Dissertation zur Erlangung des Doktorgrades
der Fakultät für Chemie und Pharmazie
der Ludwig-Maximilians-Universität München

Biocompatible and precise branched oligomers for pDNA and siRNA delivery

vorgelegt von

Eveline Edith Salcher (geb. Barth)

aus Temeschburg, Rumänien

2013

Erklärung

Diese Dissertation wurde im Sinne von § 7 der Promotionsordnung vom 28. November 2011 von Herrn Prof. Dr. Ernst Wagner betreut.

Eidesstattliche Versicherung

Diese Dissertation wurde eigenständig und ohne unerlaubte Hilfe erarbeitet.

Augsburg, den 10. 03. 2013

.....
(Unterschrift des Autors)

Dissertation eingereicht am: 11. 04. 2013

1. Gutachter: Prof. Dr. Ernst Wagner

2. Gutachter: Prof. Dr. Franz Bracher

Mündliche Prüfung am: 04. 06. 2013

Table of Contents

1 INTRODUCTION

1.1 Therapeutic approach for genetic disorders

Many severe diseases like congenital disorders and various cancer forms can be traced back to inaccurate processes on cellular level and are still beyond remedy. Therefore, many scientists have dedicated themselves to the quest for finding a cure for such disorders. By replacing or interfering with missing and defective genes they tackle the problem at its origin.

Meanwhile, there are several possibilities of approaching this topic. Therapeutic DNA, for instance, can be delivered to the nucleus of the target cells so as to replace missing or defective genes (**Fig. 1**). More than thirty years ago, T. Friedmann and R. Roblin discussed the at that time controversial issue of treating genetically determined disorders with therapeutic DNA [1]. During the last decades vast progress has been made in this field and although gene therapy is not an established treatment form yet, there are several clinical trials ongoing [2-5]. The spectrum of the treated disorders is broad, trying to cure inherited monogenic diseases (e.g. Severe combined immunodeficiency (SCID), Leber`s congenital amaurosis (LCA), Hemophilia B), infectious diseases (e.g. HIV, Hepatitis C) or cardiovascular disorders, to mention but a few examples. Nevertheless, the majority of clinical trials address various cancer forms, among others gastrointestinal and prostate tumors or cancer of the nervous system, as they occur with a very high prevalence and often are fatal.

Another approach which got in the last twenty years more and more into focus is the use of oligonucleotides aiming for specific targets within the cell. Oligonucleotides are short fragments of nucleic acids which can fulfill, depending on their nature, various tasks, thereby following one aim: regulation of inaccurate processes within the cell. Different classes have been evaluated for their therapeutic potential, either taking advantage of the antisense technology [6-9], or making use of other short nucleic acids such as decoy oligodeoxynucleotides [10], aptamers [11], polyinosine-cytosine RNA (polyIC) [12, 13] or antagomirs [14, 15].

However, the perhaps best-known oligonucleotide and its applications is small interfering RNA (siRNA). Meanwhile, it is more or less general knowledge that Andrew Fire and Craig Mello, received the Nobel Prize in 2006 for their work on RNA

interference (RNAi) in 1998. They described the impact of exogenous double-stranded RNA (dsRNA) on specific silencing of genes compared to delivered single strands in the nematode *Caenorhabditis elegans* [16]. Almost equally famous is the work of T. Tuschl and colleagues on the application of exogenous synthetic 21-nucleotide dsRNAs (also: small interfering RNAs; siRNAs) and their capability for gene silencing in mammalian cells three years later [17]. The pathway of RNA interference (RNAi) with double-stranded siRNA starts in the cytosol with its incorporation into the RNA-induced silencing complex (RISC). In the so-called Pre-RISC complex the `passenger` strand is degraded by an Argonaute (AGO) protein. The thus activated RISC contains AGO and the `guide` strand, which can then associate with the complementary target messenger RNA (mRNA). Subsequent mRNA cleavage leads to suppression of transcription of the corresponding gene (**Fig. 1**). Therefore, RNA interference leads to highly sequence-specific and efficient posttranscriptional gene silencing of target genes. Since the discovery that this pathway can be harnessed for therapeutic purposes, application in humans has rapidly advanced towards clinical trials [18, 19].

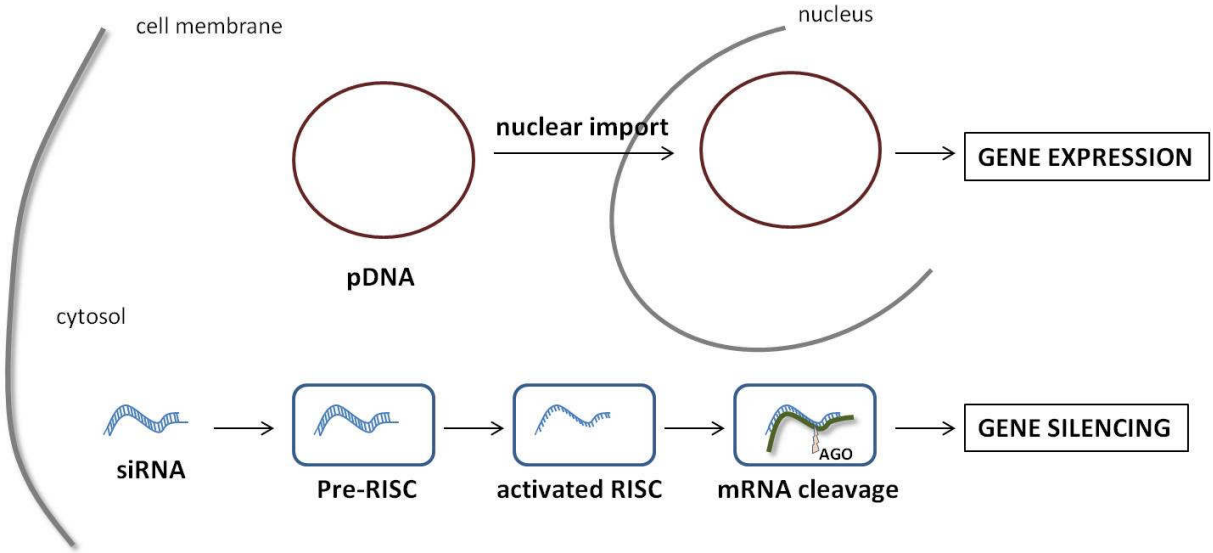

Fig. 1. pDNA and siRNA pathway within the cell.
pDNA, after entering the cell, is imported into the nucleus, where it leads to gene expression. SiRNA, for its part, is incorporated into the Pre-RISC complex, where the `passenger` strand is cleaved. The `guide` strand within the activated RISC binds to the target mRNA which is subsequently cleaved by the Argonaute (AGO) protein, thus leading to gene silencing.

1.2 Bottlenecks within nucleic acid delivery

Although research in the field of nucleic acid delivery is already far advanced, there is still need for the optimal delivery system, as the payload encounters several obstacles on the way to its site of action. Therefore, nucleic acid delivery to the target cell compartment is not an easy task, but as the drawbacks are known, they can be targeted for optimization.

When aiming at systemic administration of the pure therapeutic nucleic acid, reaching the target cells within the body undamaged is the major challenge after application. Enzymatic degradation during blood circulation by nucleases [20] and rapid renal clearance [21] are the first drawbacks which must be overcome. When applied locally, passing the anionic barrier cell membrane is an almost insuperable task due to electrostatic repulsion of the negatively charged nucleic acid phosphate backbone. Furthermore, as the size of both pDNA and siRNA is relatively large, internalization by passive diffusion is hampered. Additionally, in contrast to siRNA which acts in the cytosol, pDNA has to reach and enter the nucleus in order to allow transcription and thus mediate gene expression. A major obstacle within the cell is the transport to the nucleus, as the cellular actin cytoskeleton impedes migration of the pDNA towards its site of action [22, 23]. Active nuclear import through the nuclear pore complex (NPC) is hampered in non-dividing cells for particles lager than approximately 10 nm [24-26]; proliferating cells allow passive nuclear import during cell division [27, 28].

Therefore, the nucleic acid needs an efficient carrier with the ability to condense it to an appropriate small particle size, to protect it during blood circulation without inducing unspecific interactions with blood components and to mediate cellular uptake in target cells without damaging the cell membrane.

After internalization, the carrier has not completed its task; it has to help the payload escape endosomal entrapment. The particles are mostly found in intracellular vesicles after cellular uptake, which fuse to early endosomes. The pH within these early endosomes drops to 5.9 – 6, whereas maturation takes place by further acidification due to ATP-driven proton pumps in the endosomal membrane. As the the composition of the intra-endosomal environment cannot facilitate digestion of all proteins and lipids, late endosomes undergo fusion with lysosomes. Lysosomes contain additional enzymes, including nucleases, which would lead to nucleic acid degradation, unless the carrier facilitates endosomal escape before reaching this state. Finally, after release into the cytosol, the carrier has to set free its undamaged

cargo in or near the desired target cell compartment, namely the nucleus for DNA and the cytosol for siRNA. Concerning pDNA, late endosomal escape after microtubular transport of the vesicles to the perinuclear region is of advantage [29, 30], in order to avoid hampered cargo transport within the cell. **Fig. 2** shows exemplarily the pathway of a polyplex assembled with a cationic polymer containing a degradable disulfide linkage and the negatively charged nucleic acid.

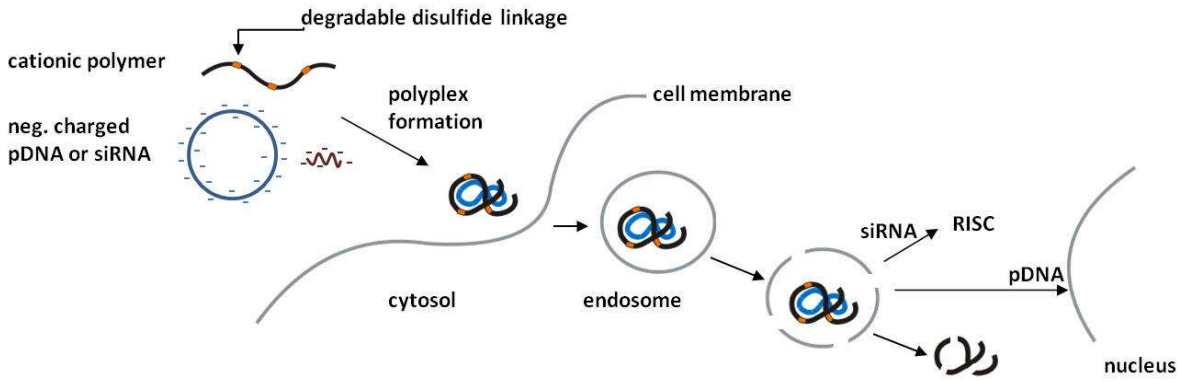

Fig. 2. Nucleic acid delivery exemplified by using a cationic polymer containing degradable disulfide linkages as carrier system. Polyplex formation takes place due to electrostatic interactions. After cellular uptake of the polyplex by endocytosis and endosomal escape, siRNA is further processed in the cytosol whereas pDNA has to enter the nucleus.

1.3 Overcoming the barriers: Nucleic acid carrier systems

1.3.1 Viral vectors

In search of efficient and biocompatible gene therapy, manifold carrier systems have been developed and investigated. However, the ideal carrier was already invented by nature – the virus. Due to its natural programming of inserting viral genetic material into target cells, it is capable of adapting to differing environmental conditions between extra- and intracellular compartments like enzymes, pH or redox potential. And indeed, this is the secret of its high efficiency, as it can dynamically change its conformation on environmental demand, securely leading the genetic material to its biological site of action [31].

Different viral vector systems have been evaluated during the last decade for gene and oligonucleotide delivery, whereas adenoviruses [32], adeno-associated viruses

(AAV) [33] and lentiviruses (LV) [34], a subclass of retroviruses, were the most commonly vectors used for gene therapy.

Gene silencing by taking advantage of the RNAi pathway could be achieved also by means of viral vectors [35]. Delivery of siRNA itself has only a transient effect, though, as siRNA acts in the cytosol and the amount decreases rapidly during cell division. Hence, another strategy was explored, namely the sustained intracellular expression of siRNA from plasmid DNA as shRNA, as shown by Brummelkamp *et al*. [9] and Paddison and colleagues [36]. Insertion of cassettes encoding for the corresponding shRNA, which are transcribed in the nucleus and further processed in the cytosol led to prolonged siRNA expression.

Nevertheless, there are good reasons why viral gene therapy is still handled with caution – the risk for serious host immune response [37], occurrence of mutagenic integration [38], limited loading capacity and high production costs still limit clinical application [39].

1.3.2 Non-viral vectors

In the field of non-viral gene delivery systems, cationic polymers and cationic lipids have meanwhile received much attention [40, 41] as they are able to circumvent some of the disadvantages associated with viral vectors, e.g. by displaying higher biocompatibility as they do not provoke such high immune response [42], higher loading capacity and feasibility for large-scale production. Unfortunately, they still cannot achieve comparable transfection efficiency. Hence, as such carriers offer manifold possibilities for optimization, much effort has been put into increasing the therapeutic potential.

A cationic lipid formulation entrapping DNA for *in vitro* transfection was first reported by Felgner *et al.* in 1987 [43]. Due to ionic interactions between the positively charged lipid head group and the negatively charged DNA, so called “lipoplexes” were formed. Since then, cationic lipid formulations for nucleic acid delivery have been further developed, even entering clinical trials [44-46].

In 1962, Smull and Ludwig observed an infection enhancement of eukaryotic tumor cells when RNA was mixed with the cationic proteins histone and protamine before adding it to cell culture medium [47]. Such complexes formed due to electrostatic interactions between a cationic compound and the negatively charged nucleic acid were later termed “polyplexes” [48]. The advantage of such interplay between carrier and cargo is that the interaction takes place in a non-damaging reversible manner. A

further benefit of cationic polymers is that these can be chemically designed and produced which leaves room for further specific modifications directed to creating non-immunogenic, bioresponsive and dynamically acting molecules.

Non-adaptable, synthetic cationic polymer-based systems, such as branched and linear poly(ethylenimine); PEI, poly(lysine); PLL, dendritic poly(amido amine); PAMAM and poly(propylenimine); PPI were already widely evaluated as nucleic acid delivery systems. The correlation between transfection efficiency and cytotoxicity has been shown to be unsatisfactory though, i.e. effective transfection agents like PEI displayed also undesired cytotoxic effects [49, 50].

Although within the polyplex the nucleic acid should be protected during blood circulation, unspecific interactions with blood components and therefore rapid clearance from the blood stream [51, 52], unspecific interactions with non-target cells, formation of aggregates at physiological salt concentrations [53] and resultant cytotoxic effects still can occur. Chemical incorporation of hydrophilic moieties like the widely used PEG for electrostatic shielding offers a way to overcome these problems. PEGylation shows not only an elongated blood circulation time, but also better water solubility and reduced cytotoxicity [54]. Transfection efficiency, however, is also reduced [55, 56] due to limited interaction of the shielded positive polymer charges with the negatively charged cell membrane. Besides that, PEG shielding hampers intracellular release of DNA and siRNA from endosomal vesicles [57, 58]. Including targeting ligands in PEGylated polyplexes is one way to enhance transfection efficiency as cellular uptake is improved due to receptor-mediated endocytosis [59-61]. An additional possibility is to increase the cytosolic release of DNA or siRNA by chemically programmed PEG-polymer linkages to be pH-sensitive and thus cleavable in the endosome [62-64].

Reaching the target tissue after systemic delivery faces an enormous challenge: the vascular barrier. Extravasation barriers differ from tissue to tissue. While CNS is extremely well protected against extravasating agents by the blood brain barrier, hepatocytes, inflammation sites or tumor sites are much more accessible. In the latter case the tumor tissue can be achieved either by “passive” or “active” targeting. Passive targeting takes advantage of the enhanced permeability and retention (EPR) effect [65]. This phenomenon implies polymer accumulation in tumor tissue due to its leaky vasculature and deficient lymphatic clearance [66].

Active targeting implies the conjugation of targeting ligands to nucleic acid carrier systems which specifically bind to receptors expressed on cell surfaces, as tumor cells often show an over-expression of a series of specific receptors. First shown for DNA delivery by conjugation of hepatocyte target moiety asialoorosomucoid (ASOR) to polylysine over twenty years ago [67], there are various ligands which can be used for active targeting, such as transferrin [68], epidermal growth factor (EGF) [30], RGD [69, 70] or folic acid [71, 72].

Once internalized, the essential step for the polyplex is to rapidly escape the endosomal vesicle in order to release the nucleic acid in the cytosol and prevent its lysosomal degradation. As the endosomal and lysosomal pH presents values between 4.5 and 6.5 and therefore differs from the neutral pH of 7.4 in other biological compartments [73], this characteristic can be taken advantage of by using different strategies.

Within the class of cationic polymers, polyethylenimine (PEI) has unique favorable properties for intracellular nucleic acid delivery. Synthetic variations in both molecular weight and structure are possible, also with differing effect on efficiency and biocompatibility [74, 75]. PEI has outstanding properties concerning pDNA binding ability and buffering capacity for endosomal escape due to the 1,2-diaminoethane motif [76-78]. Due to its high charge density [74] it facilitates endosomal escape by taking advantage of the so-called “proton sponge effect” [79]. PEI nitrogens are only moderately protonated at physiological pH [80], whereas protonation increases upon endosomal acidification. Due to proton accumulation within the vesicle and therefore high density of positive charge, the influx of chloride and water is increased. Finally, the osmotic pressure and membrane destabilization effect of the cationic compound leads to endosome disruption and thus to particle release into the cytosol. Current investigation on the impact of the length of such moieties containing the diaminoethane motif revealed the correlation between amount of protonable amines, position within the chain and buffering capacity [81-83].

The imidazole group within the histidine side chain can be also used as a buffering domain. Due to its chemical structure protonation occurs only at an acidic pH value, which makes this amino acid interesting for enhancing endosomal escape by the proton sponge effect. Therefore, it was often chemically integrated in nucleic acid carriers and various research groups could show enhanced transfection efficacy due to histidine introduction. Midoux and Monsigny showed first enhanced pDNA

transfection of the cationic polymer polylysine modified with histidine residues in 1999 [84]. Since then, histidine or the imidazole group has been widely used for nucleic acid carrier optimization [85-90].

Of course, endosomal escape can be further enhanced by introduction of specific endosomal membrane disrupting or pore forming domains, such poly(vinyl ether) [91] or endosomolytic peptides like melittin or the influenza peptide [92, 93]. Melittin, for instance, a peptide from bee venom consisting of 26 amino acids, is able to enhance transfection efficiency of polycations [12, 94-97] by damaging interactions with the endosomal membrane [98]. As its lytic potential, though, is not pH-selective, various modifications led to specific activation of the lytic activity at acidic pH, thus preventing cytotoxic side effects before internalization [99-102].

Efficient gene carriers like linPEI, though, have the disadvantage that, when applied *in vivo*, they cannot be degraded and metabolized by the body and accumulation occurs with consequent undesired toxic effects [49, 103]. Therefore, a strategy towards uniting appropriate carrier molecular weight, adequate nucleic acid condensation and cytosolic release for efficient transfection with low toxicity is the design of biodegradable vectors. These are composed of low molecular weight (LMW) monomers linked via degradable bonds resulting in a high molecular weight (HMW) polymer. Triggered by environmental conditions, these polymers are thus chemically programmed to degrade into their LMW non-toxic decomposition products.

There are also different strategies for creating such biodegradable nucleic acid carriers. One possibility is to take advantage of the acidic endosomal environment by introduction of acid-sensitive linkers [63, 104, 105]. Another option is connecting low Mw compounds by hydrolysable linkages, which degrade in a time-dependent manner [106-108]. Furthermore, one can take advantage of the redox difference between oxidizing extracellular and reducing intracellular environment. Chemically incorporated disulfide linkages into polymeric compounds remain therefore relatively stable during blood circulation and can then be cleaved in the cytosol by the reducing agent glutathione (GSH), the most abundantly occurring thiol-source in mammalian cells [109]. Similar to hydrolysable ester-linked polymers, cationic carriers with integrated disulfide bonds can decompose into their smaller molecular weight compounds and therefore release the nucleic acid in the cytosol with lower cytotoxicity than larger non-degradable carriers [110-112]. Polyplex stabilization by

introduction of reducible cross-linking agents before [113] or after [114] complexation with the nucleic acid has also shown promising results in terms of transfection efficiency. This strategy has proven to be even more of advantage also for siRNA delivery [115-117], as siRNA differs from pDNA in size and charge, which makes polyplex stabilization a more crucial feature.

Therefore, it has to be distinguished between vectors for pDNA and vectors for siRNA delivery. As already mentioned, these cargos differ in size and chemical properties i and thus efficient pDNA delivery is not a warrant that the same carrier will deliver siRNA in an equally efficient manner.

Consequently, there is need for better defined delivery systems, so as to allow conclusions on structure-activity relationships for the respective nucleic acid and thus provide information for concerted optimization.

1.4 Towards better defined delivery systems

Chemical programming of polymers has proven to be a crucial tool in mimicking virus-like features. Thus, alterations in polymer structure and conformation can be correlated to transfection efficiency and cytotoxicity. It has to be considered: the better the polymer structure is defined, the more detailed study of structure-activity relationships is possible. First approaches towards better defined polymer structure with narrow molecular weight distribution have been made by poly(amino ester) [106, 118] and pseudodendrimer synthesis [119]. An additional advantage of these structures is also their biodegradablility, which allows high molecular weights for nucleic acid condensation and transfection, but without toxicity, as the carriers decompose into small Mw, nontoxic compounds.

A class of molecules with defined architecture are dendrimers. These are characterized by a relatively low polydispersity due to the synthetic process, whereas stepwise synthesis can be performed by two different methods, divergent or convergent [120-122]. Cationic dendrimers like commercially available polyamidoamine (PAMAM) [123-125] or polypropylenimine (PPI) [126, 127] have already been investigated as nucleic acid carriers. These studies, however, show that there is still room for improvement concerning transfection efficiency and cytotoxicity. As the synthetic process allows changing the surface character of the dendrimer by introducing specific residues for enhanced gene transfection, several modified

poly(amido amine); PAMAM [128-131] and PPI [132-136] based structures were investigated for DNA and siRNA transfection.

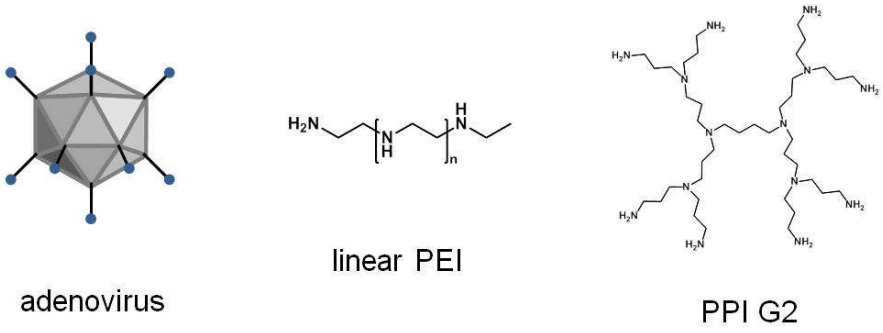

Fig. 3. Nucleic acid carrier systems.
Schematic structure of an adenovirus, chemical structures of linear PEI and PPI G2.

Lipidoids are also a class of efficient nucleic acid carriers and Akinc *et al.* showed a synthetic method of such compounds suitable for combinatorial chemistry. Thus, diverse parallel functionalization and screening of a large lipidoid library allowed fast determination of efficient carriers [137]. Further development of a combinatorial approach of this nucleic acid carrier class was used for the determination of functional group effects on siRNA delivery [138].

The group around J.-P. Behr followed another strategy, namely the generation of monodisperse nucleic acid delivery systems by monomolecular condensation of pDNA with cationic detergents [139-141].

A further possibility of assembling defined nucleic acid carrier systems which bears many advantages is solid-phase peptide synthesis. This synthetic strategy will be introduced in the following section.

1.5 Solid-phase peptide synthesis (SPPS) allows assembly of precise, sequence defined nucleic acid carriers

In 1963, R. B. Merrifield published his work on peptide synthesis following a novel strategy, namely the use of an insoluble but porous chloromethylated polystyrene polymer as a solid support for stepwise amino acid assembly [142]. This synthetic method mainly makes use of simple chemical principles: the backbone of amino acids contains a carboxylic acid and a primary amine. Activation of the carboxylic acid enables reaction with a primary amine, resulting in a stable amide bond (**Fig. 4**). Thus, the chain can be elongated in a controlled manner. Accomplishing this reaction

on solid phase has the advantage that excess reagents or by products can be discarded by washing steps. After finishing the desired sequence, the product can be easily cleaved off the solid support and collected by filtration.

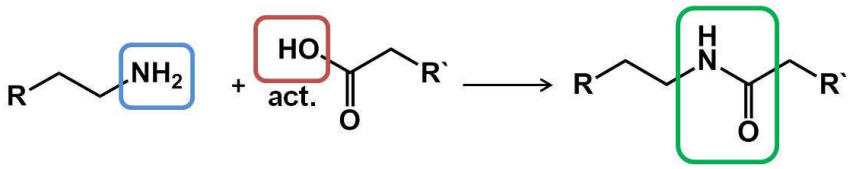

Fig. 4. Reaction of a primary amine with an activated carboxylic acid to a stable amide bond.

After first difficulties, Merrifield further improved this method himself [143] and since then great advance has been made towards optimization of reaction conditions, such as development of suitable amino acid side chain protection groups in order to prevent undesired side reactions or novel cleavage strategies. Furthermore, adequate analytical and purification methods for the products make SPPS a reliable synthetic method for sequence-defined, precise structures. Also, novel synthetic devices enable using SPPS for combinatorial chemistry, as parallel synthesis of multiple sequences is possible either manually or using automatic peptide synthesizers. Thus, different structural combinations can be generated at the same time.

Due to its many advantages, SPPS was used during the last decades also for the synthesis of precise nucleic acid carriers.

Dendritic structures, for instance, can be easily generated by the introduction of lysines with two primary amines in α- and ε-position as branching points. Using this attribute, 25 years ago J. Tam generated in a single solid-phase synthesis multiple antigenic peptides (MAPs), based on a lysine core matrix and antigenic peptides of 9 – 16 amino acids [144]. Pursuing the aim of efficient nucleic acid delivery, other dendritic structures containing functional amino acids such as histidines as additional buffering domains were synthesized by the group around A. J. Mixson [145-147].

Due to the advantages of SPPS, also cationic lipid-like structures can be generated. Wang *et al.* created a small library of reversibly polymerizable surfactants using combinatorial solid phase synthetic strategy. These vectors contain a protonable amino head group, two cysteine residues and two lipophilic tails, exhibiting pH-sensitive membrane disruption potential. By hence facilitated endosomal escape, the

surfactants mediated efficient *in vitro* luciferase silencing, comparable with the effectivity of cationic lipids [148].

When thinking of pDNA of siRNA delivery, assembly of poly(amido amines) is an interesting and promising approach, as introduction of longer building blocks containing the buffering diaminoethane motif enhance nucleic acid binding and endosomal escape. Only few reports were published on the application of the SPPS methodology for the synthesis of shorter poly(amido amines), those also without aiming at nucleic acid delivery [149-151].

In 2006, Hartmann *et al.* designed linear peptidomimetic polymers with poly(amido amine; PAA) as a structural pattern. Dicarboxylates and diamines were stepwise coupled in an alternating manner, thus generating a monodisperse oligopeptide. By exact introduction of functionalities in the linear PAA chain, such as poly(ethylene oxide); PEO, a single component block copolymer was synthesized, thus proving the versatility of the method [152]. PEO modified PAAs were studied in a subsequent work concerning dsDNA complexation and condensation qualities, resulting in clearly defined, non cytotoxic polyplexes [153]. The researcher in their studies applied only rather simple diamine compounds and did not include diaminoethane motifs.

In our laboratory David Schaffert introduced oligoamine building blocks containing the buffering diaminoethane unit. In order to avoid undesired side reactions such as on-resin crosslinking, Schaffert *et al.* modified the diaminoethane unit containing polyamines with a carboxylic anchor and adequate protection groups, thus making them feasible for solid-phase synthesis. By the means of these artificial oligoamino acids, precise, sequence-defined oligomers could be assembled [154]. In a subsequent publication, cationic oligomers with different topologies and modifications, such as introduction of cysteines and/or lipophilic domains, were designed, showing efficient transfection results for both pDNA and siRNA delivery and allowing conclusion on structure-activity relationships [155].

1.6 Aims of the thesis

In the current thesis, SPPS had to be used for overcoming the drawback of polymer polydispersity combined with maintaining important carrier features such as higher molecular weight, cargo binding properties and the buffering diaminoethane motif. In particular, the SPPS methodology should be used for the design of branched

oligomers, which are supposed to be biocompatible and sequence-defined, using cationic artificial and natural amino acids.

Firstly, branched structures had to be generated directly on solid support by introduction of two subsequent lysines. Due to two primary amines in α- and ε-position of lysine, the generated four amino- groups should act as starting points for four arms which could be elongated in a parallel manner, allowing gain in molecular weight in only few synthetic steps (**Fig. 5. A, C, D**). Also, the impact of stepwise increase of arm length on cargo binding and delivery should be evaluated. Further modifications of this class of oligomers like the introduction of cysteines for polyplex stabilization, variation in building block length or insertion of histidines as additional buffering domain should bring further insights in structure-activity relationships. The thus generated compounds had to be evaluated not only for their potential for efficient and safe gene delivery, but also for siRNA-mediated gene silencing, so as to determine differences in carrier requirements for the respective nucleic acid.

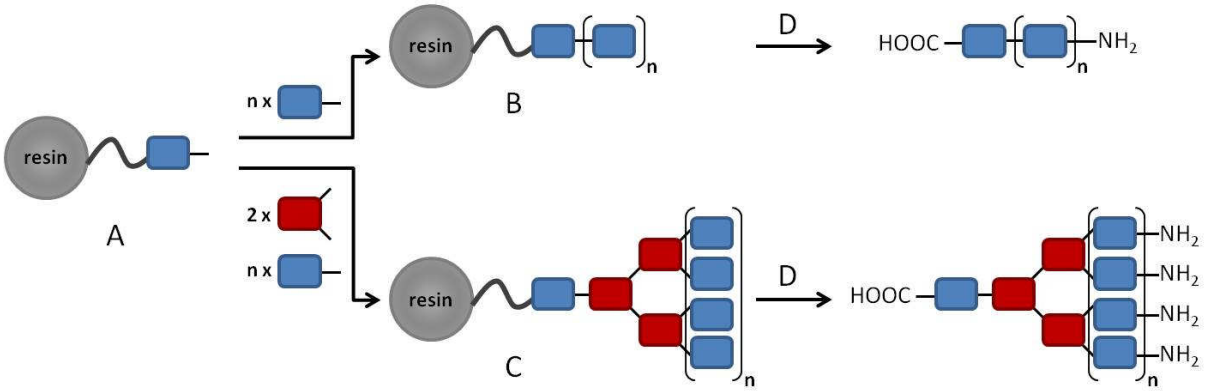

Fig. 5. Solid-phase supported synthesis (SPS) of sequence-defined oligomers. A preloaded resin **(A)** can be further modified in a stepwise manner so as to generate either linear **(B)** or, by introduction of lysines, branched **(C)** oligomers. After finishing the desired sequence, the oligomer is cleaved from the solid support **(D)**.

Secondly, a novel approach towards avoiding toxicity related to higher molecular weight should be also developed, namely assembly of defined biodegradable oligomers for gene delivery. This class of pDNA carriers should consist of the structurally defined dendritic core polypropylenimine with eight primary amines on the surface (PPI G2), which is non-toxic but also does not mediate transfection efficiency. This PPI core had to be modified in so far as to allow linkage of precise, sequence-defined cysteine-containing oligo(ethane amino)amides (**Fig. 5 A, B, D**) via disulfide bond formation. The disulfide linkages can be cleaved in the reducing cytosolic

environment, hence allowing the carrier to decompose into its non-toxic, low Mw compounds.

Therefore, due to the sequence control allowed by SPPS and also by the concerted coupling in solution to the PPI core, due to reliable purification and analytical methods, two strategies should be followed for the generation of branched, precise, biocompatible nucleic acid carriers.

The final aim of this thesis is, beyond synthesis of the above mentioned compounds, to gain interesting new insights on structure-activity relationships concerning pDNA and siRNA delivery by biophysical and biological evaluation.

2 MATERIALS AND METHODS

2.1 Chemicals and reagents

Fmoc-Ala-Wang resin Low Load was purchased from Novabiochem (Darmstadt, Germany); pentafluorophenol (Pfp), dicyclohexylcarbodiimide (DCC), 0.5 M tris(2-carboxyethyl)phosphine (TCEP), 2-chloro-1-methylpyridinium iodide (CMPI), (3-(4,5-dimethylthiazol-2-yl)-2,5-diphenyltetrazolium bromide) (MTT), 1-hydroxy-benzotriazol (HOBt), triisopropylsilane (TIS), Triton X-100, 2-(N-morpholino)ethanesulfonic acid (MES) and 50mM sodium hydroxide solution from Sigma-Aldrich (Munich, Germany); benzotriazol-1-yl-oxy-tris-pyrrolidino-phosphonium hexafluorophosphate (PyBOP) and microreactors from MultiSynTech (Witten, Germany).

All amino acids, peptide grade dimethylformamide (DMF), diisopropylethylamine (DIPEA) and trifluoroacetic acid (TFA) were obtained from Iris Biotech (Marktredwitz, Germany). Boc-Cys(NPys)-OH (BCNP) was purchased from Bachem (Bubendorf, Switzerland). Polypropylenimine (PPI) G2 was obtained from SyMO-Chem (Eindhoven, The Netherlands).

Spectra/Por dialysis membranes were purchased from Carl Roth GmbH (Karlsruhe, Germany).

Linear PEI (linPEI with an average molecular weight of 22kDa) is described in [13].

Plasmid pEGFPLuc (encoding a fusion of enhanced green fluorescent protein EGFP and *Photinus pyralis* luciferase under control of the CMV promoter) was produced with the Qiagen Plasmid Giga Kit (Qiagen, Hilden, Germany) according to the manufacturer specifications.

Ready to use siRNA duplexes were synthesized and provided by Axolabs GmbH (formerly: Roche Kulmbach, Germany): GFP-siRNA (sense: 5'-AuAucAuGGccGAcAAGcAdTsdT-3'; antisense: 5'-UGCUUGUCGGCcAUGAuAUdTsdT-3'; small letters: 2'methoxy-RNA; s: phosphorothioate) for silencing of the eGFPLuc protein and control-siRNA (sense: 5'-AuGuAuuGGccuGuAuuAGdTsdT-3'; antisense 5'-CuAAuAcAGGCcAAuAcAUdTsdT-3') as a control.

Water was used as purified, deionized water.

2.2 General methods for SPPS-based oligomer synthesis

2.2.1 Syntheses of cationic building blocks

Cationic building block Stp was synthesized as described in [154]. Gtt was used as described and synthesized by Dr. Naresh Badgujar (Wagner lab) in [154]. New cationic building block Sph was developed and synthesized by Dr. Naresh Badgujar as described in [156].

2.2.2 General methods for oligomers synthesis by manual SPPS

Synthetic step	Reagent	Reaction time	Wash
Resin swelling	DMF[1] DMF + 1% Triton-X 100[2]	1[1]-16[2] h	1 x DMF[1] (+1% Triton-X 100[2])
Coupling	DMF[1] (+ 1% Triton-X 100[2])	1-2 h	4 x DMF[1] (+ 1% Titon-X 100[2])
Fmoc deprotection	20% piperidine in DMF[1] 2% piperidine, 2% DBU in DMF + 1% Triton[2]	1 x 10, 1 x 20 min[1] 6 x 5 min[2] 8 x 5 min[3]	6 x DMF[1] 6 x DMF + 1% Triton-X 100[2]
Cleavage	TFA: water 95:5[4] TFA:TIS:water 95:2.5:2.5[5] TFA:TIS:water 92.5:5:2.5[3]	1-2 h	2 x TFA 2 x DCM

[1] for generation of four-arm core / five-arm Stp tail and subsequent branching / linear oligomer
[2] for synthesis after four-arm branching
[3] for histidine-containing oligomers
[4] for not cysteine-containing oligomers
[5] for cysteine-containing oligomers

2.2.3 DMF test on amine impurities

6 µl of a bromophenol blue stock solution (5 mg/ml in DMSO) were added to 1 ml DMF. DMF was accepted for use if the solution color was yellow or slightly green.

2.2.4 Fmoc quantification

5 – 10 mg of dry resin was weighed in duplicates in Eppendorf tubes and agitated with 1.0 ml 20% piperidine in DMF for 1.5 h. Thereafter, the tube was vortexed briefly and the resin was allowed to settle for approximately 2 min. 25 µl of the supernatant of each sample, of a positive control (Fmoc-Ala-Wang resin) and of a blank solution (20% piperidine in DMF) were diluted to 1 ml with DMF. A_{301} of each sample was determined in duplicates. The Fmoc-substitution (FS) of the resin was calculated using following equation:

$$\text{FS (mmol/g)} = \frac{A_{301} \cdot 1000}{m \cdot 7800 \cdot D}$$

A_{301}: absorbance at λ = 301 nm

m: resin mass [mg]

7800: molar extinction coefficient [L mol^{-1} cm^{-1}]

D: dilution factor (0.025)

2.2.5 Kaiser Test

Reagent A: 5% ninhydrin in ethanol (w/v)

Reagent B: 80% phenol in ethanol (w/v)

Reagent C: 2 ml 0.001 M KCN in 98 ml pyridine

A few resin beads were taken into an Eppendorf cap and washed three times with DMF and three times with methanol. Two drops of each reagent were added and the beads were heated at 99°C for 4 min. The presence of free amino groups gave a positive test (blue beads), whereas a negative outcome indicated no presence of free amino groups (colorless beads).

2.2.6 Introduction of Triton X-100

In order to avoid intramolecular chain aggregation due to hydrophobic interactions and yield improvement, 1% Triton X-100 was added to the coupling solvent or deprotection solvent mixture used for chain elongation of four- and five-arm oligomers after branching.

2.3 Syntheses of four- and five-arm oligomers

2.3.1 Synthesis of four-arm core

After swelling 0.2 mmol of Fmoc-Ala-Wang resin Low Load (Novabiochem) in DMF and cleavage of the Fmoc protecting group by double treatment with 20% piperidine in DMF, a solution of Fmoc-Lys(Fmoc)-OH (0.4 eq), PyBOP/HOBt (0.4 eq) and DIPEA (0.8 eq) in DMF was added to the resin and the vessel was agitated for 1 h. The unreacted amino groups were subsequently acetylated using 20 equivalents of acetic anhydride and 40 equivalents of DIPEA in DMF before removal of the Fmoc protecting group. The second coupling was performed by adding a solution of Fmoc-Lys(Fmoc)-OH (4 eq), DIPEA (8 eq) and PyBOP/ HOBt (4 eq) in DMF and incubation for 1 h. Reaction progress was monitored by Kaiser test. After completion of the reaction the resin was washed five times with DMF and five times with DCM and dried for 12 h in vacuo. The loading of the resin was determined by spectrophotometric Fmoc-quantification using 20% piperidine in DMF.

2.3.2 Synthesis of four-arm Stp oligomers

The preloaded resin (0.02-0.04 mmol according to Fmoc loading) was swollen over night in DMF. After the swelling 1% Triton X-100 was added to the DMF for use, and all subsequent steps including washing, coupling and Fmoc-deprotection were performed using this mixture. Fmoc protecting groups were cleaved by six-fold treatment (each 5 min) with 2% piperidine, 2% DBU in DMF/Triton. After washing the resin, a solution of Fmoc-Stp-OH (4 eq), DIPEA (8 eq) and PyBOP/ HOBt (4 eq) in DMF/Triton was added for 90 min. The reaction solvent was drained and the resin was washed five times with DMF. Reaction progress was monitored by Kaiser test. The whole process was repeated depending on the desired sequence. The resin was treated six times (each 5 min) with 2% piperidine, 2% DBU in DMF/Triton in order to deprotect the Fmoc group. The resin was washed five times with DMF and five times with DCM and dried over KOH in vacuo. For cleavage the resin was suspended in a solution of TFA/H_2O (95/5, v/v) and agitated for 3 h. The cleavage solution was drained and collected. The resin was washed twice with TFA and twice with DCM. The collected solutions were concentrated under reduced pressure to minimum volume. The residue was washed twice with ice-cold MTBE, then dissolved in water and lyophilized. The lyophilized product was dissolved in a minimal volume 10mM HCl and dialyzed against 10 mM HCl using a Spectra/Por® Dialysis Membrane,

MWCO 3500 Da. After 16 h the buffer was exchanged and the dialysis proceeded for another 8 h. The sample was lyophilized and characterized via cation exchange chromatography.

2.3.3 Synthesis of terminally modified four-arm Stp, Gtt and Sph oligomers

Oligomers were synthesized as described above. Additionally, depending on the sequence, either Boc-Cys(Trt)-OH or Boc-Ala-OH was coupled as last amino acid in the same manner. For cleavage the resin was suspended in a solution of TFA/TIS/H_2O (95:2.5:2.5, v/v/v) for cysteine containing oligomers, or TFA/H_2O (95:5, v/v) for alanine containing oligomers, and agitated for 2 h. The cleavage solution was drained and collected. The resin was washed twice with TFA and twice with DCM. The collected solutions were concentrated under reduced pressure to approximately 2 ml. The product was precipitated in a 1:1 mixture (40 ml) of cooled (0 °C) MTBE and n-hexane and centrifuged at 4 °C for 5 min (3000 rpm). The pellet was then dissolved in 10mM HCl containing 30% acetonitrile and purified by size exclusion chromatography (SEC). Product fractions were pooled and freeze dried. Identity was confirmed by ^{1}H-NMR. Purity of selected oligomers was determined by RP-HPLC.

2.3.4 Synthesis of five-arm Stp oligomers

After swelling 0.1 mmol of Fmoc-Ala-Wang resin Low Load (Novabiochem) in DMF and cleavage of the Fmoc protecting group by double treatment with 20% piperidine in DMF, a solution of Fmoc-Stp-OH (0.5 eq), PyBOP/HOBt (0.5 eq) and DIPEA (1.0 eq) in DMF was added to the resin and the vessel was agitated for 1 h. The unreacted amino groups were subsequently acetylated using 20 equivalents of acetic anhydride and 40 equivalents of DIPEA in DMF. Reaction progress was monitored by Kaiser test. After completion of the reaction the resin was washed five times with DMF and five times with DCM and dried for 12 h in vacuo. The loading of the resin was determined by spectrophotometric Fmoc-quantification using 20% piperidine in DMF.

The preloaded resin (0.01 mmol) was swollen in DMF for 1 h. After cleavage of the Fmoc protecting group by double treatment with 20% piperidine in DMF, a solution of Fmoc-Stp-OH (4 eq), PyBOP/HOBt (4 eq) and DIPEA (8 eq) in DMF was added to the resin and incubated for 1 h. In the next two coupling steps Fmoc-Lys(Fmoc)-OH was used as described above, 4 eq for the first coupling and 8 eq for the second.

After removal of the Fmoc protection group with 20% piperidine in DMF the synthesis was carried on according to synthesis of four-arm oligomers, using 16 eq building block and amino acid, 16 eq HOBt/PyBop and 32 eq DIPEA in each coupling step. In the last coupling step Boc-Cys(Trt)-OH was used. Cleavage from the resin and further purification was performed as described above.

2.3.5 Synthesis of histidine-containing four-arm oligomers

Oligomers were synthesized as described above, with following modifications: Fmoc-His(Trt)-OH was used as additional amino acid. Fmoc-deprotection cycles were increased to eight times five minutes. Cleavage from the resin was performed with TFA/TIS/H_2O (92.5/5/2.5, v/v/v).

Compounds **582** and **584** (based on [146]) were synthesized automatically using a SyroWAVE Peptide synthesizer (Biotage Sweden AB, Uppsala, Sweden). Couplings were performed 2 x 5 min using a microwave device, deprotection steps were performed using 20%piperidine, 2% DBU in DMF for 3 x 20 min. Cleavage, purification and characterization was performed as described above.

Synthetic methods for the generation of polypropylenimine (PPI) conjugates

2.3.6 Synthesis of linear Stp oligomers

A Fmoc-Cys(Trt)-Wang resin was preswollen in DMF for 1 h. Fmoc-deprotection was performed by double treatment with 20% piperidine in DMF. After washing the resin five times with DMF, a solution of Fmoc-Stp-OH (4 eq), PyBOP/HOBt (4 eq) and DIPEA (8 eq) in DMF was added to the resin and the vessel was agitated for 1 h. Reaction progress was monitored by Kaiser test. The procedure was repeated, depending on the sequence, up to four times. After the last Fmoc-deprotection the resin was washed five times with DMF, five times with DCM and dried over night *in vacuo*. Cleavage from the resin was performed by treatment with TFA/TIS/H_2O (92.5/2.5/2.5, v/v/v) for two hours. The cleavage solution was then drained and collected; the resin was washed twice with TFA and twice with DCM. The collected solutions were concentrated to approximately 1 ml and precipitated in ice-cold MTBE/n-hexane (1/1). After centrifugation, the pellet was rewashed with ice-cold MTBE. The product was then dissolved in water and freeze dried. Identity was confirmed by ^{1}H-NMR.

2.3.7 Synthesis of Boc-Cys(NPys)-pentafluorophenyl ester (BCNP-OPfp)

BCNP-OPfp was synthesized according to [157] with slight modifications. 500 mg Boc-Cys(NPys)-OH (1.33 mmol) and 269.3 mg pentafluorophenol (Pfp, 1.463 mmol, 1.1 eq) were suspended in 5 ml DCM. 1 eq dicyclohexylcarbodiimide (DCC, 274.4 mg) was dissolved in 1 ml DCM and added to the solution. The mixture was stirred for 15 min at 0°C and subsequently for 3.5 h at room temperature. After cooling the solution to 0°C, precipitated dicyclohexylurea (DCU) was filtered and the solvent evaporated. Completion of the reaction was monitored by TLC (R_f in ethylacetate: BCNP: 0; Pfp: 0.6, sample: 0.8; in chloroform/methanol 3:1: BCNP: 0.2, Pfp: 0.8, sample: 0.9).

Yield: 650 mg (90%)

2.3.8 Synthesis of activated PPI core (PPI-CNP)

30 mg PPI G2 (0.039 mmol) was dissolved in 1 ml DCM. 588.4 mg Boc-Cys(NPys)-OPfp (28 eq, 1.087 mmol) was dissolved in 5 ml DCM and added to the PPI solution. The mixture was stirred for 24 h at room temperature. The solvent was concentrated to a minimal volume and precipitated in ice-cold MTBE. After centrifugation and decantation of the supernatant, the residue was washed with ice-cold MTBE and the procedure repeated until the washing solution was colourless. The residue was then dissolved in acetonitrile, freeze dried and analyzed by ^{1}H-NMR.

Yield: 108 mg (46%)

^{1}H-NMR: δ (ppm) = 1.4-1.5 (s, 72 H, -CH_3 boc), 1.6-1.7 (m, 28 H, -CH_2-CH_2-CH_2-PPI), 2.4-3.3 (m, 68 H, βH cysteine, PPI), 4.3 (t, 8 H, αH cysteine), 7.5 (dd, 8 H, *J*=4.7, 8.3 Hz, -CH=C**H**$_{NPys}$-CH=), 8.6 (dd, 8 H, *J*=1.6, 8.2 Hz, -C**H**$_{NPys}$-C(NO_2)=), 8.9 (dd, 8 H, *J*=1.5, 4.7 Hz, -C**H**$_{NPys}$=N-)

3.3 (s, MeOD), 4.9 (s, H_2O)

In order to remove the boc protection group the precipitate was dissolved in 1 ml 80% TFA in DCM. After 2 h the solvent was evaporated, the residue was dissolved in water and freeze dried. The product was subsequently analyzed by ^{1}H-NMR to ensure complete boc removal and for quantification of the NPys-groups. Additionally, surface modification was quantified spectrophotometrically. Purity was determined by RP-HPLC.

^{1}H-NMR: δ (ppm) = 1.6-2.4 (m, 28 H, -CH_2-C**H**$_2$-CH_2- PPI), 3.1-3.6 (m, 68 H, βH cysteine, PPI), 4.2 (t, 8 H, αH cysteine), 7.5 (dd, 8 H, *J*=4.7, 8.3 Hz, -CH=C**H**$_{NPys}$-

CH=), 8.5 (dd, 8 H, *J*=1.6, 8.2 Hz, -C**H**$_{NPys}$-C(NO_2)=), 8.7 (dd, 8 H, *J*=1.5, 4.7 Hz, -C**H**$_{NPys}$=N-), 4.8 (s, HDO)

2.3.9 Assembly of PPI conjugates

PPI-CNP was reacted with 24 eq of linear cationic polymer (related to SH-groups) in a minimal amount of reaction buffer (MES pH 6.1 + 20% acetonitrile). After 4 h the amount of released nitropyridinethione was measured spectrophotometrically. After completion of reaction the sample was transferred to a dialysis tube with an adequate MWCO and dialyzed in water pH 5.5 (acetic acid) for 4 h. After buffer exchange dialysis was continued for additional 20 h. The sample was then freeze dried and analyzed by ^{1}H-NMR.

2.4 Methods and devices for compound purification and chemical characterization

2.4.1 Dialysis

Dialysis was performed using SpectraPor tubes of an adequate MWCO. Dialysis was performed in water for four-arm Stp oligomers and in water pH 5.5 for PPI conjugates at 4°C with buffer exchange after 4 h and total dialysis time of 24 h.

2.4.2 Size exclusion chromatography

Size exclusion chromatography of all polymers was run on an Äkta Basic HPLC system using a self-packed Sephadex G-10 column (GE Healthcare). The buffer used was 10 mM HCl + 30% acetonitrile at a flow rate of 2 ml/min and isocratic elution. The product fractions were pooled and freeze dried.

2.4.3 Analytical ion exchange chromatography (IEX-HPLC)

Analytical IEX-HPLC was performed using an ÄKTA Basic system (GE Healthcare) and a Resource S 1 mL column. Buffer A: 10 mM HCl. Buffer B: 10 mM HCl + 3 M NaCl. Flow rate 2 ml/min. Gradient: 2% B to 100% B in 15 min. UV detection at 214 nm and 280 nm.

2.4.4 Analytical reversed phase HPLC (RP-HPLC)

Analytical RP-HPLC was performed using a Waters HPLC System containing a P-900 gradien pump system under the control of the Millenium software and a C_{18}-RP analytical column (Waters SunFire C_{18}, 4.6 x 150 mm). Buffer A: H_2O + 0.1% TFA,

buffer B: acetonitrile + 0.1 % TFA at a flow rate of 1 ml/min. The gradient was run from 5% to 100% buffer B in 20 min. Absorption of the amide bond was monitored at λ = 214 nm with a 996 Photodiode array detector.

2.4.5 ^{1}H-NMR

^{1}H NMR spectra were recorded using a Jeol JNMR-GX 400 (400 MHz) or JNMR-GX 500 (500 MHz) device. Chemical shifts are reported in ppm and refer to the solvent as internal standard. Data are reported as s=singlet, d=doublet, t=triplet, m=multiplet; integration was performed manually. The spectra were analyzed using NUTS (2 D professional version 20020107 by Acron NMR, 2002) or MestreNova (Ver. 5.2.5-4119 by MestReLab Research).

2.4.6 Mass Spectrometry

MALDI-MS analysis was carried out on a Bruker Autoflex MALDI-TOF system.

2.4.7 3-Nitro-2-pyridinesulfenyl (NPys) quantification

A standard Boc-Cys(NPys)-OH (BCNP) solution was serially diluted in methanol and measured spectrophotometrically at 340 nm. The sample was diluted accordingly and measured against methanol as a blank. Concentration of NPys was calculated via the calibration curve.

2.4.8 Quantification of 3-Nitro-pyridine-2-thione (NPythione)

For the calibration curve, a standard BCNP solution was serially diluted in MES buffer:acetonitrile 4:1 and measured spectrophotometrically at 440 nm. Subsequently, the dilutions were treated with 4 µl TCEP (500 µmol/ml) each and incubated at room temperature for 30 min. The released NPythione was measured at 440 nm against the buffer mixture as a blank. The sample was diluted and treated accordingly. Concentration of the released NPythione was calculated after subtraction of the absorption values of untreated BCNP via the calibration curve.

2.4.9 Ellman`s assay [158]

The colorimetric reaction between Ellman's reagent (5,5'-dithiobis(2-nitrobenzoicacid), DTNB) and the free thiol groups was performed as follows: 0.4 mg DTNB dissolved in 1 ml of Ellman´s buffer (0.2 M Na_2HPO_4 with 1 mM EDTA at pH 8.0) was used as stock solution. Standard cystein solution and samples were serially diluted in Ellman’s buffer and 10% (v/v) of the stock solution. After 20 minutes

incubation at 37 °C the solutions were measured at 412 nm. Ellman´s stock diluted 1:10 in Ellman´s buffer was taken as blank. Concentration of the thiol group was calculated via the calibration curve.

2.4.10 Tris(2-carboxyethyl)phosphine (TCEP) assay

A standard cysteine solution (0.05 µmol/ml) was serially diluted with Ellman`s buffer and incubated with 40 µl TCEP (5 µmol/ml) for 10 min at room temperature. Subsequently, 10 µl 2-chloro-1-methylpyridinium iodide (CMPI, 100 µmol/ml) were added and further incubated for 10 min at 37°C. Absorbance was measured at 314 nm with buffer/TCEP/CMPI mixture as a blank. Concentration of reduced disulfide bonds and resulting free thiols was calculated via the calibration curve.

2.5 Biophysical and biological characterization

2.5.1 Acidimetric titrations of histidine containing oligomers

The protonation behaviour was investigated over a pH range of pH 2 to 11. The titrations were carried out with an automated potentiometric titrator Metrohm Titrando 905 equipped with a Biotrode pH electrode (METROHM GmbH & Co. KG, Filderstadt, Germany). The oligomer amount corresponding to 15 µmoles protonable amines was dissolved in 3.5 ml 50 mM sodium chloride solution. The pH was adjusted < 2 with 0.5 M hydrochloric acid. Titrations were carried out with 50 mM sodium hydroxide solution until the endpoint of pH 11 was reached. To distinguish polymer and solvent effects a control titration of 50 mM sodium chloride solution without polymer was performed. Volume differences (ΔV) from pH 2 to 11 and pH 5.5 to 7.4 (endosomal pH range) were determined.

Buffer capacity was calculated according to the following formula:

$$\text{Buffer Cap [\%]} = \frac{(\Delta V(\text{pH5.5-7.4 sample}) * \Delta V(\text{pH5.5-7.4 NaCl})\,\text{ml} * 50\,\mu\text{moles/ml}}{15\,\mu\text{moles}} * 100$$

2.5.2 Polyplex formation

Polyplex formulations for transfection and binding assay experiments were prepared as follows: 200 ng of DNA or 500 ng of siRNA and the corresponding amount of polymer were diluted in separate tubes in 10 µL of 20 mM HEPES buffered 5%

glucose pH 7.4 (HBG) each. The polycation solution was added to the nucleic acid, mixed and incubated for 30-40 min at room temperature.

2.5.3 Measurement of particle size and zeta potential

Particle size and zeta potential of pDNA and siRNA formulations were measured by laser-light scattering using a Zetasizer Nano ZS (Malvern Instruments, Worcestershire, U.K.). PDNA and siRNA polyplexes were prepared in HBG pH 7.4, whereas siRNA polyplexes were diluted in 20 mM HEPES prior to measurement.

2.5.4 pDNA binding assay

A 1% agarose gel was prepared by dissolving agarose in TBE buffer (trizma base 10.8 g, boric acid 5.5 g, disodium EDTA 0.75 g, and 1 l of water) and boiling it up to 100 °C. After cooling down to about 50 °C and addition of GelRed, the agarose gel was casted in the electrophoresis unit. Polyplexes containing 200 ng of pDNA in 20 µL HBG and loading buffer (prepared from 6 ml of glycerine, 1.2 ml of 0.5 M EDTA, 2.8 ml of H_2O, 0.02 g of bromophenol blue) were placed into the sample pockets. Electrophoresis was performed at 80 V for 80 min.

2.5.5 siRNA binding assay

A 2.5% agarose gel was prepared containing GelRed as described above. Polyplexes containing 500 ng of siRNA in 20 µl HBG and loading buffer (containing xylene cyanol) were placed into the sample pockets. Electrophoresis was performed at 80 V for 40 min.

2.5.6 pDNA polyplex dissociation assay

An agarose gel was prepared as for pDNA binding assay. Polyplexes were formed and incubated for further 30 min with 0.1, 0.2 and 0.4 I.U. heparin, with TCEP (0.5 M, 0.5 µl) and with 0.2 I.U. heparin and TCEP. Electrophoresis was run as described above.

2.5.7 Ethidium bromide exclusion assay

Polymer ability to bind pDNA and siRNA was evaluated by an ethidium bromide (EtBr) exclusion assay. The effect of stepwise addition of polymer solution to 10 µg pDNA or siRNA in 1 ml HBG containing 0.4 µg EtBr was measured at increasing N/P ratios using a Cary Eclipse spectrophotometer (Varian, Germany). Maximal

fluorescence intensity was set 100% for the EtBr solution containing free nucleic acid and fluorescence decrease was measured after each addition of polymer aliquot.

2.6 Cell culture

Mouse neuroblastoma cells Neuro2A and Neuro2A/EGFPLuc cells, stably expressing the CMV-EGFPLuc cassette (Clontech) encoding a fusion of enhanced green fluorescent protein and GL3 firefly luciferase under the control of the CMV promoter as described in [159], were grown in Dulbecco's modified Eagle's medium (DMEM), supplemented with 10% FCS, 4 mM stable glutamine, 100 U/mL penicillin and 100 µg/mL streptomycin.

2.6.1 Luciferase reporter gene expression

Neuro2A cells were seeded 24 h prior to pDNA delivery using 10000 cells per well in 96-well plates. In vitro transfection efficiency of the polymers was evaluated using 200 ng pEGFPLuc encoding plasmid per well. All experiments were performed in quintuplicates. Before transfection, medium was replaced with 80 µL fresh medium containing 10% FCS. Polyplexes formed at different protonable nitrogen/phosphate (N/P) ratios in 20 µL HBG were added to each well and incubated at 37 °C. At 24 h after transfection, cells were treated with 100 µL cell lysis buffer (25 mM Tris, pH 7.8, 2 mM EDTA, 2 mM DTT, 10% glycerol, 1% Triton X-100). Luciferase activity in the cell lysate was measured using a luciferase assay kit (100 µL Luciferase Assay buffer, Promega, Mannheim, Germany) and a Lumat LB9507 luminometer (Berthold, Bad Wildbad, Germany).

2.6.2 Cell viability assay (MTT assay)

Neuro2A cells were seeded into 96-well plates at a density of 1×10^4 cells/well. After 24 h, culture medium was replaced with 80 µL fresh growth medium containing 10% FCS and transfection complexes (20 µL in HBG) at different N/P ratios were added. All studies were performed in quintuplicates. 24 h post transfection, 10 µl MTT (5 mg/ml) were added to each well reaching a final concentration of 0.5 mg MTT/mL. After an incubation time of 2 h, unreacted dye and medium were removed. Optical absorbance was determined at 590 nm (reference wavelength 630 nm) using a micro plate reader (Spectrafluor Plus, Tecan Austria GmbH).

2.6.3 Luciferase gene silencing

Gene silencing experiments were performed in Neuro2A/EGFPLuc cells stably expressing the CMV-EGFPLuc cassette (Clontech) encoding a fusion of enhanced green fluorescent protein and GL3 firefly luciferase under the control of the CMV promoter as described in [159] The cells were grown as described above. For transfection either GFP-siRNA for silencing of the EGFPLuc protein, or control-siRNA as a control were used at a concentration of 0.5µg/well each. SiRNA delivery was performed in 96-well plates with 5000 cells per well in triplicates. Cells were seeded 24 h prior to transfection and then medium was replaced with 80 µL fresh growth medium containing 10% FCS. Transfection complexes for siRNA delivery (20 µL formed in HBG) at different N/P ratios were added to each well and incubated at 37 ℃. At 48 h after transfection, luciferase activity was determined as described above. The relative light units (RLU) were presented as percentage of the luciferase gene expression obtained with only buffer treated control cells.

3 RESULTS

3.1 Four- and five-arm oligo(ethanamino)amides for pDNA and siRNA delivery

3.1.1 Introduction

Linear PEI with an average molecular weight of 22kDa is often termed the `gold standard` for gene delivery. It has outstanding properties concerning pDNA binding and transfection [76] not only due to its chemical structure containing the `proton sponge` 1,2-diaminoethane motif [77], but also due to its high molecular weight. Nevertheless, its polydispersity hampers precise conclusions on structure-activity relationships.

In order to overcome this drawback, SPPS was used as synthetic tool for the generation of precise branched oligomers. Lysine, due to two primary amines per amino acid in α- and ε- positon, offers the possibility for assembly of branched structures (**Scheme 1**). By subsequent coupling of two lysines, four arms can be elongated in a parallel manner with the corresponding building blocks or amino acids. Thus, increase in molecular weight in only few synthetic steps is facilitated.

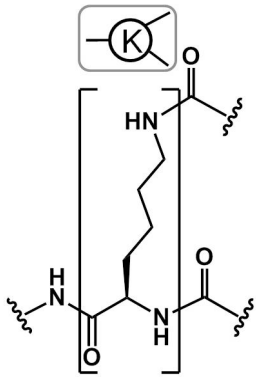

Scheme 1. Lysine as branching point

For the generation of four- and five-arm oligomers, different artificial amino acids containing the 1,2-diamioethane motif were used (**Fig. 6 A**). The cationic building block Fmoc-Stp(boc)$_3$-OH with three protonable amino groups was first developed and synthesized by Dr. David Schaffert in the Wagner lab [154]. Dr. Naresh Badgujar (Wagner lab) similarly developed and synthesized two further building blocks which were used in this thesis, namely the shorter Fmoc-Gtt(boc)$_2$-OH with two [154] and the new, longer building block Fmoc-Sph(boc)$_4$-OH with four protonable amino groups (**Fig. 6 A**). All building blocks consist of an oligoamine unit with protonable secondary amines, a terminal primary amine and a carboxylic handle for coupling.

The building block unit was abbreviated with three letters as follows:

Carboxylic handle	Oligoamine unit	Abbreviation
Glutaroyl-	**t**riethylen**t**etraamine	**Gtt**
Succinoyl-	**t**etraethylen**p**entamine	**Stp**
Succinoyl-	**p**entaethylen**h**examine	**Sph**

All reactive sites were protected with adequate groups (**Fig. 6 A, C**) in order to avoid undesired side reactions. Boc is acid-labile, whereas Fmoc can be cleaved under basic conditions, setting free the primary amine for subsequent coupling on solid phase.

The natural amino acids used in SPPS in this thesis (**Fig. 6 B**) bear also adequate side chain protection groups. Trt for thiol protection within the amino acid cysteine is, similar to boc, cleavable under acidic conditions (**Fig. 6 B, C**).

A

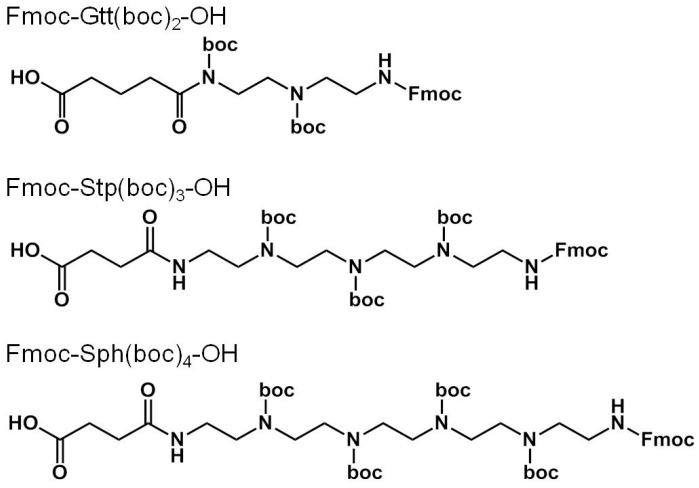

B

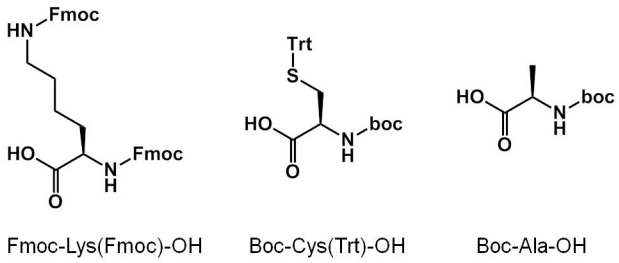

C

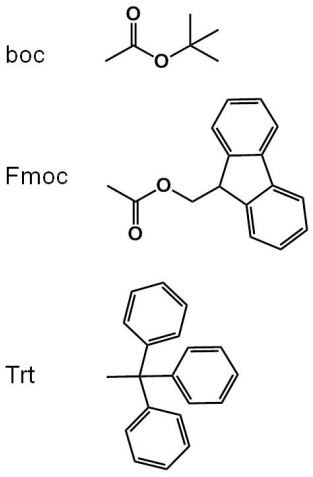

Fig. 6. **(A)** Protected building blocks Gtt, Stp and Sph. The protection groups boc and Fmoc can be cleaved in an orthogonal manner, i.e. boc is stable under basic conditions and Fmoc is stable under acidic conditions. Fmoc is cleaved during synthesis for chain elongation; boc and Trt are cleaved simultaneously with the finished sequence from the solid support under acid treatment. **(B)** Structures of the used protected natural amino acids. **(C)** Structures of the used protection groups.

After completion of the desired sequence, the generated oligomer was cleaved off the solid support by acid treatment. Simultaneously, also the acid-labile protection groups were cleaved and the desired product was collected by filtration.

In contrast to the convention of writing peptide sequences from N → C terminus, the sequences of the described oligomers in this thesis are shown from C → N terminus.

Amino acids were abbreviated according to the one-letter code:

Amino acid	One-letter-code
Alanine	**A**
Cysteine	**C**
Lysine	**K**

3.1.2 General synthesis and library design

Monomers were assembled using standard amide bond formation between terminal amino groups and activated carboxylic groups of the next building block. Alanine-loaded resin was modified with *bis*-Fmoc-lysine. Repetition of this step generated four amino groups which were elongated into four arms with the building blocks (BB) Stp, Gtt, or Sph, and in the last step with cysteine or alanine (C/A) (**Scheme 2**). For the generation of five-arm oligomers, a building block tail was introduced before lysine branching.

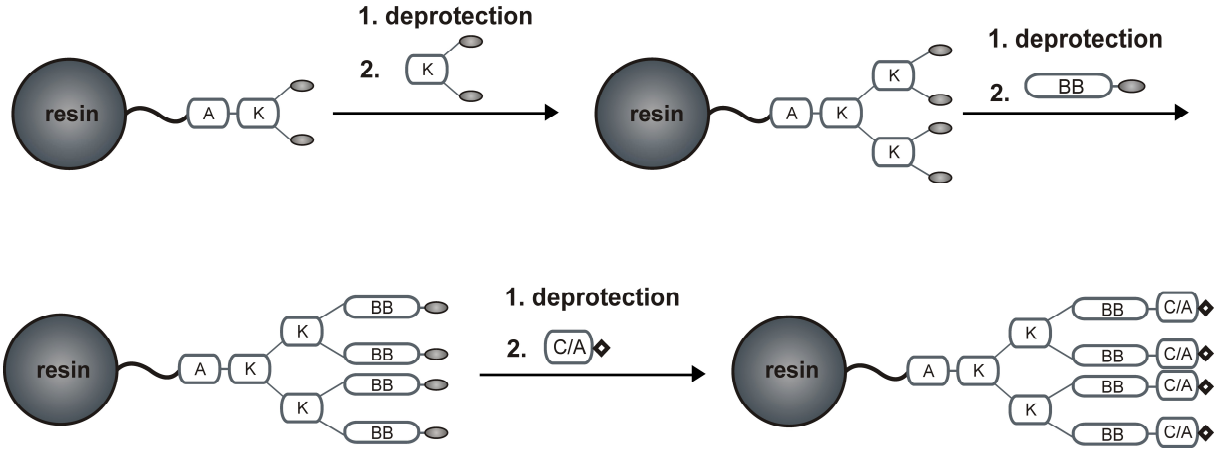

Scheme 2. Schematic representation of four-arm generation and oligomer synthesis.
An alanine preloaded resin was modified with *bis*-Fmoc-lysine, thus generating four arms. Subsequently, cationic building blocks were reacted and, depending on the sequence, terminal cysteines or alanines.

After cleavage from the solid support, the oligomers provide a carboxylic end (C-terminus) and four N-terminal primary amines (**Fig. 7**). By these means, a small library of various four- and five-arm oligomers was generated (**Fig. 7**, left panel), first using Stp with three protonable amines as building block. Different chain lengths and thus increasing molecular weight were tested for Stp oligomers, starting with one up to five building blocks per arm. Subsequently, terminal cysteines were introduced for polyplex stabilization by intramolecular disulfide formation. Furthermore, as Stp was not the only available building block suitable for solid-phase synthesis, for the most efficient oligomers Stp was replaced with two further building blocks: on the one hand the shorter Gtt with only two, on the other hand the longer Sph with four protonable amines (**Fig. 7**, right panel). By this variation, conclusions could be drawn on the impact of the length of the diaminoethane unit on cargo binding and delivery.

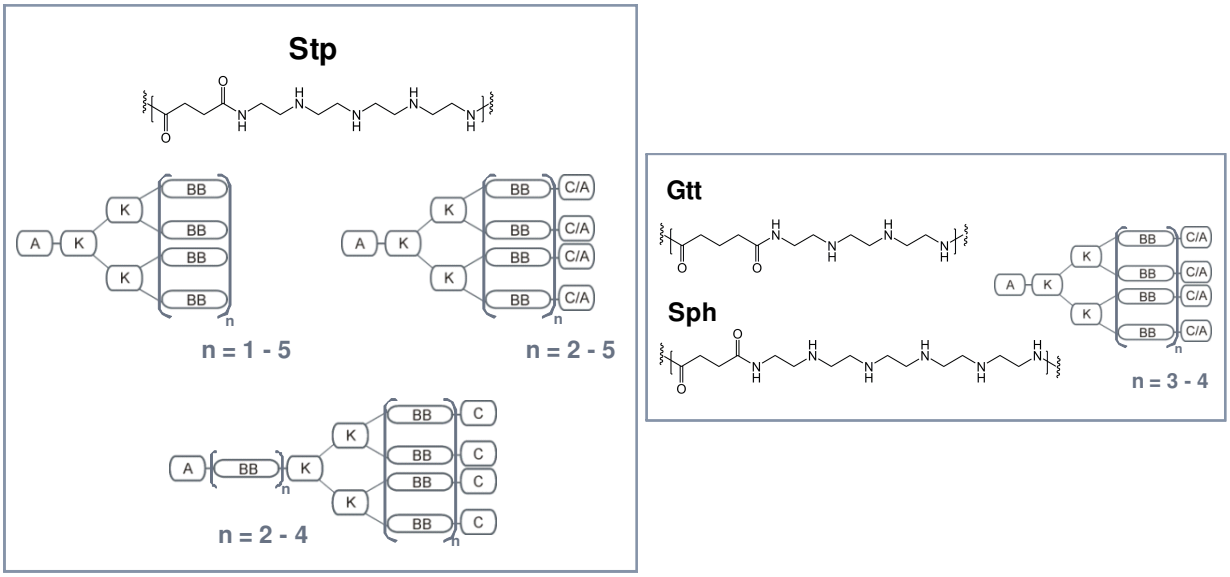

Fig. 7. Library design of four- and five-arm oligomers containing different building blocks and terminal cysteine or alanine modification.

All oligomers were purified by either by dialysis (unmodified Stp oligomers) or SEC in order to remove residual scavengers or small molecular weight impurities. **Fig. 8** shows exemplary analytical IEX (unmodified Stp oligomers) and RP-HPLC traces of selected compounds. No significant impurities could be observed. Further analytical IEX traces of unmodified Stp compounds are shown in Appendix **7.3**.

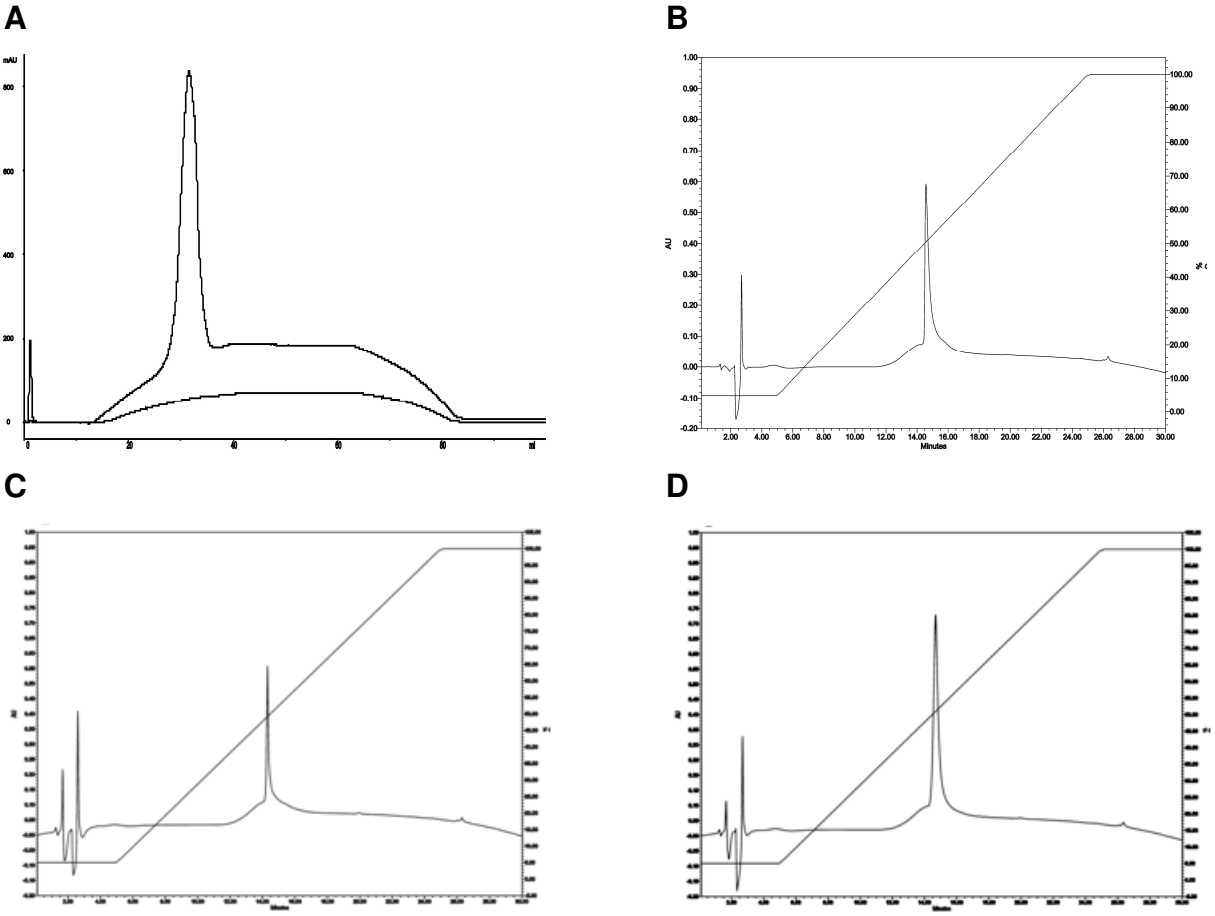

Fig. 8. (A) Analytical IEX trace of four-arm Stp oligomer 403 with 5 Stp/arm and analytical RP-HPLC traces of **(B)** 533, Stp5-A **(C)** 527, Gtt4-A **(D)** 535, Sph4-A.

3.1.3 Four-arm Stp oligomers for pDNA delivery

First, the cationic building block Stp was used for the generation of four-arm gene carriers with increasing arm length up to five Stp/arm.

Measurements on particle size and surface charge of pDNA polyplexes (**Fig. 9 A**) show that with increasing N/P ratio (i.e. molar ratio of protonable nitrogens to phosphates) the particle size decreases due to higher charge density, whereas oligomers with 5 Stp/arm complex pDNA to the smallest particle size. Oligomers with only 1 Stp/arm are not able neither to form measurable particles, nor to compact pDNA efficiently so as to result in positive surface charge. Starting with 2 Stp/arm, all particles display a positive zeta potential.

The binding efficiency of unmodified Stp oligomers to pDNA was evaluated by agarose gel electrophoresis (**Fig. 9 B**). This assay displays the effect of increasing amount of building block/arm. The longer the sequence, the stronger also the binding

of the cargo, whereas oligomers with 1 Stp/arm did not bind pDNA at all and starting with three Stp/arm pDNA is fully bound at all N/P ratios.

A

Oligomer	N/P	Mean Size [nm]	Mean PDI	Mean Zeta Potential [mV]
286 Stp1	3	762 ± 33	0.32 ± 0.04	-7.1 ± 0.4
	12	n.d.	-	0.6 ± 0.2
	24	n.d.	-	2.7 ± 0.2
287 Stp2	3	n.d.	-	5.3 ± 0.7
	12	515 ± 51	0.28 ± 0.01	13.6 ± 0.1
	24	337 ± 52	0.17 ± 0.02	16.0 ± 0.4
288 Stp3	3	605 ± 34	0.35 ± 0.05	10.6 ± 0.2
	12	188 ± 4	0.07 ± 0.02	19.1 ± 0.4
	24	160 ± 1	0.09 ± 0.02	17.7 ± 0.3
289 Stp4	3	296 ± 3	0.13 ± 0.03	14.1 ± 0.6
	12	143 ± 2	0.12 ± 0.03	17.9 ± 0.8
	24	123 ± 10	0.13 ± 0.02	23.2 ± 0.6
403 Stp5	3	232 ± 2	0.04 ± 0.01	16.4 ± 0.4
	12	102 ± 1	0.11 ± 0.02	25.0 ± 0.6
	24	90 ± 2	0.14 ± 0.02	20.6 ± 0.3

n.d.: not detectable

B

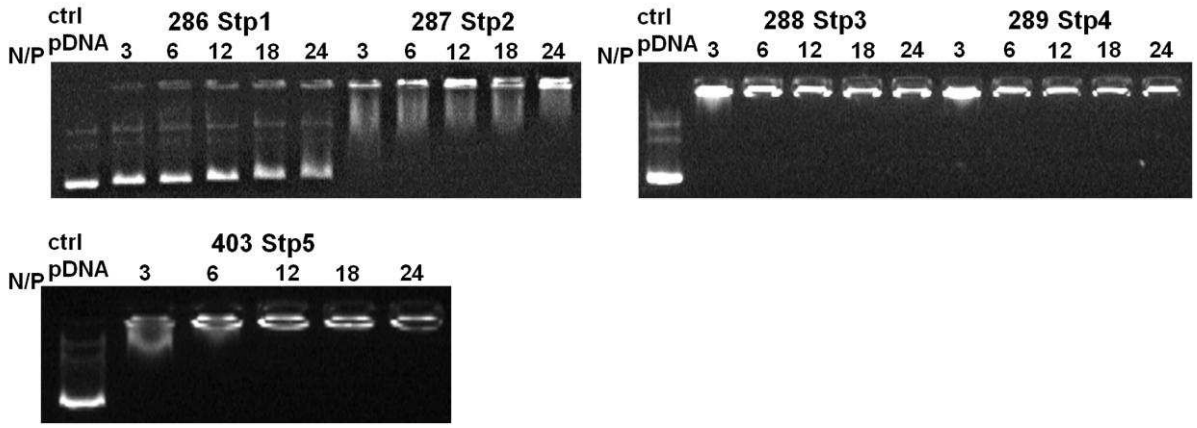

Fig. 9. (A) Particle size and zeta potential of Stp oligomers/pDNA polyplexes at increasing N/P ratios. **(B)** pDNA binding assay of Stp oligomers at different N/P ratios.

Four-arm Stp oligomers were tested *in vitro* on Neuro2A cells on their efficiency as gene carriers by Thomas Fröhlich (Wagner lab). **Fig. 10, upper panel,** shows the results of the luciferase reporter gene assay. Oligomers with one or two building blocks/arm did not have any effect, whereas starting with three Stp/arm gene delivery efficiency increases. Nevertheless, a maximum in efficiency is achieved with compound **289** containing four Stp/arm; a longer chain does not show any further benefit. Furthermore, even the best compounds showed only a moderate transfection

efficiency compared to `gold standard` linPEI. No negative effects on cell metabolic activity could be observed in the MTT assay, though (**Fig. 10, lower panel**).

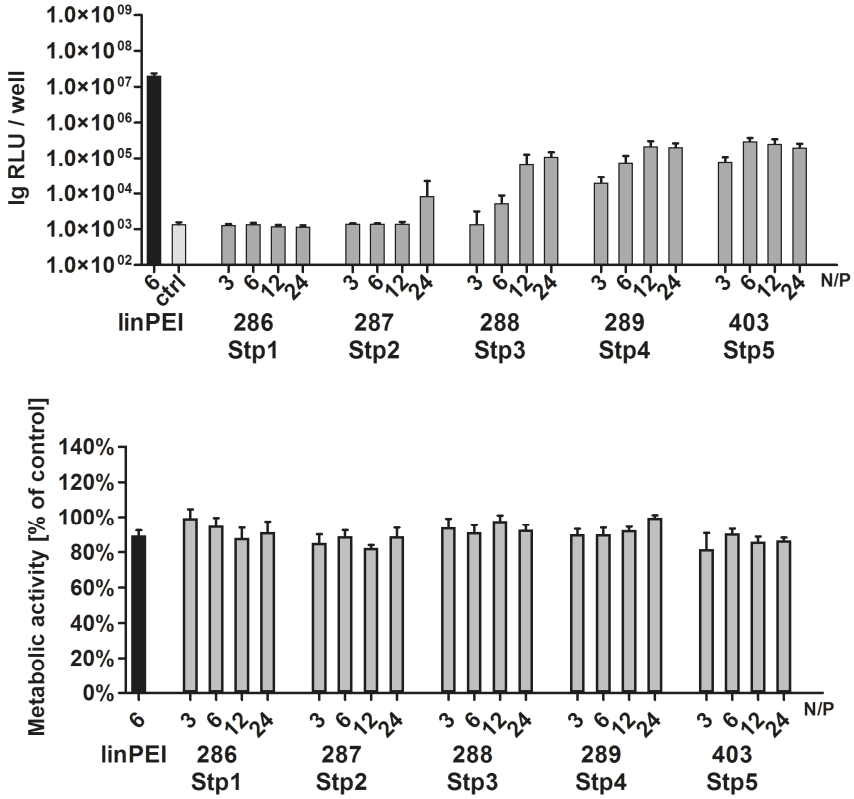

Fig. 10. Luciferase reporter gene assay of four-arm Stp oligomers at increasing N/P ratios and corresponding cell viability data below (experiment performed by Thomas Fröhlich, Wagner lab).

Therefore, as these oligomers left room for optimization in terms of gene delivery, cysteines were introduced as activity enhancing amino acids.

3.1.4 Effect of introduction of cysteines

As cysteines are known to be able to stabilize polyplexes by cross-linking due to disulfide bond formation, these amino acids were introduced at the N-terminus of Stp oligomers with 2 -5 building blocks/arm and evaluated biophysically and biologically. Alanines were used as control amino acid in order to exclude possible effects due to arm elongation.

The strength of the electrostatic interaction between cationic Stp oligomers and negatively charged pDNA was investigated by agarose gel electrophoresis (**Fig. 11 A**). At first, oligomers were pre-incubated with pDNA at room temperature in air-saturated buffer to allow (in the case of cysteine-containing oligomers) oxidative disulfide formation after initial complex formation as described [155]. All Stp

oligomers showed good pDNA binding abilities, independent of cysteine modification. Transfections (performed by Petra Kos, Wagner lab) demonstrated that the presence of terminal cysteines has a very positive impact on luciferase gene transfer (similar efficiency as linPEI), whereas chain length is a less important feature (**Fig. 11 B**, upper panels). Optimal efficiency is reached with cysteine modified four-arm Stp oligomers **392** and **402** with three and four Stp units per arm, respectively. **421** with five Stp per arm shows no further improvement. The alanine-ended mutants are by far not as effective as the cysteine oligomers. pDNA polyplexes were well tolerated by cells even at high N/P ratios (**Fig. 11 B**, lower panels).

As the standard binding assay did not disclose differences in pDNA binding affinity, a polyplex dissociation assay was carried out (**Fig. 11 C**). Oligomers were incubated with pDNA under oxidative conditions and then treated with different concentrations of heparin to challenge electrostatic interactions between cationic carrier and negatively charged cargo. In parallel, polyplexes were also treated with TCEP for cleavage of formed disulfide bonds, and with both TCEP and heparin at a medium dose. Agarose gel electrophoresis (**Fig. 11 C**) after treatment with heparin at increasing concentrations showed that polyplexes formed with cysteine-modified oligomers are more stable than the alanine mutants. Low dose heparin dissociates all alanine but none of the cysteine containing structures. At medium heparin dose, cysteine containing polyplexes with four Stp units per arm are more stable than those with three Stp units. The effect of combined heparin/TCEP treatment can be seen best for polyplex formed with oligomer **402**. It is stable under single treatment with each heparin or TCEP, but the cargo is released when both reagents are present.

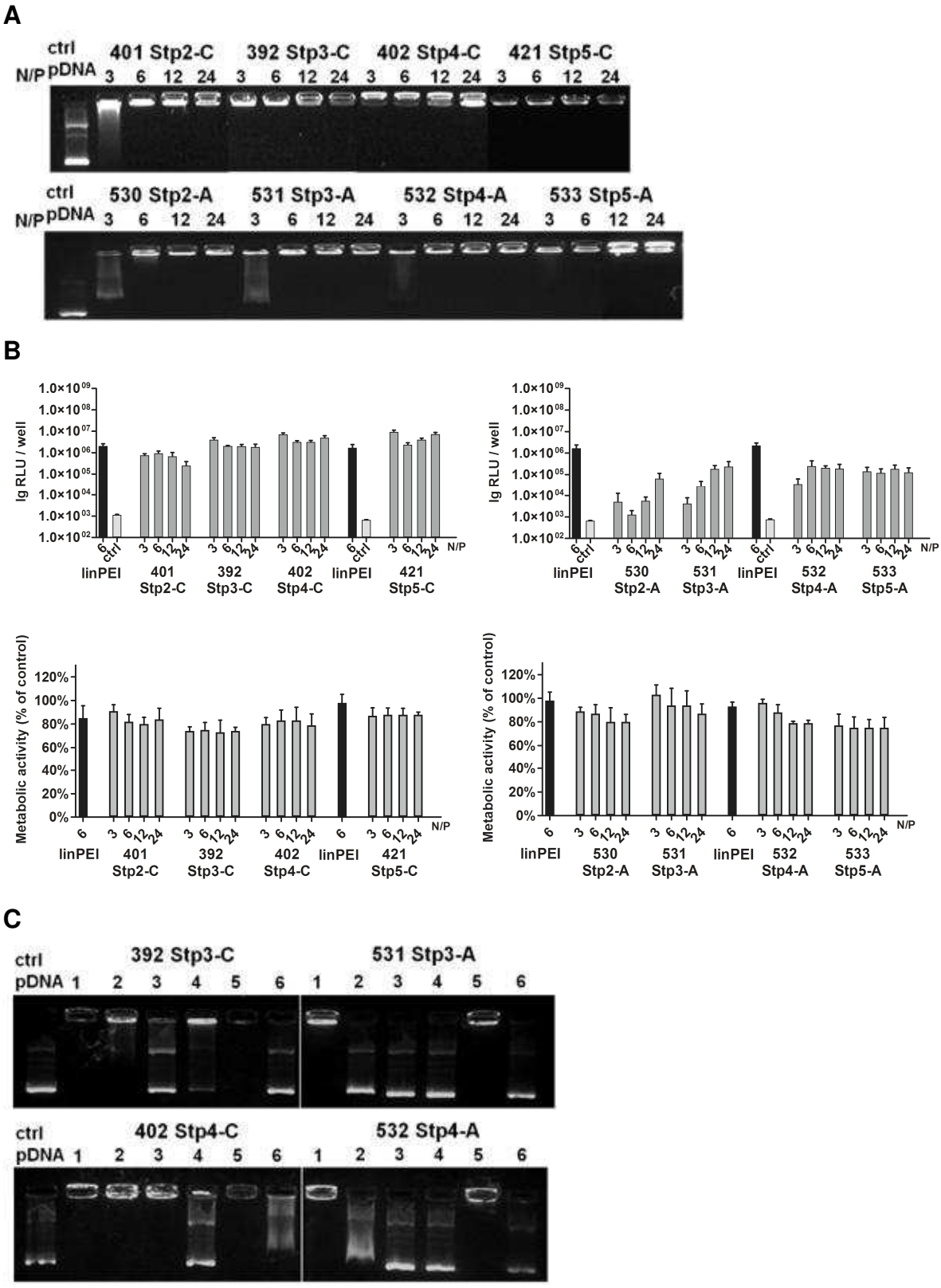

Fig. 11. (A) pDNA binding assay of cysteine- and alanine-modified four-arm Stp oligomers. **(B)** Luciferase gene transfer (Neuro2A cells) and corresponding metabolic cell activities below (experiment performed by Petra Kos, Wagner lab). **(C)** pDNA polyplex dissociation assay of four-arm Stp oligomers. Polyplexes were formed at N/P 12 and treated as follows: lane 1: polyplex, 2: polyplex + 0.1 I.U. heparin, 3: polyplex + 0.2 I.U. heparin, 4: polyplex + 0.4 I.U. heparin, 5: polyplex + TCEP, 6: polyplex + TCEP + 0.2 I.U. heparin.

3.1.5 Effect of Stp replacement by shorter building block Gtt

Next, the shorter triethylene tetramine-based building block Gtt was used for assembly of analogs of the most efficient Stp oligomers with three and four building blocks/arm. Only the cysteine-modified Gtt oligomers formed oligomer/pDNA complexes stable in the electrophoretic binding assay (**Fig. 12 A**, left panel); the alanine mutants did not bind pDNA effectively, as shown by the laddering in **Fig. 12 A**, right panel. This is the result of either not completely bound pDNA or polyplex instability during electrophoresis. Consistently, only Gtt3-C (**492**) and Gtt4-C (**494**) mediated luciferase gene transfer (**Fig. 12 B**), whereas the alanine-modified Gtt four-arms displayed even lower activity than the alanine-modified Stp four-arms (experiment performed by Petra Kos, Wagner lab).

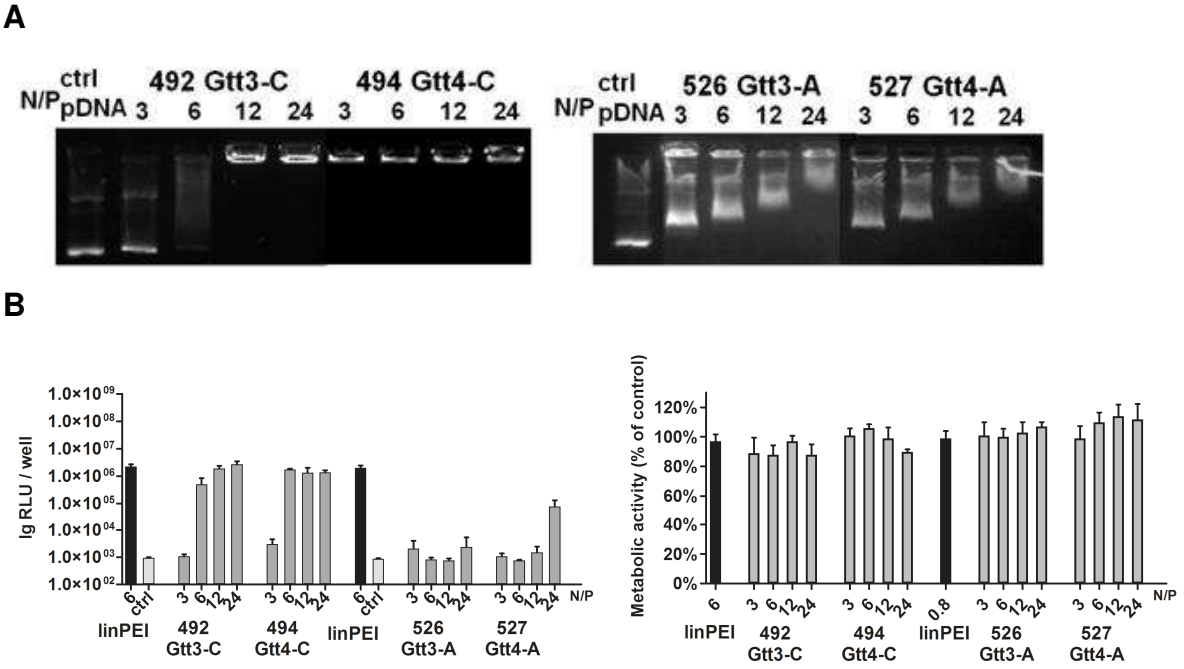

Fig. 12. (A) pDNA binding assay of cysteine- and alanine modified Gtt oligomers. **(B)** Luciferase assay and corresponding cell metabolic activities (experiment performed by Petra Kos, Wagner lab).

3.1.6 Effect of Stp replacement by longer building block Sph

The new building block Sph (with one additional amino ethane unit) was applied in assembly of oligomers with three and four building blocks per arm and N-terminal cysteines or alanines. Sph oligomers did bind their cargo very efficiently independent of end-modification (**Fig. 13 A**). A polyplex dissociation assay (**Fig. 13 B**) confirms the stabilizing effect of the cysteines.

A

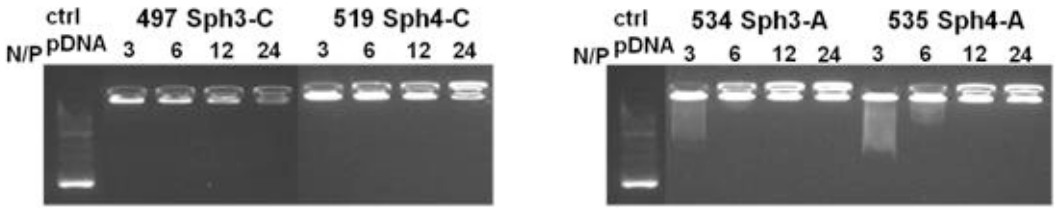

B

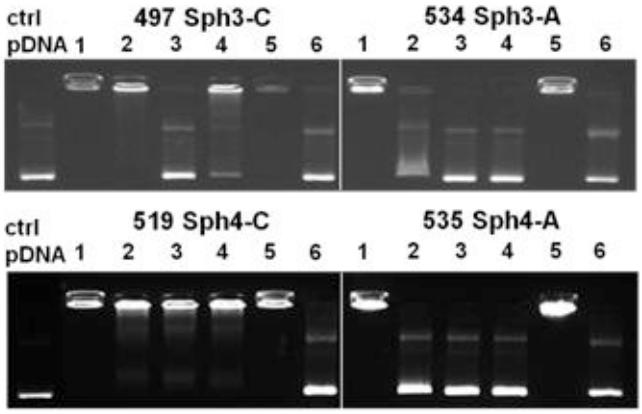

Fig. 13. (A) pDNA binding assay of cysteine-/alanine-Sph oligomers. **(B)** Dissociation assay of polyplexes (N/P 12) treated as follows: lane 1: polyplex, 2: polyplex + 0.1 I.U. heparin, 3: polyplex + 0.2 I.U. heparin, 4: polyplex + 0.4 I.U. heparin, 5: polyplex + TCEP, 6: polyplex + TCEP + 0.2 I.U. heparin.

Biological evaluation of polyplexes displayed the superiority of the Sph building block in terms of luciferase reporter gene transfer and no notable cytotoxicity even at high N/P ratios (**Fig. 14 A**, experiment performed by Petra Kos, Wagner lab). The alanine-ended oligomers showed equal transfection efficiency as linPEI, the cysteine modified compounds were even up to 60-fold more efficient than linPEI.

The cysteine-ended four-arms Gtt4-C, Stp4-C and Sph4-C were compared in their pDNA compaction ability in an ethidium bromide exclusion assay (**Fig. 14 B**). When a polycation binds and compacts pDNA, the intercalator fluorescence is significantly reduced. LinPEI was used as a control with high compaction activity. This assay shows that Sph oligomers were the most potent in terms of pDNA compaction ability, whereas Gtt oligomers do not compact pDNA efficiently.

A

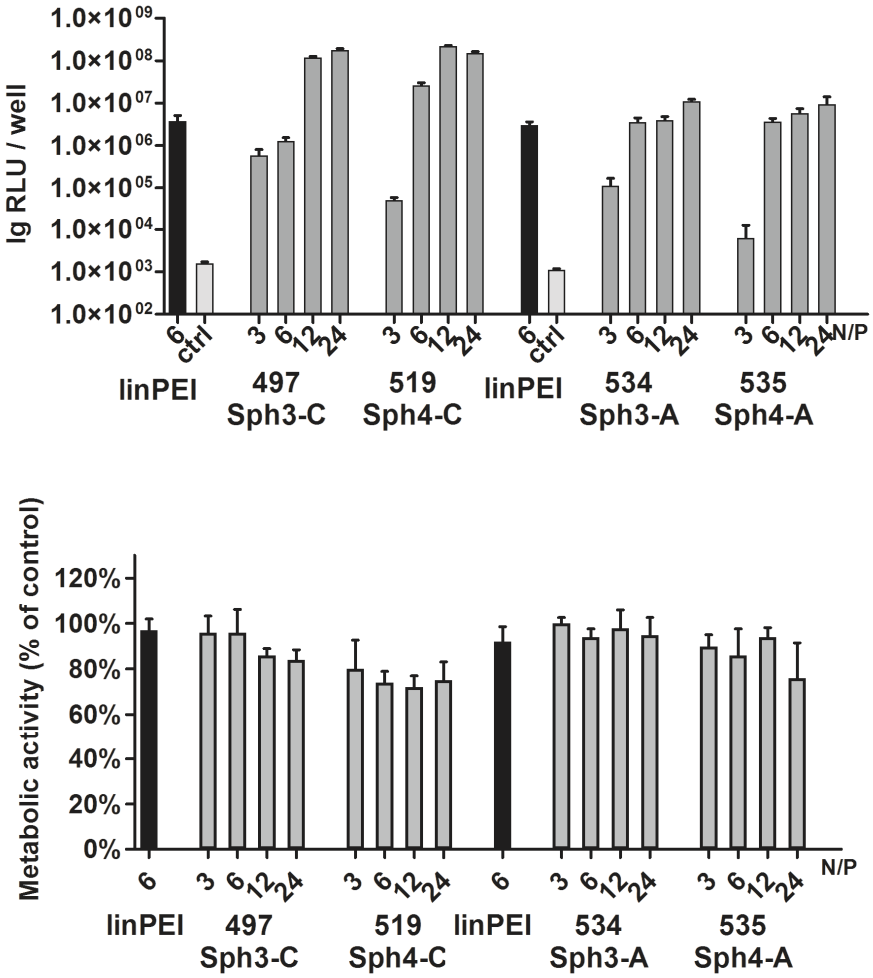

B

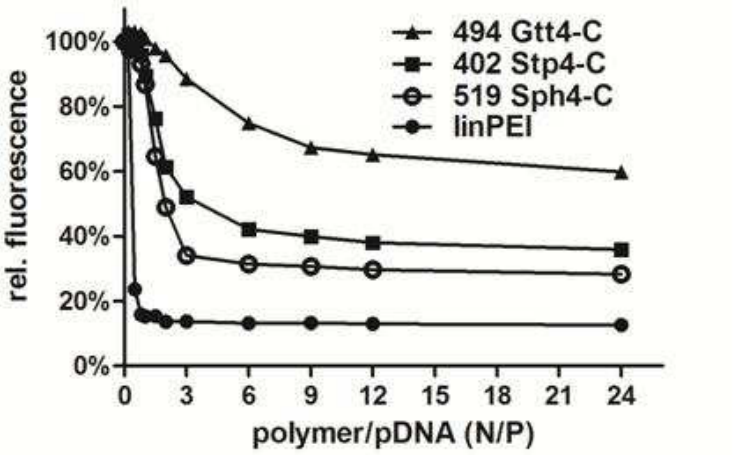

Fig. 14. (A) Luciferase gene transfer and corresponding metabolic cell activities (experiment performed by P. Kos). **(B)** Ethidium bromide exclusion assay of cysteine-modified oligomers of different building blocks (4 units per arm).

Particle sizes and zeta potential of four-arm polyplexes are listed in **Table 1**. Zeta potential obtained with cysteine-modified four-arms Gtt4-C, Stp4-C and Sph4-C (all with 4 units per arm) were around +25 mV. Particles sizes of 496 nm, 367 nm and 258 nm, respectively, however clearly differed and indicated a correlation of pDNA compaction with aminoethane numbers in the building block.

Oligomer Id	Sequence	Mean Size [nm]	Mean PdI	Mean Zeta Potential [mV]
401	A-K-(K-(Stp_2-C)$_2$)$_2$	1062.7 ± 136.9	0.396 ± 0.06	22.6 ± 1.2
392	A-K-(K-(Stp_3-C)$_2$)$_2$	344.8 ± 88.6	0.267 ± 0.01	24.8 ± 1.3
402	A-K-(K-(Stp_4-C)$_2$)$_2$	367.0 ± 13.0	0.273 ± 0.01	25.2 ± 0.3
421	A-K-(K-(Stp_5-C)$_2$)$_2$	351,6 ± 13.9	0.271 ± 0.02	27.9 ± 1.3
530	A-K-(K-(Stp_2-A)$_2$)$_2$	423.1 ± 102.1	0.371 ± 0.02	14.2 ± 0.4
531	A-K-(K-(Stp_3-A)$_2$)$_2$	410.0 ± 53.6	0.319 ± 0.03	12.1 ± 1.4
532	A-K-(K-(Stp_4-A)$_2$)$_2$	381.6 ± 81.9	0.372 ± 0.04	26.8 ± 0.6
533	A-K-(K-(Stp_5-A)$_2$)$_2$	263.0 ± 31.2	0.280 ± 0.01	25.4 ± 0.6
492	A-K-(K-(Gtt_3-C)$_2$)$_2$	n.d.	-	25.0 ± 0.0
494	A-K-(K-(Gtt_4-C)$_2$)$_2$	496.0 ± 109.8	0.316 ± 0.03	24.9 ± 0.0
526	A-K-(K-(Gtt_3-A)$_2$)$_2$	n.d.	-	10.8 ± 0.6
527	A-K-(K-(Gtt_4-A)$_2$)$_2$	445.3 ± 33.5	0.340 ± 0.02	16.2 ± 0.7
497	A-K-(K-(Sph_3-C)$_2$)$_2$	370.3 ± 65.4	0.310 ± 0.04	28.3 ± 1.0
519	A-K-(K-(Sph_4-C)$_2$)$_2$	258.1 ± 35.1	0.314 ± 0.03	23.2 ± 0.6
534	A-K-(K-(Sph_3-A)$_2$)$_2$	284.4 ± 43.9	0.302 ± 0.02	28.3 ± 1.8
535	A-K-(K-(Sph_4-A)$_2$)$_2$	338.0 ± 54.8	0.275 ± 0.01	19.4 ± 1.8

Table 1. Particle size and zeta potential of four-arm oligomers after complexation with pDNA at N/P 12.

3.1.7 Four-arm cysteine containing Stp, Gtt and Sph oligomers for siRNA delivery

The synthesized oligomers were also tested in siRNA-mediated gene silencing. The binding of oligomers to siRNA evaluated by gel electrophoresis (**Fig. 15 A**) shows that cysteine-ended Stp and Sph oligomers have the strongest interaction with siRNA. Gtt analogs hardly bind siRNA, except oligomer **494** at high N/P.

The ethidium bromide exclusion assay (**Fig.15 B**) shows that Stp and Sph oligomers have equal siRNA compaction ability, much more efficiently than Gtt oligomers. LinPEI, although it compacts siRNA, shows only weak gene silencing efficiency [160].

A

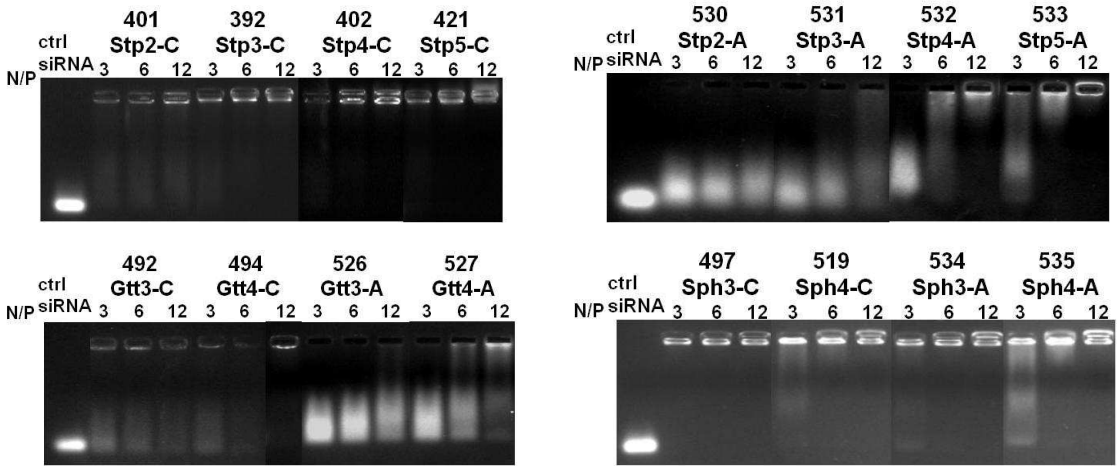

B

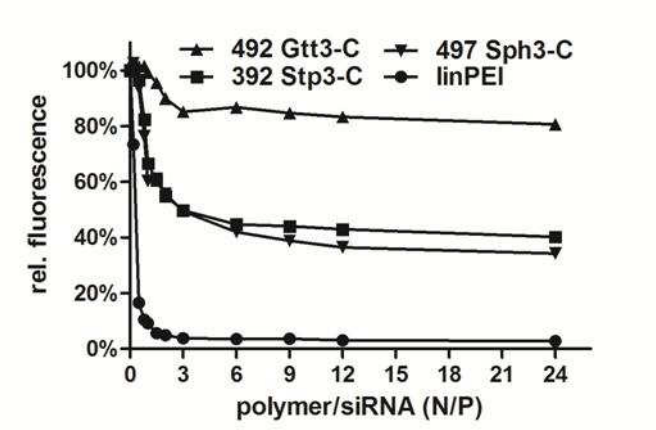

Fig. 15. (A) siRNA binding assay of oligomers containing different building blocks. **(B)** Ethidium bromide exclusion assay.

Gene silencing experiments **(Fig. 16**; experiments performed by Thomas Fröhlich and Petra Kos, Wagner lab) demonstrate that only cysteine-ended oligomers based on Stp or Sph (but not Gtt) were bioactive. Alanine-ended four-arms did not mediate any gene silencing effect. In contrast to pDNA delivery, Sph oligomers were not beneficial compared with Stp based oligomers.

A

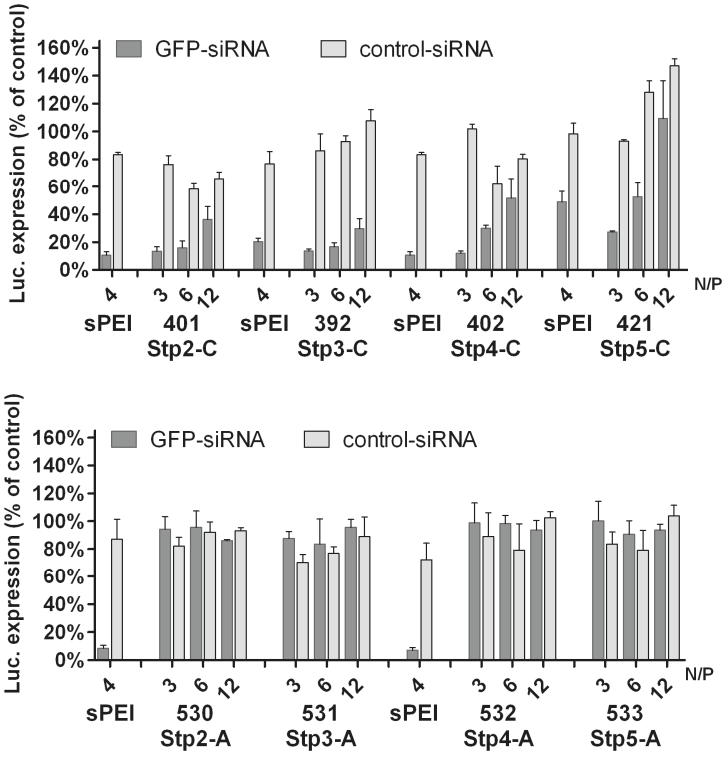

B

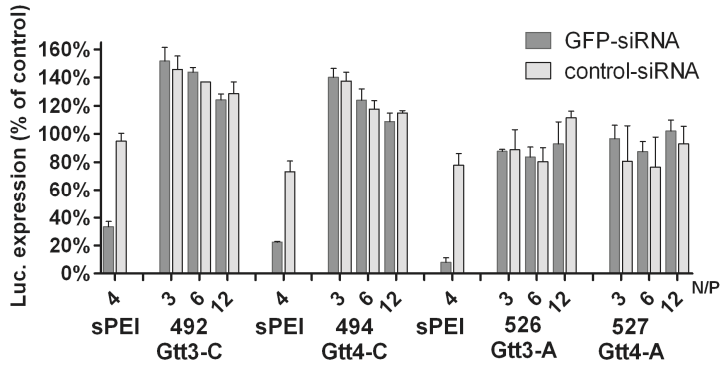

C

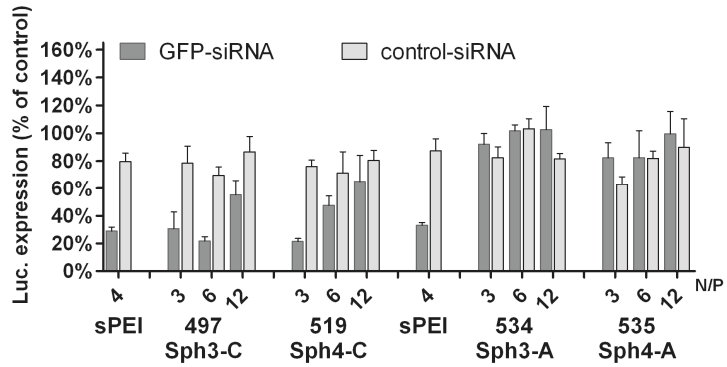

Fig. 16. Luciferase reporter gene silencing with (A) Stp- **(B)** Gtt- and **(C)** Sph-based oligomers (experiments performed by Thomas Fröhlich and Petra Kos, Wagner lab).

3.1.8 Five-arm Stp oligomers for pDNA and siRNA delivery

As it is known that polymer size is important especially for pDNA delivery, longer Stp oligomers than plain four-branch were synthesized on solid phase by introduction of a Stp tail before branching and terminal cysteines. These oligomers were also evaluated for their properties to bind and deliver pDNA and siRNA.

Fig. 17 A shows the results obtained for pDNA binding in the gel shift assay. It is obvious that all compounds can efficiently bind pDNA, as also shown in the ethidium bromide exclusion assay, where **425** has the same cargo compaction ability as the four-arm counterpart **402** (**Fig. 17 B**). Nevertheless, in the luciferase reporter gene assay the five-arm oligomers did not show any superiority compared to four-arm oligomers (**Fig. 17 C**, experiment performed by Thomas Fröhlich). As the synthesis is more time consuming, improvement of this class of oligomers was not further pursued.

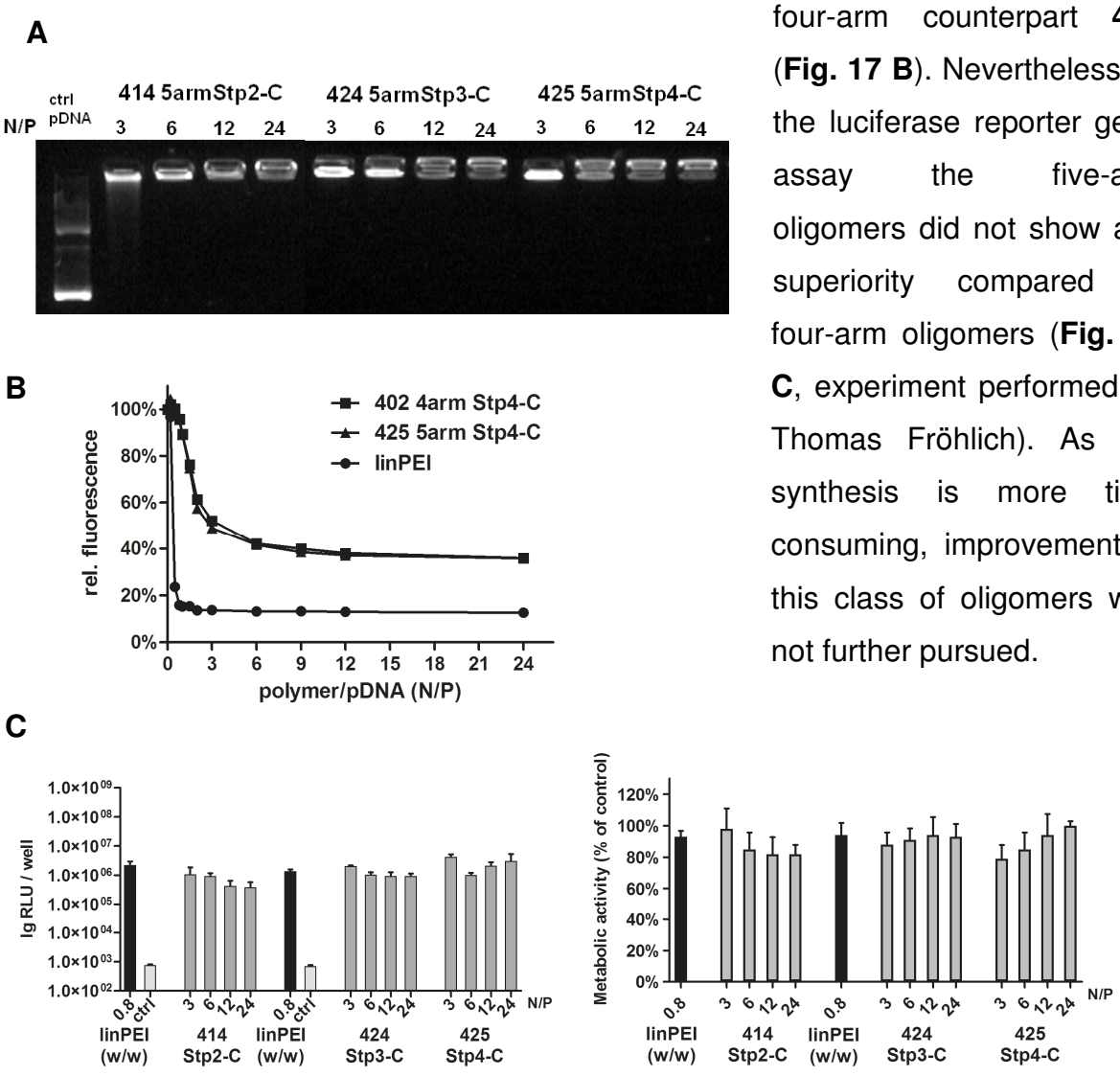

Fig. 17. (A) pDNA binding assay. **(B)** Ethidium bromide exclusion assay **(C)** Luciferase assay of cysteine-containing five-arm Stp oligomers and corresponding cell viability data (experiment performed by Thomas Fröhlich, Wagner lab).

Nevertheless, the five-arm oligomers were also tested for their efficiency to bind and deliver siRNA. The siRNA binding assay shows that only the biggest compound **425** can efficiently bind siRNA (**Fig. 18 A**). Although comparable in compaction efficiency to the four-arm counterpart (**Fig. 18 B**), efficient gene silencing could only be achieved with **414** (**Fig. 18 C**, experiment performed by Thomas Fröhlich, Wagner lab).

A

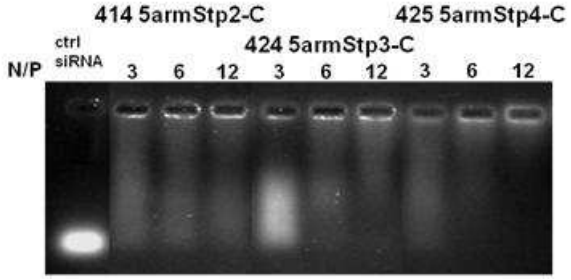

B

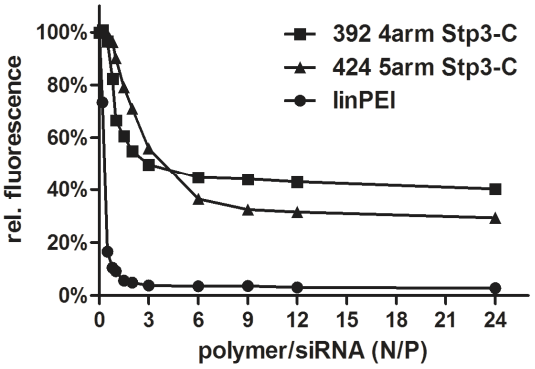

C

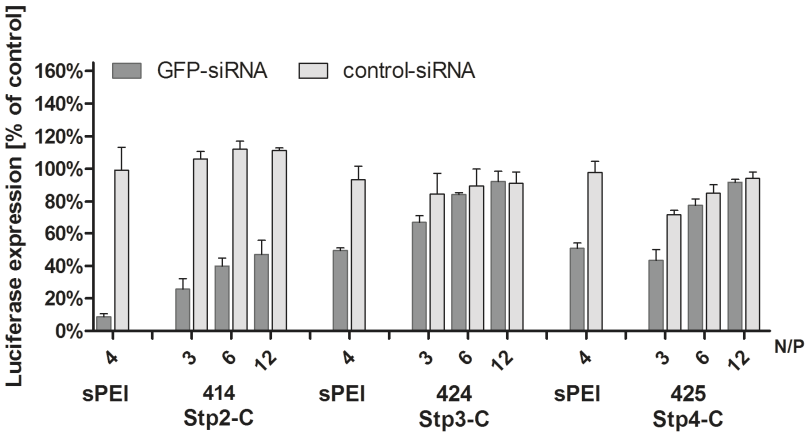

Fig. 18. (A) siRNA binding assay **(B)** Ethidium bromide exclusion assay. **(C)** Luciferase gene silencing of cysteine-modified five-arm Stp oligomers (experiment performed by Thomas Fröhlich, Wagner lab).

3.2 Histidine-containing Stp and Gtt oligomers

3.2.1 Introduction

Escaping the cellular endosome before its maturation to lysosomes is a crucial and transfection limiting step before the nucleic acid reaches its site of action. Different strategies have been exploited so as to overcome this obstacle.

One possibility is to take advantage of the proton sponge effect, as described for PEI [77]. Therefore, protonable amino groups at an acidic pH of 5-6 are required. Secondary amines within the PEI chain fulfill this demand, but also the amino acid histidine, for instance, with its imidazole side chain (**Fig. 19**). This residue serves as pH-selective proton sponge, as protonation does not occur before entering the acidic endosome.

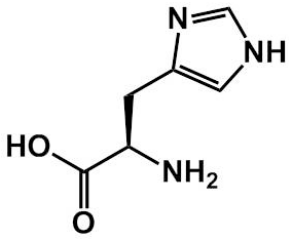

Fig. 19. Amino acid histidine

Due to this side chain feature, namely facilitation of endosomal escape and thus enhanced payload delivery, various synthetic carriers [161], such as dendrimers [162], cationic polymers [163-165] and lipids [166, 167] have been modified with histidine or imidazole.

Therefore, selected Stp and Gtt oligomers were modified with additional histidines and evaluated for the impact on biophysical polyplex properties and nucleic acid transfection. Additionally, as control compounds, four-arm lysine-histidine oligomers based on previous publications by the group around A. J. Mixson [146, 147] were synthesized and compared to Stp and Gtt containing oligomers.

3.2.2 Library design and chemical characterization

Based on results described in section 3.1, cysteine and alanine containing four-arm Stp and Gtt oligomers were further modified with histidines. First, additional histidines were introduced after each coupling of the corresponding building block (**Fig. 20 A;** ‘lowHis’, bottom left scheme). A higher amount of histidines was synthetically achieved by introduction of the amino acid before coupling the second branching

point and also, additionally, before coupling the terminal cysteine or alanine (**Fig. 20 A**; 'highHis', bottom right scheme). Alanine was applied as substitute control amino acid for cysteine and histidine, respectively. As additional control sequences, lysine-histidine oligomers based on [146] were synthesized and evaluated (**Fig. 20 B**).

A

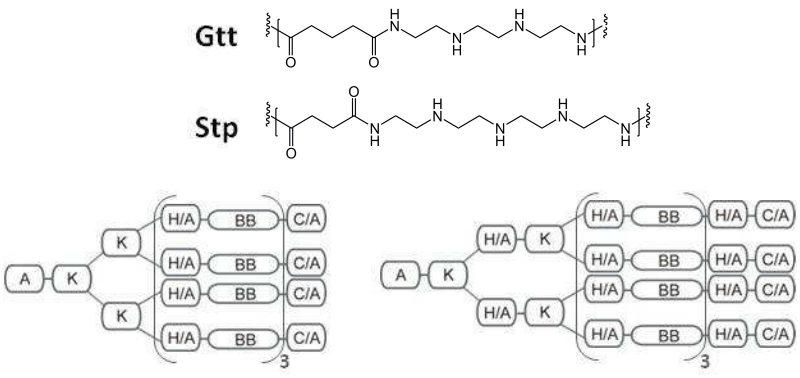

B

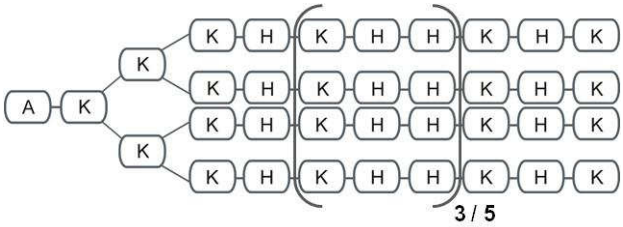

Fig. 20. (A) Histidine containing four-arm Stp and Gtt oligomers. Histidines were introduced either before building block coupling (lowHis, left scheme) or before the second branching point and before and after each building block (highHis, right scheme). Oligomers were N-terminally modified with cysteines. Alanines were used as control amino acids for both histidine and cysteine. **(B)** Control sequence based on [146].

Thus, a small library of 18 histidine-containing oligomers and corresponding mutant sequences was generated. All oligomer Ids and accordant sequences with detailed specifications on molecular formula, molecular weight and amount of protonable amines are listed below.

Oligomer Id	Sequence	Molecular Formula	Molecular weight [g/mol]	Protonable amines
487	A-K-(K-((H-Stp)$_3$-C)$_2$)$_2$	$C_{250}H_{449}N_{107}O_{44}S_4$	5786.19	52
528	A-K-(K-((A-Stp)$_3$-C)$_{2)2}$	$C_{214}H_{425}N_{83}O_{44}S_4$	4993.45	40
490	A-K-(K-((H-Stp)$_3$-A)$_2$)$_2$	$C_{250}H_{473}N_{107}O_{44}$	5682.12	52
495	A-K-(K-((A-Stp)$_3$-A)$_2$)$_2$	$C_{214}H_{425}N_{83}O_{44}$	4865.19	40
521	A-K-(K-((H-Gtt)$_3$-C)$_2$)$_2$	$C_{237}H_{411}N_{95}O_{45S4}$	5439.67	40
524	A-K-(K-((A-Gtt)$_3$-C)$_2$)$_2$	$C_{201}H_{387}N_{71}O_{45}S_4$	4646.93	28
522	A-K-(K-((H-Gtt)$_3$-A)$_2$)$_2$	$C_{237}H_{411}N_{95}O_{45}$	5311.41	40
525	A-K-(K-((A-Gtt)$_3$-A)$_2$)$_2$	$C_{201}H_{387}N_{71}O_{45}$	4518.67	28
573	A-K-(H-K-((H-Stp)$_3$-H-C)$_2$)$_2$	$C_{285}H_{489}N_{125}O_{51}S_4$	6611.00	58
575	A-K-(A-K-((A-Stp)$_3$-A-C)$_2$)$_2$	$C_{231}H_{453}N_{89}O_{51}S_4$	5421.89	40
574	A-K-(H-K-((H-Stp)$_3$-H-A)$_2$)$_2$	$C_{285}H_{489}N_{125}O_{51}$	6482.74	58
576	A-K-(A-K-((A-Stp)$_3$-A-A)$_2$)$_2$	$C_{231}H_{453}N_{89}O_{51}$	5293.63	40
577	A-K-(H-K-((H-Gtt)$_3$-H-C)$_2$)$_2$	$C_{261}H_{429}N_{113}O_{51}S_4$	6094.19	46
579	A-K-(A-K-((A-Gtt)$_3$-A-C)$_2$)$_2$	$C_{207}H_{393}N_{77}O_{51}S_4$	4905.08	28
578	A-K-(H-K-((H-Gtt)$_3$-H-A)$_2$)$_2$	$C_{261}H_{429}N_{113}O_{51}$	5965.93	46
580	A-K-(A-K-((A-Gtt)$_3$-A-A)$_2$)$_2$	$C_{207}H_{393}N_{77}O_{51}$	4776.82	28
582	A-K-(K-(K-H-(K-H$_2$)$_3$-K-H-K)$_2$)$_2$	$C_{357}H_{555}N_{151}O_{61}$	7938.20	56
584	A-K-(K-(K-H-(K-H$_2$)$_5$-K-H-K)$_2$)$_2$	$C_{389}H_{597}N_{167}O_{67}$	11157.97	80

Table 2. **List of histidine-containing oligomers.** First eight sequences (shaded light gray) are lowHis oligomers, subsequent eight sequences are highHis oligomers and sequence **582** and **584** (shaded dark grey) are control compounds based on [146].

The purity of the terminal alanine-containing oligomer with the highest molecular weight out of each class (lowHis and highHis) was determined, besides ^{1}H-NMR, by RP-HPLC. No significant impurities could be observed (**Fig. 21**).

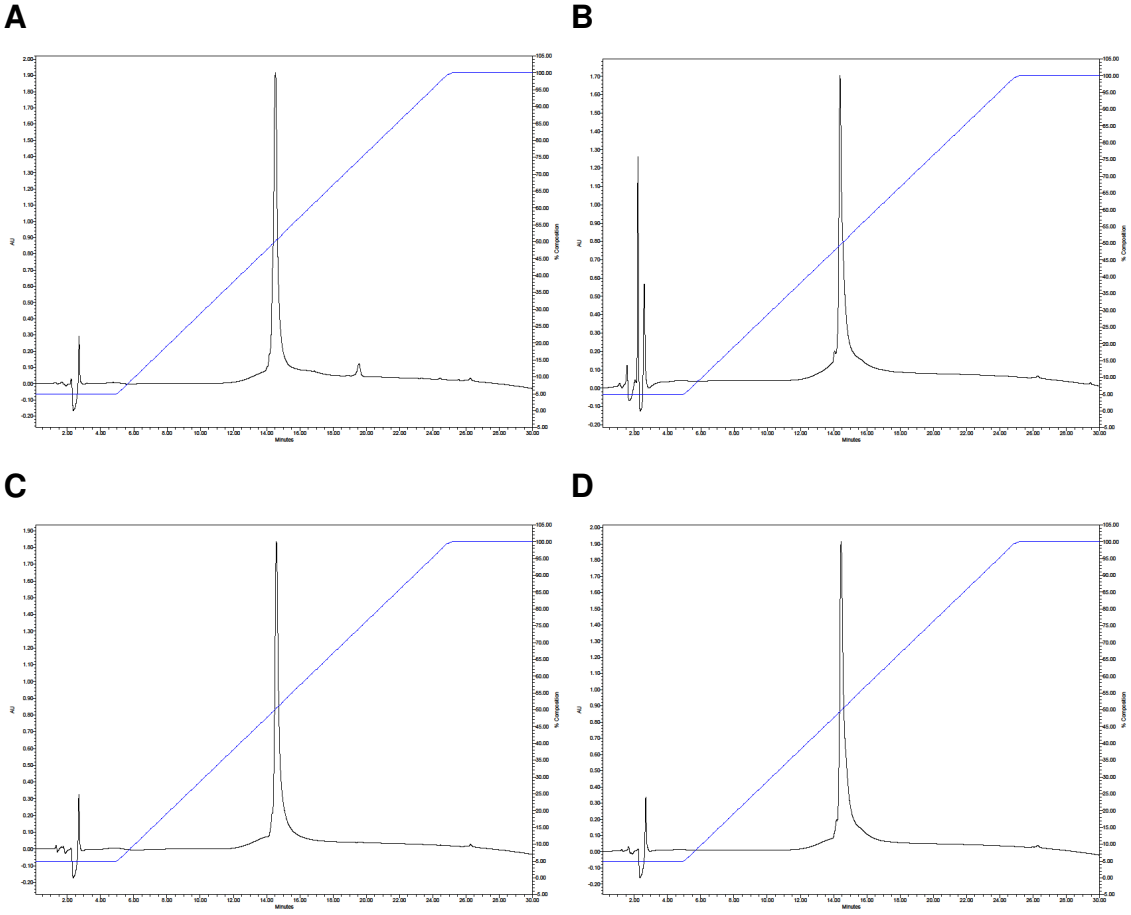

Fig. 21. Analytical RP-HPLC traces of histidine-containing oligomers. (A) (H-Stp)$_3$-A, 490 **(B)** (H-Gtt)$_3$-A, 522 **(C)** (H-Stp)$_3$-H-A, 574 **(D)** (H-Gtt)$_3$-H-A, 578.

3.2.3 Biophysical and biological characterization

The effect of histidine introduction on oligomer buffering capacity was determined via acidimetric titrations (experiment performed by Ulrich Lächelt, Wagner lab). The results show the enhanced buffering effect mediated by histidines compared to alanine-containing compounds (**Fig. 22**), also increasing with the amount of histidines within the oligomers (**Fig. 22**, left panel vs. right panel). Moreover, the building block Gtt containing two protonable amines shows a higher buffering capacity than Stp with three protonable amines per unit. The results with control oligomer **584** (KHH$_5$) are in the range of His-containing Stp compounds.

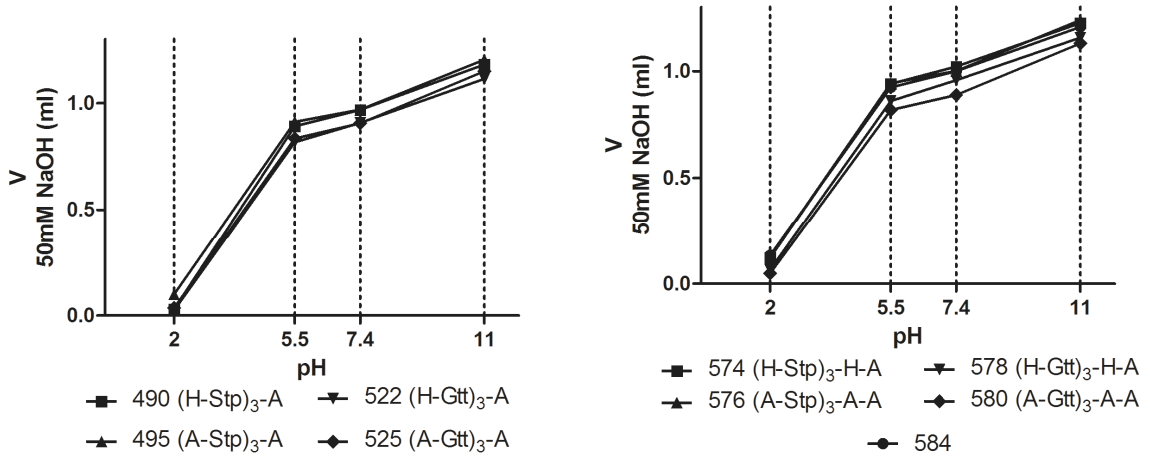

Buffer Capacity (%)

490	23,3%	**522**	27,7%
495	16,6%	**525**	21,5%

Buffer Capacity (%)

574	24,8%	**578**	30,0%
576	16,7%	**580**	21,0%
584	22,7%		

Fig. 22. Acidimetric titration of selected histidine-containing oligomers compared to alanine controls (experiment performed by Ulrich Lächelt, Wagner lab).

LowHis oligomers were tested for their pDNA binding ability by gel electrophoresis. This assay revealed that all Stp oligomers apart from compound **490** (with histidines and terminal alanine) bind their cargo efficiently. For the Gtt oligomers, in contrast, histidine containing compounds distinctly exceed the alanine controls (with or without terminal cysteines) in their binding capacity (**Fig. 23 A**).

The luciferase assay displays the difference in the impact of histidines on Stp and Gtt oligomers (**Fig. 23 B,** upper panels). Concerning Stp oligomers, histidines were beneficial in case of cysteine-containing compounds, whereas for the terminal alanine modification no improvement could be observed. For Gtt oligomers, histidines increased gene delivery efficiency for both terminal cysteine and alanine modification;for the latter the difference in transfection efficiency at higher N/P ratios was highly significant.

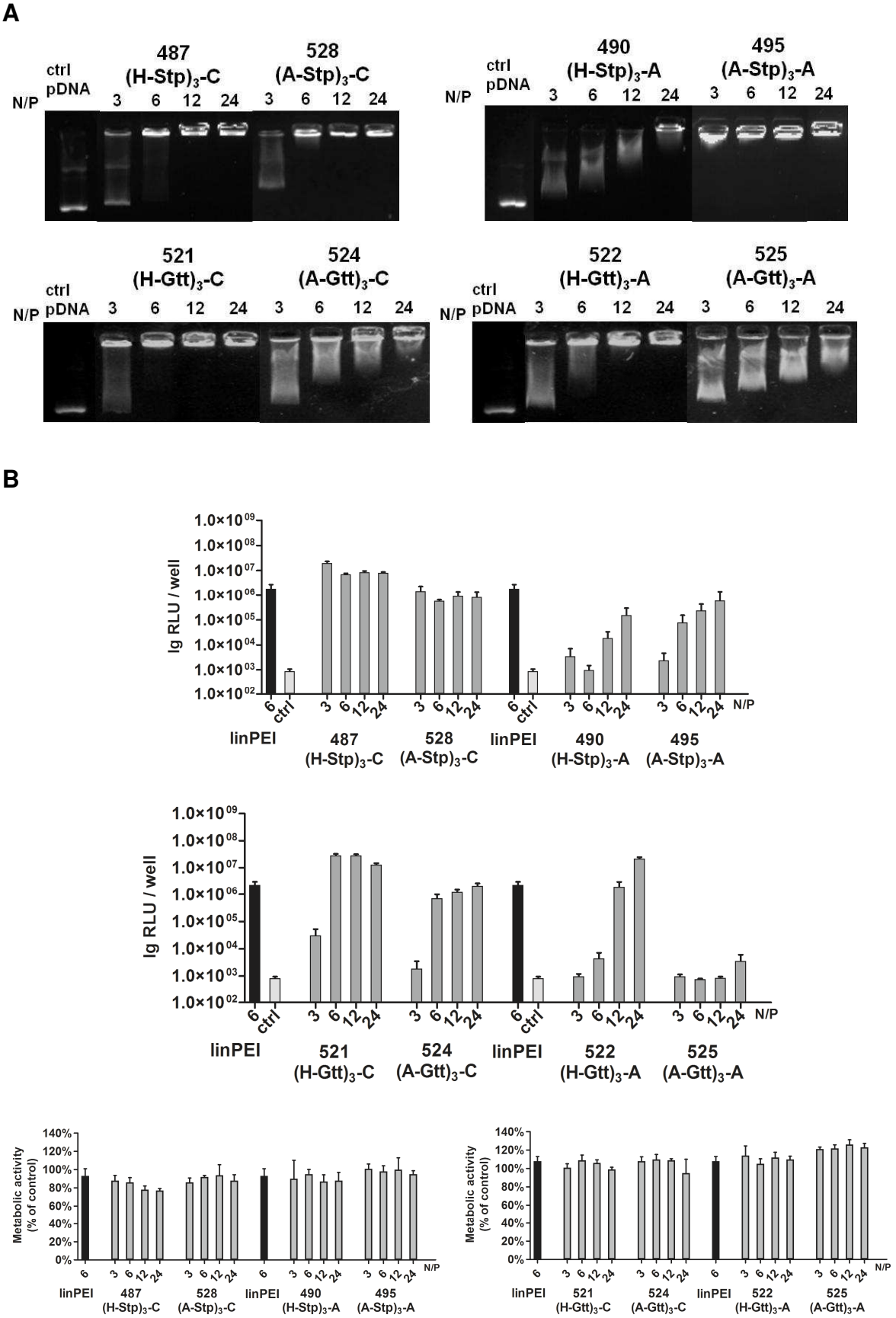

Fig. 23. (A) pDNA binding assay of histidine containing oligomers. Luciferase assay of histidine containing **(B)** Stp oligomers and Gtt oligomers and corresponding cell viability data below (experiments performed by Petra Kos, Wagner lab).

Furthermore, these compounds were also tested for the ability to mediate gene silencing with siRNA. The capability to bind siRNA was tested by agarose gel electrophoresis and revealed that cysteine containing Stp oligomers, consistent with previous findings, have the best binding abilities due to polyplex stabilization, whereas histidines do not have a positive influence on cargo binding (**Fig. 24 A**).
However, gene silencing experiments showed that histidines definitely have an impact on siRNA transfection and are beneficial as an additional buffering domain, even leading to a gene silencing effect for Gtt oligomers, although some unspecific toxicity could also be observed (**Fig. 24 B**).

A

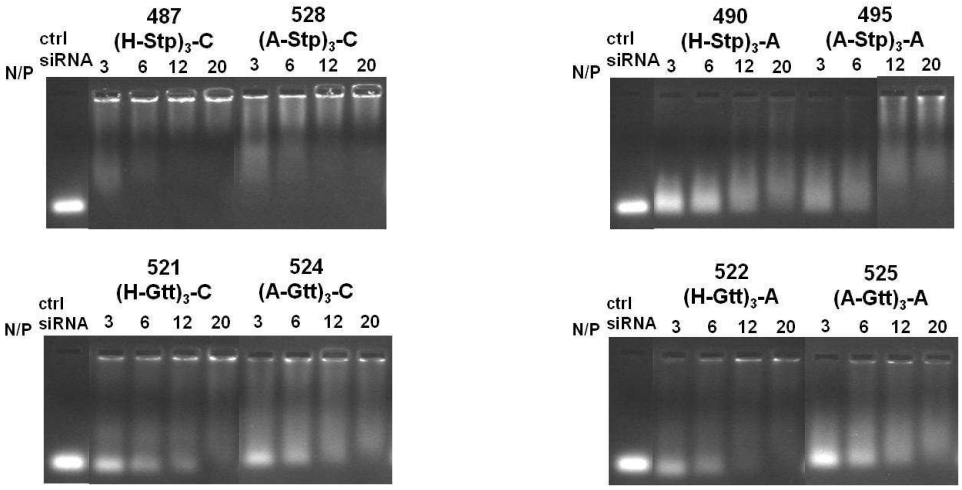

B

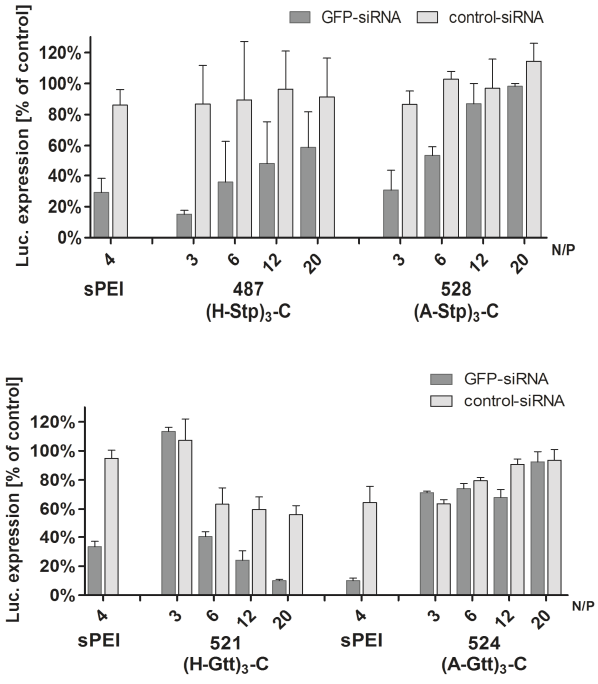

Fig. 24. (A) siRNA binding assay. **(B)** Gene silencing evaluation of histidine containing oligomers (experiments performed by Petra Kos, Wagner lab).

Oligomers with a higher amount of histidines (highHis) were also tested for their pDNA binding capacity. **Fig. 25** shows that both cysteine-containing Stp and Gtt oligomers do efficiently bind their cargo. Binding ability declines for histidine-containing oligomers with terminal alanine. Compound **580** ((A-Gtt)$_3$-A-A) cannot retain pDNA at all.

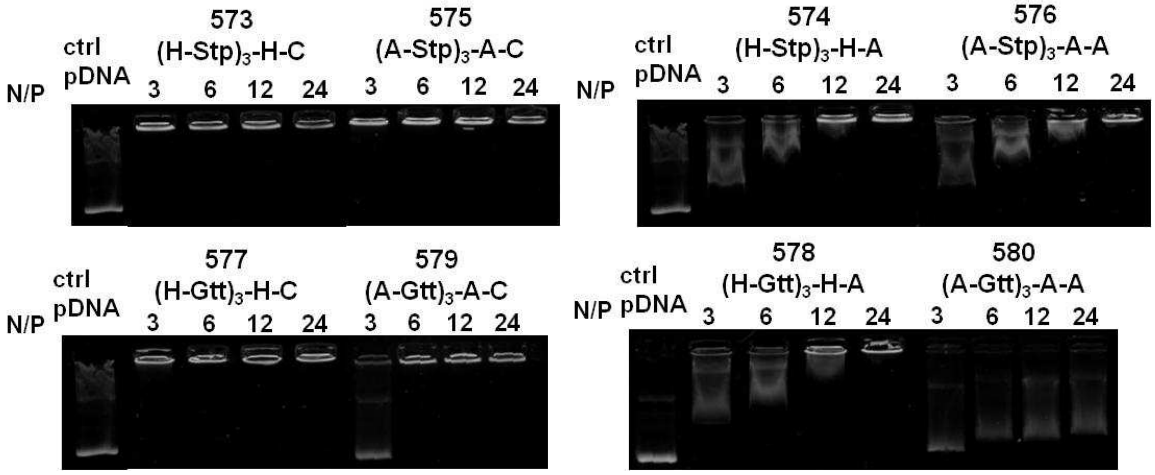

Fig. 25. pDNA binding assay of highHis oligomers.

Subsequent gene delivery experiments (**Fig. 26**) displayed similar results as obtained with lowHis compounds, showing no significant improvement due to additional histidines.

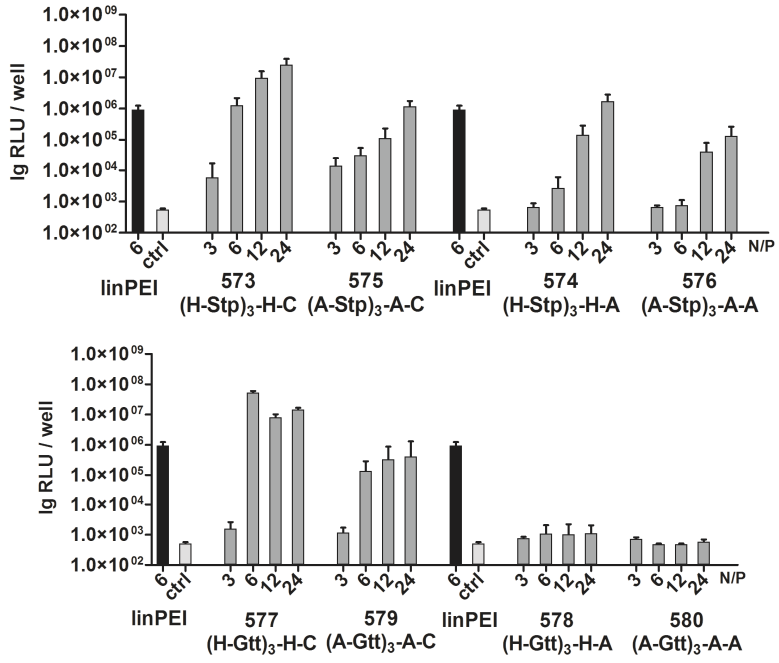

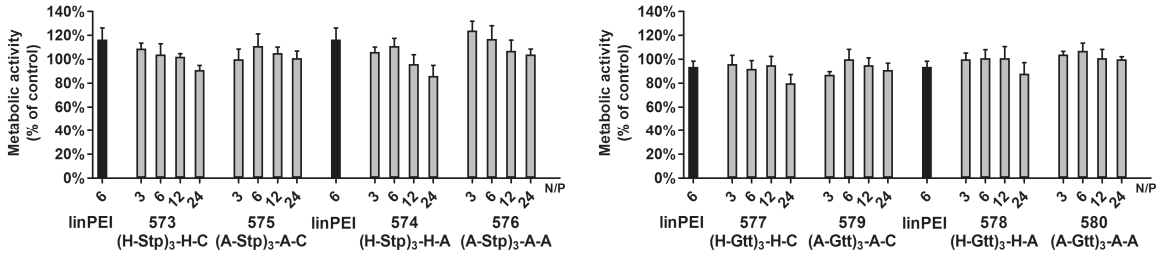

Fig. 26. Luciferase assay of highHis oligomers and corresponding cell viability data below (experiments performed by Petra Kos, Wagner lab).

Control oligomers **582** (KHH_3) and **584** (KHH_5) both showed in the gel electrophoresis assay efficient pDNA binding (**Fig. 27 A**). Transfection efficiency, though, did not exceed linPEI level (**Fig. 27 B**). Therefore, four-arm Stp and Gtt oligomers containing histidines and terminal cysteine remain the most efficient compounds.

A

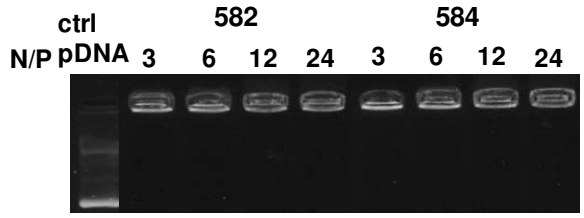

B

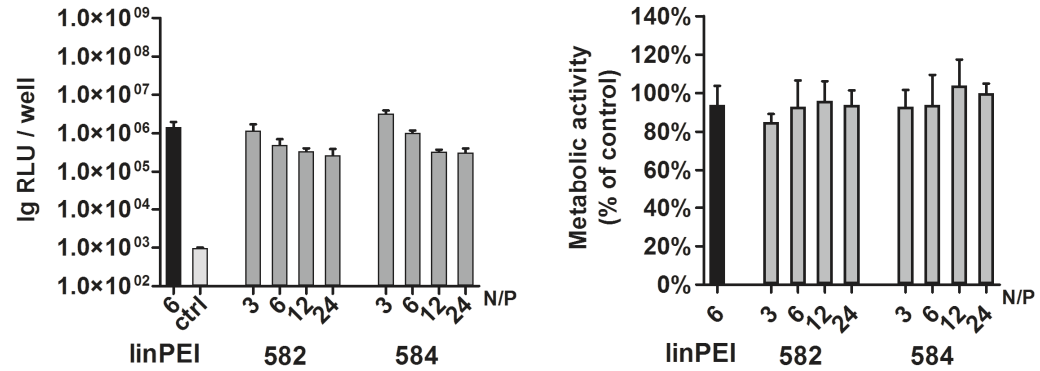

Fig. 27. (A) pDNA binding assay of control lysine-histidine oligomers. **(B)** Luciferase assay and corresponding cell viability data (experiments performed by Petra Kos, Wagner lab).

3.3 Polypropylenimine (PPI) conjugates for pDNA delivery

3.3.1 Introduction

Efficient pDNA delivery with cationic oligomers is known to be dependent also on polymer size. The `gold standard` in terms of transfection linear PEI, for instance, has a molecular weight of 22 kDa and owes its effectivity also to this feature. High molecular weight, though, is also strongly associated with carrier toxicity [49, 103]. Due to its static structure, accumulation occurs in cells or organs of living systems, causing undesired toxic effects. Low Mw gene vectors, on the other hand, may not provide sufficient polyplex stability in vivo during blood circulation [114, 168, 169]. Therefore, connection of non-toxic small Mw compounds by biodegradable linkages into larger polymeric structures is a possible solution [106, 114, 168, 170-174] for this problem.

In 2008, our lab (Russ and colleagues) presented a method for assembly of better defined structures to so-called `pseudodendrimers` by connecting oligoethylenimine (OEI) units with the biodegradable linker hexanedioldiacrylate (HD) (**Fig 28 A**), resulting in efficient, high Mw, biocompatible gene carriers [119]. In a subsequent work, the structurally defined dendrimer polypropylenimine (PPI) was used as a core structure and was connected with the same HD linker to either PPI or oligoethylenimine units [135]. Nevertheless, uncertainty of the resulting structure still remained due to its polydisperse nature and absence of precise connection sites.

In 2007 Kim *et al.* could show that simple PPI surface modification with arginine as additional cationic domain can enhance pDNA transfection efficiency [134].

In order to allow more precise conclusions on structure-activity relationships, this part of the thesis focuses on the generation of more defined biodegradable gene vectors with higher molecular weight and biocompatibility. Therefore, the dendrimer polypropylenimine (PPI) G2 was used again as a core, as it has a defined structure and does not display noteworthy toxicity. Furthermore, its moderate efficiency concerning pDNA transfection leaves room for improvement. Small linear, sequence-defined oligomers consisting of increasing numbers of the building block Stp were used for further modification, as previous experiments in our lab showed that these small oligomers are neither efficient for gene delivery, nor toxic. The aim was to find out whether a combination of these compounds would bring any benefit. Disulfide bonds were chosen as a biodegradable linkage between these compounds, as these

could be generated in a controlled manner and are rather stable in the extracellular environment, not leading to polymer degradation until reaching the reducing cytosolic environment (**Fig. 28 B**).

A **B**

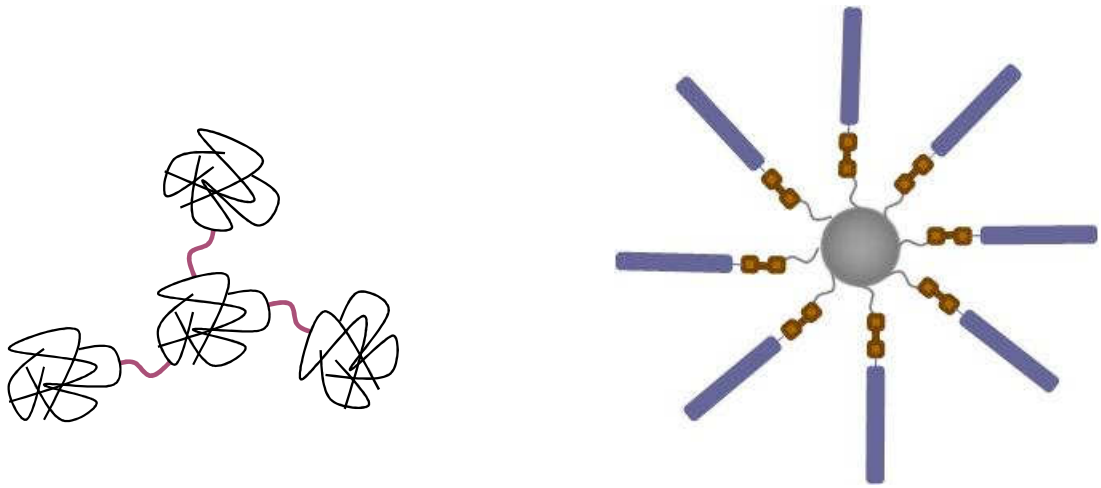

Fig. 28. (A) Pseudodendrimers consisting of HD-linked OEI units (see Russ et al [135]). **(B)** Defined dendritic structures consisting of PPI G2 core linked via disulfide linkages to sequence-defined Stp oligomers.

3.3.2 Synthetic concept

In order to facilitate reaction of PPI with cysteine-containing linear Stp oligomers, the eight primary amines on the PPI dendrimer surface had to be activated. 3-Nitro-2-pyridinesulfenyl (NPys) modified cysteine (BCNP, **Fig. 29** compound **1**) was chosen for this purpose, as the NPys acts as both protecting and activating group for the cysteine thiol, thus allowing concerted disulfide bond formation.

Therefore, the BCNP carboxylic group was activated with pentafluorophenol (**Fig. 29**, compound **2**), in order to facilitate reaction with the PPI primary amines. After PPI modification to PPI-BCNP (**Fig. 29**, compound **4**), the excess BCNP was removed and the acid-labile boc protecting group was cleaved, leading to PPI-CNP (**Fig. 29**, compound **5**). Subsequently, PPI-CNP was reacted with cysteine containing linear oligomers with 1 - 4 and 5 Stp units. The generated nitropyridine-thione was removed by dialysis (**Fig. 29**, last reaction step), resulting in compound **6**.

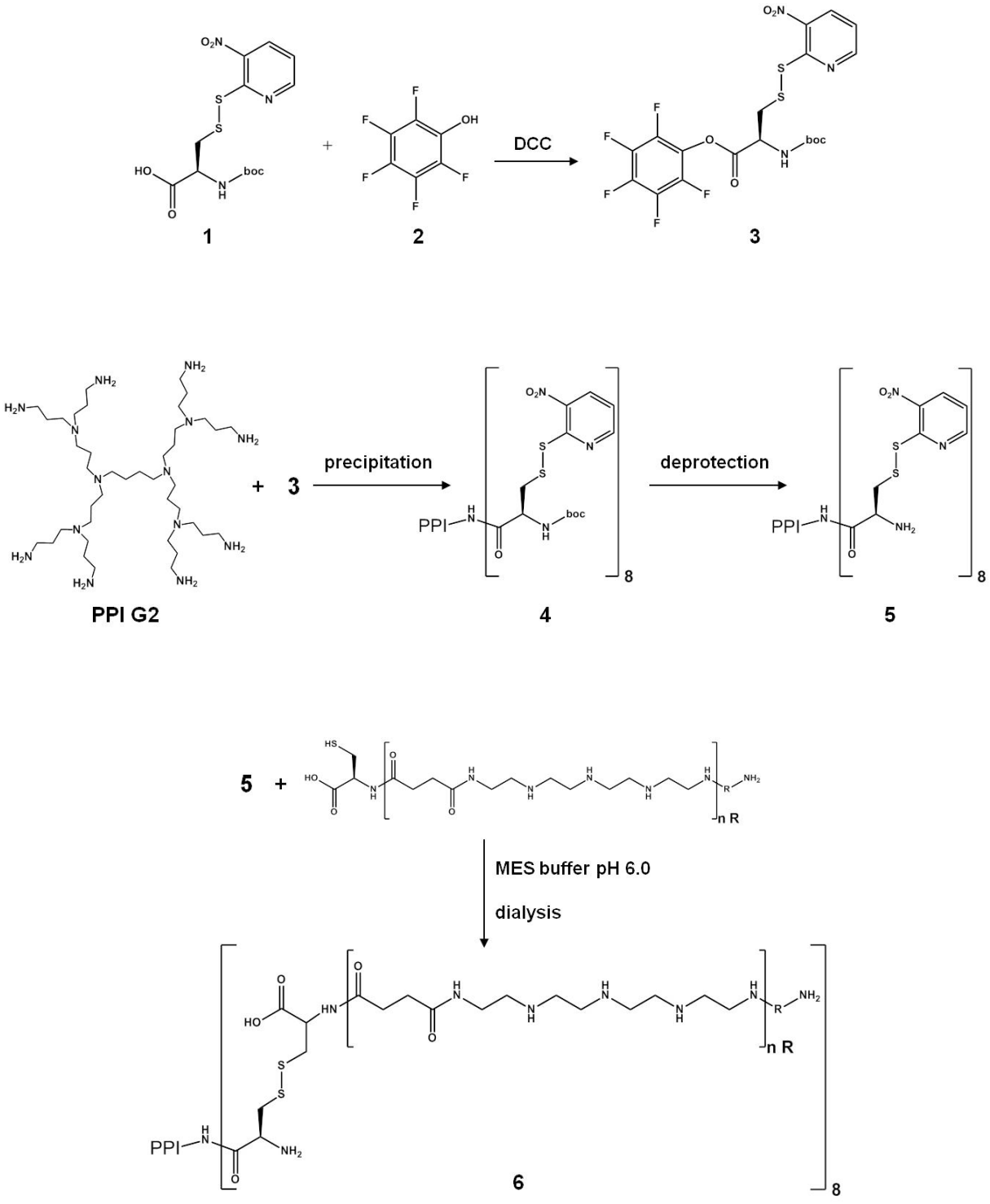

Fig. 29. Synthetic concept of PPI conjugates.
First, Boc-Cys(NPys)-OH was activated with pentafluorophenol to BCNP-OPfp **3** and subsequently reacted with PPI G2 to PPI-BCNP **4**. After precipitation for excess BCNP-OPfp removal, PPI-BCNP **4** was deprotected, resulting in PPI-CNP **5**. PPI-CNP was subsequently reacted with linear, cysteine-containing Stp oligomers and purified by dialysis to yield compound **6** (n = 1-3, 5).

3.3.3 Chemical characterization

Identity of synthesized intermediates **4** and **5** was confirmed by ^{1}H-NMR. **Fig. 30** shows the spectra of PPI after reaction with BCNP (**A**) and after cleavage of the boc protection group (**B**). Integration confirmed full modification of the PPI core with BCNP.

A **B**

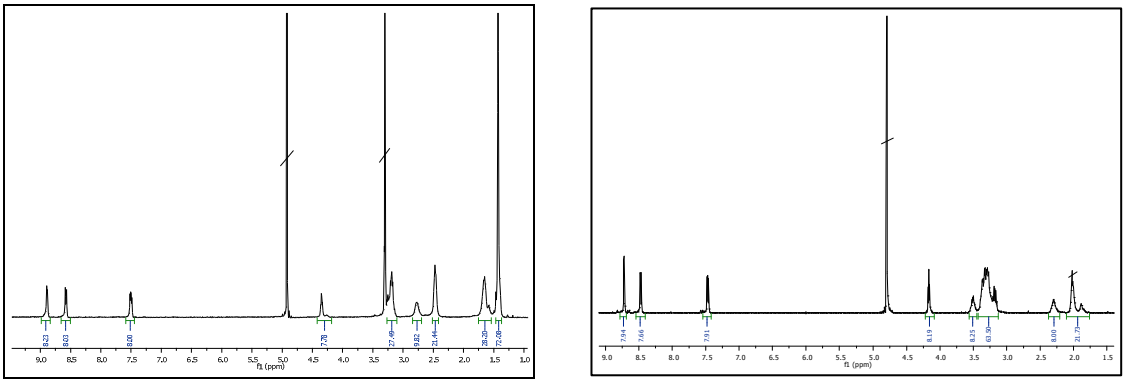

Fig. 30. ^{1}H-NMR spectra of **(A)** PPI-BCNP **4** in MeOH-D_4 and **(B)** PPI-CNP **5** in D_2O.

In order to allow concerted and precise modification of the activated PPI, purity of the PPI-CNP core compound had to be ensured. This was confirmed by analytical RP-HPLC (**Fig. 31**). The analytical run was monitored at two wavelengths: 220 nm (**Fig. 31**, red chromatogram) for amide bond and 340 nm (black chromatogram) for NPys detection. The overlay shows that NPys can only be found in the highly pure product peak.

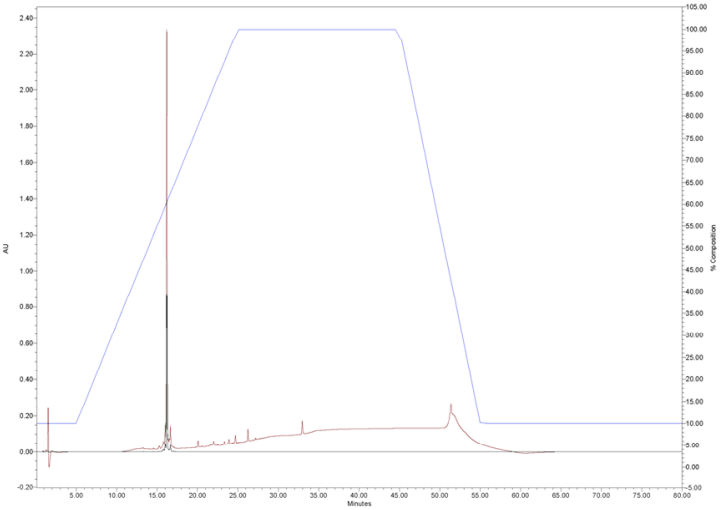

Fig. 31. Analytical RP-HPLC trace of purified PPI-CNP **5** performed on a C_{18} column and monitored at 220 nm (red chromatogram) and 340 nm (black chromatogram).

Linear Stp oligomers with increasing chain length (n= 1-3, 5) were generated by SPPS and product identity was confirmed by ^{1}H-NMR. Subsequently, reaction progress of PPI-CNP with linear Stp oligomers was monitored *in situ* by spectrophotometric quantification of the released nitropyridine-thione. After dialysis and lyophilization of the products **6** with n=1-3, 5 (see **Figure 33 A**), completion of reaction could be confirmed by lack of NPys protons in the ^{1}H-NMR spectrum (**Fig. 32**). Successful synthesis of the desired compound was further confirmed by additional quantification of generated disulfide bonds by the TCEP assay and lack of free thiols (Ellman`s assay).

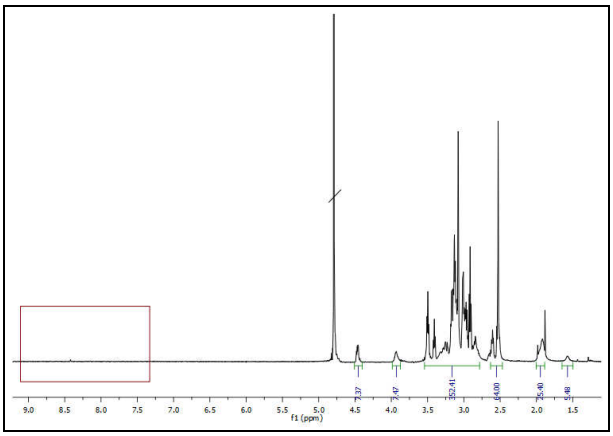

Fig. 32. Exemplary ^{1}H-NMR spectrum of compound **6**, n=2, obtained by reaction of PPI-CNP **5** with C-Stp$_2$.

3.3.4 Biophysical and biological characterization

Dynamic light scattering measurements show that all PPI-(C-C-Stp$_n$)$_8$/pDNA polyplexes are approximately 200 – 400 nm in size. Attempted particle formation of pDNA with PPI G2 displayed only aggregates with a size of > 1 µm. Surface charge of all polyplexes was above +20 mV (**Fig. 33 A**).

The binding efficiency of the PPI conjugates to pDNA was determined by gel electrophoresis. Only **PPI G2** and compound **536** with 5 Stp/chain were able to fully bind pDNA at all N/P. Concerning the smaller conjugates, the longer the Stp chain, the higher also the binding affinity (**Fig. 33 B**).

A

Conjugate Id	n (Stp units)	Sequence	Mean Size [nm]	Mean PdI	Mean Zeta Potential [mV]
418	1	PPI-(C-C-Stp)$_8$	155.3 ± 60.6	0.140 ± 0.04	21.7 ± 0.3
427	2	PPI-(C-C-Stp$_2$)$_8$	272.8 ± 94.8	0.245 ± 0.01	25.6 ± 1.3
428	3	PPI-(C-C-Stp$_3$)$_8$	321.5 ± 32.9	0.320 ± 0.01	32.1 ± 1.3
536	5	PPI-(C-C-Stp$_5$)$_8$	266.7 ± 29.5	0.278 ± 0.03	29.5 ± 0.6
PPI G2	0		1198 ± 636	0.496 ± 0.02	27.1 ± 1.6

B

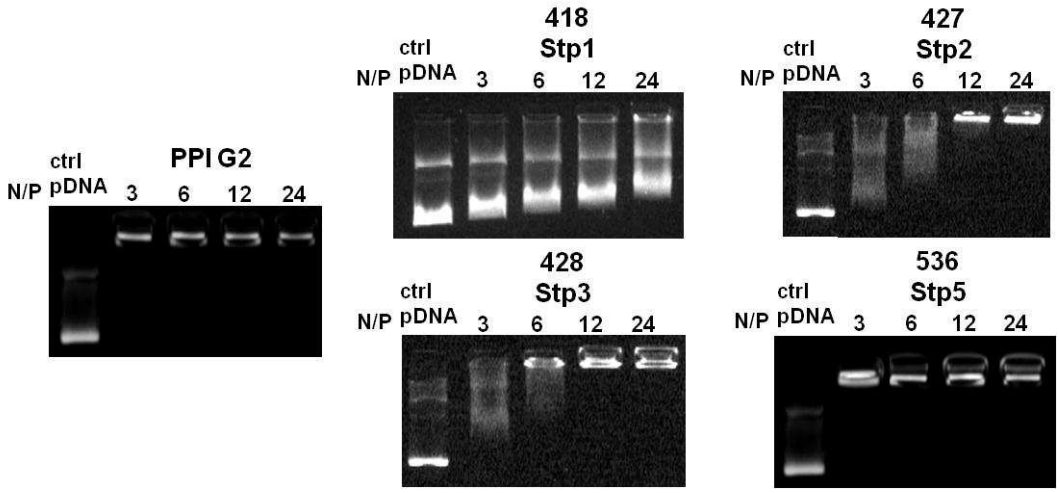

Fig. 33. (A) Particle size and zeta potential of PPI conjugate/pDNA polyplexes formed at N/P 12. **(B)** pDNA binding assay.

PPI conjugates were evaluated for their gene delivery efficiency and cytotoxicity on Neuro2A cells. Consistent with the biophysical characterization results, in the luciferase assay compound **418** with 1 Stp/chain showed the lowest efficiency compared to PPI G2 alone and control linPEI. Best results in terms of transfection efficiency could be achieved with conjugates containing 3 and 5 Stp/chain, whereas the longest chain did not bring any significant benefit. All compounds did not affect the cell metabolic activity, thus displaying high biocompatibility (**Fig. 34**, experiments performed by Petra Kos).

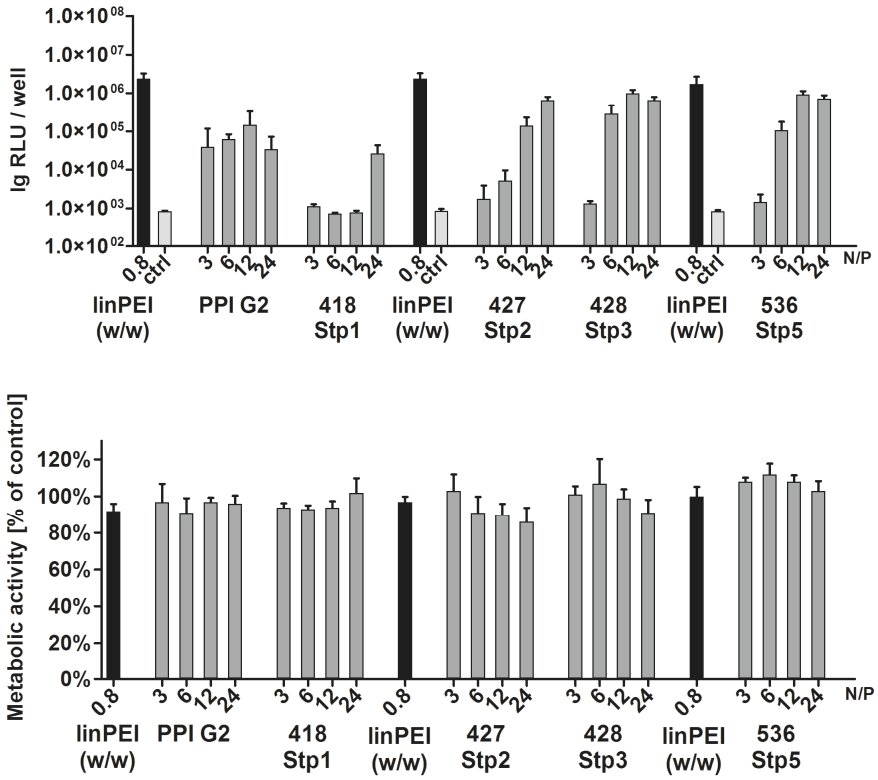

Fig. 34. Luciferase assay of transfections with PPI-C-(C-Stp$_n$)$_8$ polymer **6**/pDNA complexes and corresponding cell viability data (experiments performed by Petra Kos).

4 DISCUSSION

Nucleic acid delivery with cationic polymers is often hindered by low efficiency and toxicity. Among others, cationic polymers like polyethylenimine have the ability to reversibly compact pDNA through electrostatic interaction into stable polyplexes. Thus, the payload can reach undamaged the target cell compartment, namely the nucleus, where it can fulfil its task.

Such polymers, although showing promising results in terms of transfection efficiency and cytotoxicity, are still accompanied by a crucial drawback which hampers essential structure-activity relationship studies: polydispersity.

The concept of solid-phase supported synthesis (SPS) shows a way out of this dilemma. This method allows step-by-step polymer chain elongation and therefore exact position control of the inserted compound. Beyond linear compounds, introduction of lysines with two primary amines each facilitates the synthesis of branched oligomers and easy increase of molecular weight by parallel arm elongation Thus, generation of precise, sequence-defined oligomers is possible, allowing conclusions on structure-activity relationships.

4.1 Four- and five-arm oligo(ethanamino)amides for pDNA and siRNA delivery

As already mentioned, solid-phase supported synthesis can facilitate fast assembly of sequence-defined cationic oligomers [153, 175-177] with exact control on the position of introduced modifications. Using artificial amino acids which contain the 1,2-diaminoethane motif [154], this strategy was applied for assembling carriers for pDNA and siRNA [155, 159]. In the first chapter of this thesis, a small library of branched, four-arm oligomers was described. Two simple, straightforward modifications converted moderately active pDNA transfection carriers, four-arm Stp3 (**288**) or Stp4 (**289**) [155] into 1000-fold more potent pDNA transfection agents, Sph3-C (**497**) and Sph4-C (**519**).

The first successful modification was the incorporation of cysteines at the N-terminal end of the four arms. Disulfide bonds, either directly incorporated into transfection carriers or, as in the current study, formed after nucleic acid complexation, can be very beneficial [174, 178-180], both for complex stability in the extracellular space,

and for biocompatibility due to cleavage of the carrier into low-molecular fragments in the reducing intracellular environment [109]. Consistently, the cysteine-ended oligomers displayed pDNA and siRNA transfection activity without significant cytotoxicity. Polyplex dissociation assays of Stp and Sph polyplexes confirmed the importance of cysteine stabilization, whereas stronger binding of the oligomers containing 4 building blocks/arm did not improve transfection significantly. This result shows that a higher binding and compaction ability is not necessarily beneficial, as it may hamper cargo release in the cytosol.

In order to further increase molecular weight, a Stp tail was added before introduction of the lysine branching points in four-arm oligomers, thus creating cysteine-terminated five-arm Stp compounds. Stp tails and arms correlated in length, thus containing 2, 3 and four Stp units. Biophysical and biological evaluation of these compounds, though, did not reveal any benefit compared to their four-arm counterparts. This finding further emphasizes the importance of the optimal structure for maximal activity.

The second optimization resulted from defined variation of the artificial oligoamino acid building block, differing in the repeats of 1,2-diaminoethane units. This motif [78, 83] is responsible for the high transfection activity of PEI [13, 76, 77, 174, 181] and related polymers [81, 82, 155, 180, 182], due to unique dynamic properties, reversibly changing the cationic character by endosomal protonation and mediating endosomal escape. Within the polyamide chains of the four-arm oligomers, each building block Gtt, Stp and Sph provides two terminal amide nitrogens and two, three, or four protonable secondary amine nitrogens per unit. For both pDNA compaction and transfection activity, the building blocks ranked in the very clear order of Sph>Stp>>Gtt. Interestingly, extending the chain lengths beyond 3 building blocks per arm had marginal impact on the performance. Stp_5-C (**421**, with 64 protonatable nitrogens) has a far lower efficiency than Sph_3-C (**497**, 52 protonatable nitrogens) and Sph4-C (**519**, 68 protonatable nitrogens). For the much smaller siRNA cargo, Sph and Stp however displayed very similar binding activity, with Stp providing best gene silencing efficiency. Cysteine mediated stabilization by disulfide formation was strictly required for siRNA delivery. In conclusion, compaction ability (especially in case of pDNA) and polyplex stabilization (especially for siRNA) are major delivery requirements. Defined carriers generated by solid-phase supported synthesis can

accomplish this effectively, also providing insight into structure-activity relationships and manifold possibilities for further improvement.

4.2 Histidine-containing Stp and Gtt oligomers

The amino acid histidine has due to its imidazole side chain the property for selective protonation at acidic pH. This feature is crucial for one of the main bottlenecks within nucleic acid delivery with cationic carriers – endosomal escape. Therefore, this additional proton sponge was already used for enhancing the transfection efficiency of various gene carriers [161].

As SPS allows selective introduction of activity-enhancing moieties, histidines were inserted in an alternating manner into four-arm oligomers with three Stp or Gtt/arm and terminal cysteine. Thus, compounds with a low amount (`lowHis`) and with a higher amount (`highHis`) of histidines were generated. By replacing histidine and/or the terminal cysteine with alanine as a control amino acid, direct conclusions on structure-activity relationships could be drawn.

By these means, a library of sixteen histidine-containing oligomers and alanine counterparts was generated. Identity and purity was confirmed by ^{1}H-NMR and RP-HPLC. Acidimetric titrations (experiment performed by Ulrich Lächelt, Wagner lab) confirmed the higher buffering capacity at acidic pH mediated by histidines compared to alanine-containing mutants. Also, Gtt oligomers with two protonable amines per unit showed a higher buffering capacity than Stp oligomers with three protonable amines per unit.

In the gel electrophoresis assay, the `histidine effect` had the highest impact on Gtt oligomers. LowHis and highHis Gtt oligomers with terminal cysteines (**521, 577**) equalized the Stp counterparts (**487, 573**) in terms of pDNA binding. Consistently, in the luciferase assay all these compounds showed similar transfection efficiency, exceeding linPEI levels and showing no cytotoxic effects. Moreover, cysteine-terminated oligomers were, consistent with previous findings, more efficient than the alanine mutants due to polyplex stabilization, whereas replacement of histidine with alanine had a greater impact for the Gtt oligomers, leading to clearly lower transfection rates.

Nevertheless, significant improvement in terms of transfection efficiency due to introduction of additional histidines (lowHis vs. highHis oligomers) could not be observed.

The impact of histidine-introduction could also be observed in gene silencing experiments. SiRNA transfection with cysteine-containing lowHis oligomers revealed that introduction of histidines considerably improved gene silencing compared to alanine mutants. Even for Gtt oligomers a silencing effect could be shown, even though unspecific toxicity could also be observed.

Also, the new histidine-containing Stp and Gtt oligomers were compared with histidine-rich structures (**582, 584**) based on the work of A. J. Mixson [146]. These control oligomers showed transfection efficiency similar to linPEI but could not reach luciferase expression levels mediated by the best Stp and Gtt compounds.

4.3 Polypropylenimine (PPI) conjugates for pDNA delivery

The `gold standard` in terms of gene delivery, namely PEI, owes its efficiency also to its high molecular weight of 22 kDa but is polydispers by nature [76]. As high molecular weight of cationic polymers, though, is associated on the one hand with better transfection efficiency but on the other hand also with cytotoxicity [49], gene carriers with the feature of environment-triggered cargo release have the potential to overcome this drawback. Therefore, in order to increase molecular weight while maintaining a defined structure, the synthetic concept implied coupling the symmetrical polypropylenimine dendrimer [126] to linear, sequence-defined Stp oligomers. Biodegradability was achieved by modification of the eight primary amines on the PPI surface with activated cysteines, making them feasible for reaction with free thiols. Linear oligomers consisting of increasing amount of the cationic building block Stp (1-3 and 5 units) and containing a terminal cysteine with a free thiol were coupled to this activated core, so as to create reducible disulfide linkages. Thus, four compounds with increasing molecular weight were assembled (**418** Stp1, **427** Stp2, **428** Stp3, **536** Stp5) and compared to unmodified generation 2 (G2) PPI. The successful reaction was confirmed by chemical characterization methods.

Biophysical evalutation of these compounds by the pDNA binding assay revealed that the binding affinity increases with oligomer chain length, whereas only the compound with the highest Mw (**536** Stp5) could efficiently bind pDNA. PPI alone is also very efficient in terms of pDNA binding.

Biological testing for pDNA transfection efficiency by the luciferase assay showed that the oligomers containing the shortest Stp chain were even less effective than PPI

alone; results consistent with the findings in the gel shift assay. PPI coupled to oligomers with 3 and 5 Stp/chain (**428, 536**) were the most efficient for pDNA delivery, whereas **536** (Stp5) did not show any significant improvement compared to **428** (Stp3), which correlates also with the results obtained with four-arm oligomers.

Size and zeta potential measurements also offered an explanation for the transfection efficiency of PPI alone – very large particle size (> 1µm) and aggregates facilitate cellular uptake.

Nevertheless, transfection efficiency of the best conjugates is in the range of PEI, thus encouraging further efforts for optimization. Furthermore, the synthetic concept of PPI primary amine activation offers a platform for novel conjugates.

5 CONCLUSION AND OUTLOOK

Solid-phase supported synthesis (SPS) and subsequent biological evaluation of branched, sequence-defined oligomers displayed their potential as efficient nucleic acid carriers. Optimized synthesis of plain four-arm oligomers consisting of the cationic building block Stp has paved the way for further carrier optimization. Significant enhancement of pDNA and, even more, of siRNA transfection efficiency was achieved by simple N-terminal cysteine introduction due to resulting enhanced polyplex stabilization. Additionally, the protonable amine density within the used building block (Gtt, Stp, Sph) has proven to also a very important feature, with Sph showing the highest efficiency; a finding which can be exploited for further structure variations. Finally, SPS facilitated introduction of histidines within four-arm oligomers, increasing pH-specific oligomer buffering capacity and thus transfection efficiency.

Thus, the four-arm oligomers described in this work may be the first steps towards highly efficient and biocompatible nucleic acid carriers. Due to the synthetic method used, namely solid phase supported synthesis, there are still manifold possibilities for improvement and optimization.

Furthermore, the synthetic pathway established for generation of PPI conjugates offers a platform for further development, as the activated dendritic core can be modified with further adequate moieties. Moreover, this method can be used for modification of other core structures with primary amines on the surface.

In conclusion, branched cationic oligomers generated by means of SPS offer a broad platform as efficient and biocompatible nucleic acid carriers. Due to controlled sequence assembly, conclusions on structure-activity relationships are possible – a crucial starting point for further development of even more effective non-viral vectors.

Furthermore, the possibility of fast combinatorial synthesis offered by SPS and feasible purification and analytical methods offer manifold possibilities for the development of novel and potent structures.

6 SUMMARY

Synthetic nucleic acid carrier systems got more and more into focus during the last decades as they offer the opportunity to overcome drawbacks associated with viral vectors. Over the years, linear polyethylenimine (linPEI) has established itself as the `gold standard` in terms of nucleic acid transfection efficiency. Various modifications have even increased its effectivity and reduced toxicity, but polydispersity hampered precise conclusions on structure-activity relationships.

Solid-phase supported synthesis shows a way out of this dilemma, as it offers the possibility for sequence-controlled assembly of cationic oligomers and also the option for directed sequential modifications.

The aim of this thesis was the synthesis and optimization of branched, sequence-defined and biocompatible oligomers via SPS for generation of highly efficient nucleic acid carriers. First, four-branched oligomers consisting of lysines as branching points and the artificial amino acid Stp were synthesized with an increasing number of Stp per arm. Chemical characterization confirmed identity and purity of the compounds; biophysical and biological evaluation showed promising results in terms of pDNA transfection.

Therefore, the most potent structures were further modified with terminal cysteines for polyplex stabilization, which led to significant improvement in terms of pDNA transfection and also of gene silencing with siRNA. These results were undermined by gel electrophoresis assays in so far, that cysteines play a crucial role concerning polyplex stabilization. Additionally, further artificial oligoamino acids besides Stp with three protonable amines per unit were evaluated, namely Gtt with two and Sph with four protonable amines, respectively. The differing repeats of the 1,2-diaminoethane units also resulted in differing impact on pDNA delivery, ranking in the order Sph>Stp>>Gtt. In terms of siRNA-mediated gene silencing, Sph and Stp showed similar results, whereas Gtt-containing oligomers did not show any effect. Hence, it could be concluded that optimal oligomer/siRNA polyplex stabilization due to electrostatic interactions and disulfide formation is required for efficient gene silencing.

Another successful modification of Stp and Gtt oligomers was the introduction of the amino acid histidine. Selective protonation of its imidazole side chain at acidic pH

enhances endosomal escape, a crucial bottleneck in the nucleic acid delivery pathway. Histidine-containing oligomers were more efficient concerning pDNA and siRNA delivery than the alanine-containing control structures, undermining the importance of endosomal escape for successful transfection.

A further aim of this thesis was to generate defined, non-toxic structures with a higher Mw consisting of low Mw subunits coupled with biodegradable linkages. The structurally defined dendrimer polypropylenimine (PPI) was chosen as a core and its primary amines on the surface were modified in so far as to react with free thiols to reducible disulfide bonds. By these means, sequence-defined, linear Stp oligomers with increasing Stp units per chain were coupled to the activated PPI core and evaluated for pDNA delivery. The resulting non-toxic compounds showed correlation between increasing Stp chain length and transfection efficiency.

7 APPENDIX

7.1 List of used compounds

7.1.1 Four- and five-arm oligomers

Oligomer Id	Sequence	Molecular Formula	Molecular weight [g/mol]	Protonable amines
286	A-K-(K-(Stp)$_2$)$_2$	$C_{69}H_{143}N_{27}O_{13}$	1559.05	16
287	A-K-(K-(Stp$_2$)$_2$)$_2$	$C_{117}H_{243}N_{47}O_{21}$	2644.48	28
288	A-K-(K-(Stp$_3$)$_2$)$_2$	$C_{165}H_{343}N_{67}O_{29}$	3729.92	40
289	A-K-(K-(Stp$_4$)$_2$)$_2$	$C_{213}H_{443}N_{87}O_{37}$	4815.36	52
403	A-K-(K-(Stp$_5$)$_2$)$_2$	$C_{261}H_{543}N_{107}O_{45}$	5900.79	64
401	A-K-(K-(Stp$_2$-C)$_2$)$_2$	$C_{129}H_{263}N_{51}O_{25}S_4$	3057.05	28
392	A-K-(K-(Stp$_3$-C)$_2$)$_2$	$C_{177}H_{363}N_{71}O_{33}S_4$	4142.49	40
402	A-K-(K-(Stp$_4$-C)$_2$)$_2$	$C_{225}H_{463}N_{91}O_{41}S_4$	5227.93	52
421	A-K-(K-(Stp$_5$-C)$_2$)$_2$	$C_{273}H_{563N111O49S4}$	6313.37	64
530	A-K-(K-(Stp$_2$-A)$_2$)$_2$	$C_{129}H_{263}N_{51}O_{25}$	2928.80	28
531	A-K-(K-(Stp$_3$-A)$_2$)$_2$	$C_{177}H_{363}N_{71}O_{33}$	4014.23	40
532	A-K-(K-(Stp$_4$-A)$_2$)$_2$	$C_{225}H_{463}N_{91}O_{41}$	5099.67	52
533	A-K-(K-(Stp$_5$-A)$_2$)$_2$	$C_{273}H_{563}N_{111}O_{49}$	6185.11	64
414	A-Stp$_2$-K-(K-(Stp$_2$-C)$_2$)$_2$	$C_{153}H_{313}N_{61}O_{29}S_4$	3599.77	34
424	A-Stp$_3$-K-(K-(Stp$_3$-C)$_2$)$_2$	$C_{213}H_{447}N_{86}O_{38}S_4$	4949.64	49
425	A-Stp$_4$-K-(K-(Stp$_4$-C)$_2$)$_2$	$C_{273}H_{563}N_{111}O_{49}S_4$	6313.37	64
492	A-K-(K-(Gtt$_3$-C)$_2$)$_2$	$C_{165}H_{327}N_{59}O_{33}S_4$	3794.00	28
494	A-K-(K-(Gtt$_4$-C)$_2$)$_2$	$C_{209}H_{415}N_{75}O_{41}S_4$	4763.27	36
526	A-K-(K-(Gtt$_3$-A)$_2$)$_2$	$C_{165}H_{327}N_{59}O_{33}$	3665.74	28
527	A-K-(K-(Gtt$_4$-A)$_2$)$_2$	$C_{209}H_{415}N_{75}O_{41}$	4635.01	36
497	A-K-(K-(Sph$_3$-C)$_2$)$_2$	$C_{201}H_{423}N_{83}O_{33}S_4$	4659.31	52
519	A-K-(K-(Sph$_4$-C)2)$_2$	$C_{249}H_{523}N_{103}O_{41}S_4$	5744.74	68
534	A-K-(K-(Sph$_3$-A)$_2$)$_2$	$C_{201}H_{423}N_{83}O_{33}$	4531.05	52
535	A-K-(K-(Sph$_4$-A)$_2$)$_2$	$C_{249}H_{523}N_{103}O_{41}$	5616.48	68
487	A-K-(K-((H-Stp)$_3$-C)$_2$)$_2$	$C_{250}H_{449}N_{107}O_{44}S_4$	5786.19	52
528	A-K-(K-((A-Stp)$_3$-C)$_{2)2}$	$C_{214}H_{425}N_{83}O_{44}S_4$	4993.45	40
490	A-K-(K-((H-Stp)$_3$-A)$_2$)$_2$	$C_{250}H_{473}N_{107}O_{44}$	5682.12	52

495	A-K-(K-((A-Stp)$_3$-A)$_2$)$_2$	$C_{214}H_{425}N_{83}O_{44}$	4865.19	40
521	A-K-(K-((H-Gtt)$_3$-C)$_2$)$_2$	$C_{237}H_{411}N_{95}O_{45S4}$	5439.67	40
524	A-K-(K-((A-Gtt)$_3$-C)$_2$)$_2$	$C_{201}H_{387}N_{71}O_{45}S_4$	4646.93	28
522	A-K-(K-((H-Gtt)$_3$-A)$_2$)$_2$	$C_{237}H_{411}N_{95}O_{45}$	5311.41	40
525	A-K-(K-((A-Gtt)$_3$-A)$_2$)$_2$	$C_{201}H_{387}N_{71}O_{45}$	4518.67	28
573	A-K-(H-K-((H-Stp)$_3$-H-C)$_2$)$_2$	$C_{285}H_{489}N_{125}O_{51}S_4$	6611.00	58
575	A-K-(A-K-((A-Stp)$_3$-A-C)$_2$)$_2$	$C_{231}H_{453}N_{89}O_{51}S_4$	5421.89	40
574	A-K-(H-K-((H-Stp)$_3$-H-A)$_2$)$_2$	$C_{285}H_{489}N_{125}O_{51}$	6482.74	58
576	A-K-(A-K-((A-Stp)$_3$-A-A)$_2$)$_2$	$C_{231}H_{453}N_{89}O_{51}$	5293.63	40
577	A-K-(H-K-((H-Gtt)$_3$-H-C)$_2$)$_2$	$C_{261}H_{429}N_{113}O_{51}S_4$	6094.19	46
579	A-K-(A-K-((A-Gtt)$_3$-A-C)$_2$)$_2$	$C_{207}H_{393}N_{77}O_{51}S_4$	4905.08	28
578	A-K-(H-K-((H-Gtt)$_3$-H-A)$_2$)$_2$	$C_{261}H_{429}N_{113}O_{51}$	5965.93	46
580	A-K-(A-K-((A-Gtt)$_3$-A-A)$_2$)$_2$	$C_{207}H_{393}N_{77}O_{51}$	4776.82	28
582	A-K-(K-(K-H-(K-H2)3-K-H-K)2)2	$C_{357}H_{555}N_{151}O_{61}$	7938.20	56
584	A-K-(K-(K-H-(K-H2)5-K-H-K)2)2	$C_{389}H_{597}N_{167}O_{67}$	11157.97	80

7.1.2 Linear cysteine-containing Stp oligomers

Sequence	Molecular Formula	Molecular weight [g/mol]	Protonable amines
C-Stp	$C_{15}H_{32}N_6O_4S$	392.52	4
C-Stp$_2$	$C_{27}H_{53}N_{11}O_6S$	659.84	7
C-Stp$_3$	$C_{39}H_{78}N_{16}O_8S$	931.20	10
C-Stp$_4$	$C_{51}H_{102}N_{21}O_{10}S$	1202.56	13
C-Stp$_5$	$C_{63}H_{128}N_{26}O_{12}S$	1473.92	16

7.1.3 PPI conjugates

Conjugate Id	Sequence	Molecular Formula	Molecular weight [g/mol]	Protonable amines
418	PPI-(C-C-Stp)$_8$	$C_{268}H_{556}N_{78}O_{24}S_{16}$	4718.51	46
427	PPI-(C-C-Stp$_2$)$_8$	$C_{280}H_{576}N_{110}O_{56}S_{16}$	6893.31	70
428	PPI-(C-C-Stp$_3$)$_8$	$C_{376}H_{776}N_{150}O_{72}S_{16}$	9064.19	94
430	PPI-(C-C-Stp$_4$)$_8$	$C_{472}H_{976}N_{190}O_{88}S_{16}$	11227.33	118
536	PPI-(C-C-Stp$_5$)$_8$	$C_{568}H_{1176}N_{230}O_{104}S_{16}$	13405.93	150

7.2 Analytical Data

^{1}H-NMR chemical shifts of the synthesized compounds (all measured at 400 MHz in D_2O). Compound mass was not determined unless otherwise stated.

7.2.1 Four- and five-arm oligomers

Oligomer Id: 286 Sequence: A-K-(K-$(Stp)_2)_2$

δ (ppm) = 1.3-1.8 (m, 21 H, γδεH lysine, -CH_3 alanine), 2.5-2.6 (m, 16 H, -CO-CH_2-CH_2-CO-), 3.1 (t, 6 H, βH lysine), 3.2-3.4 (m, 16 H, -CH_2- Tp), 3.48-3.54 (m, 48 H, -CH_2- Tp), 4.1-4.3 (m, 4 H, αH amino acids).

Calculated Mass: 1560.05 $[M+H]^+$
Mass found: 1558.823 $[M+H]^+$

Oligomer Id: 287 Sequence: A-K-(K-$(Stp_2)_2)_2$

δ (ppm) = 1.3-1.8 (m, 21 H, γδεH lysine, -CH_3 alanine), 2.5-2.6 (m, 32 H, -CO-CH_2-CH_2-CO-), 3.1 (t, 6 H, βH lysine), 3.2-3.4 (m, 32 H, -CH_2- Tp), 3.48-3.54 (m, 96 H, -CH_2- Tp), 4.1-4.3 (m, 4 H, αH amino acids).

Calculated Mass: 2645.48 $[M+H]^+$
Mass found: 2646.258 $[M+H]^+$

Oligomer Id: 288 Sequence: A-K-(K-$(Stp_3)_2)_2$

δ (ppm) = 1.3-1.8 (m, 21 H, γδεH lysine, -CH_3 alanine), 2.5-2.6 (m, 48 H, -CO-CH_2-CH_2-CO-), 3.1 (t, 6 H, βH lysine), 3.2-3.4 (m, 48 H, -CH_2- Tp), 3.48-3.54 (m, 144 H, -CH_2- Tp), 4.1-4.3 (m, 4 H, αH amino acids).

Calculated Mass: 3730.92 $[M+H]^+$
Mass found: 3729.070 $[M+H]^+$

Oligomer Id: 289 Sequence: A-K-(K-$(Stp_4)_2)_2$

δ (ppm) = 1.3-1.8 (m, 21 H, γδεH lysine, -CH_3 alanine), 2.5-2.6 (m, 64 H, -CO-CH_2-CH_2-CO-), 3.1 (t, 6 H, βH lysine), 3.2-3.4 (m, 64 H, -CH_2- Tp), 3.48-3.54 (m, 192 H, -CH_2- Tp), 4.1-4.3 (m, 4 H, αH amino acids).

Calculated Mass: 4186.36 $[M+H]^+$
Mass found: 4187.455 $[M+H]^+$

Oligomer Id: 403 Sequence: A-K-(K-$(Stp_5)_2)_2$
δ (ppm) = 1.3-1.8 (m, 21 H, γδεH lysine, -CH_3 alanine), 2.5-2.6 (m, 80 H, -CO-CH_2-CH_2-CO-), 3.1 (t, 6 H, βH lysine), 3.2-3.4 (m, 80 H, -CH_2- Tp), 3.48-3.54 (m, 240 H, -CH_2- Tp), 4.1-4.3 (m, 4 H, αH amino acids).

Oligomer Id: 401 Sequence: A-K-(K-$(Stp_2$-C$)_2)_2$
δ (ppm) = 1.3-1.8 (m, 21 H, γδεH lysine, -CH_3 alanine), 2.5-2.6 (m, 32 H, -CO-CH_2-CH_2-CO-), 3.0 (m, 8 H, βH cysteine), 3.1 (t, 6 H, βH lysine), 3.2-3.4 (m, 32 H, -CH_2-Tp), 3.48-3.54 (m, 96 H, -CH_2- Tp), 4.1-4.3 (m, 8 H, αH amino acids).

Oligomer Id: 392 Sequence: A-K-(K-$(Stp_3$-C$)_2)_2$
δ (ppm) = 1.3-1.8 (m, 21 H, γδεH lysine, -CH_3 alanine), 2.5-2.6 (m, 48 H, -CO-CH_2-CH_2-CO-), 3.0 (m, 8 H, βH cysteine), 3.1 (t, 6 H, βH lysine), 3.2-3.4 (m, 48 H, -CH_2-Tp), 3.48-3.54 (m, 144 H, -CH_2- Tp), 4.1-4.3 (m, 8 H, αH amino acids).

Oligomer Id: 402 Sequence: A-K-(K-$(Stp_4$-C$)_2)_2$
δ (ppm) = 1.3-1.8 (m, 21 H, γδεH lysine, -CH_3 alanine), 2.5-2.6 (m, 64 H, -CO-CH_2-CH_2-CO-), 3.0 (m, 8 H, βH cysteine), 3.1 (t, 6 H, βH lysine), 3.2-3.4 (m, 64 H, -CH_2-Tp), 3.48-3.54 (m, 192 H, -CH_2- Tp), 4.1-4.3 (m, 8 H, αH amino acids).

Oligomer Id: 421 Sequence: A-K-(K-$(Stp_5$-C$)_2)_2$
δ (ppm) = 1.3-1.8 (m, 21 H, γδεH lysine, -CH_3 alanine), 2.5-2.6 (m, 80 H, -CO-CH_2-CH_2-CO-), 3.0 (m, 8 H, βH cysteine), 3.1 (t, 6 H, βH lysine), 3.2-3.4 (m, 80 H, -CH_2-Tp), 3.48-3.54 (m, 240 H, -CH_2- Tp), 4.1-4.3 (m, 8 H, αH amino acids).

Oligomer Id: 530 Sequence: A-K-(K-$(Stp_2$-A$)_2)_2$
δ (ppm) = 1.3-1.8 (m, 33 H, γδεH lysine, -CH_3 alanine), 2.5-2.6 (m, 32 H, -CO-CH_2-CH_2-CO-), 3.1 (t, 6 H, βH lysine), 3.2-3.4 (m, 32 H, -CH_2- Tp), 3.48-3.54 (m, 96 H, -CH_2- Tp), 4.1-4.3 (m, 8 H, αH amino acids).

Oligomer Id: 531 Sequence: A-K-(K-(Stp_3-A)$_2$)$_2$

δ (ppm) = 1.3-1.8 (m, 33 H, γδεH lysine, -CH_3 alanine), 2.5-2.6 (m, 48 H, -CO-CH_2-CH_2-CO-), 3.1 (t, 6 H, βH lysine), 3.2-3.4 (m, 48 H, -CH_2- Tp), 3.48-3.54 (m, 144 H, -CH_2- Tp), 4.1-4.3 (m, 8 H, αH amino acids).

Oligomer Id: 532 Sequence: A-K-(K-(Stp_4-A)$_2$)$_2$

δ (ppm) = 1.3-1.8 (m, 33 H, γδεH lysine, -CH_3 alanine), 2.5-2.6 (m, 64 H, -CO-CH_2-CH_2-CO-), 3.1 (t, 6 H, βH lysine), 3.2-3.4 (m, 64 H, -CH_2- Tp), 3.48-3.54 (m, 192 H, -CH_2- Tp), 4.1-4.3 (m, 8 H, αH amino acids).

Oligomer Id: 533 Sequence: A-K-(K-(Stp_5-A)$_2$)$_2$

δ (ppm) = 1.3-1.8 (m, 33 H, γδεH lysine, -CH_3 alanine), 2.5-2.6 (m, 80 H, -CO-CH_2-CH_2-CO-), 3.1 (t, 6 H, βH lysine), 3.2-3.4 (m, 80 H, -CH_2- Tp), 3.48-3.54 (m, 240 H, -CH_2- Tp), 4.1-4.3 (m, 8 H, αH amino acids).

Oligomer Id: 414 Sequence: A-Stp_2-K-(K-(Stp_2-C)$_2$)$_2$

δ (ppm) = 1.3-1.8 (m, 21 H, γδεH lysine, -CH_3 alanine), 2.5-2.6 (m, 40 H, -CO-CH_2-CH_2-CO-), 3.0 (m, 8 H, βH cysteine), 3.1 (t, 6 H, βH lysine), 3.2-3.4 (m, 40 H, -CH_2-Tp), 3.48-3.54 (m, 120 H, -CH_2- Tp), 4.1-4.3 (m, 8 H, αH amino acids).

Oligomer Id: 424 Sequence: A-Stp_3-K-(K-(Stp_3-C)$_2$)$_2$

δ (ppm) = 1.3-1.8 (m, 21 H, γδεH lysine, -CH_3 alanine), 2.5-2.6 (m, 60 H, -CO-CH_2-CH_2-CO-), 3.0 (m, 8 H, βH cysteine), 3.1 (t, 6 H, βH lysine), 3.2-3.4 (m, 60 H, -CH_2-Tp), 3.48-3.54 (m, 180 H, -CH_2- Tp), 4.1-4.3 (m, 8 H, αH amino acids).

Oligomer Id: 425 Sequence: A-Stp_4-K-(K-(Stp_4-C)$_2$)$_2$

δ (ppm) = 1.3-1.8 (m, 21 H, γδεH lysine, -CH_3 alanine), 2.5-2.6 (m, 80 H, -CO-CH_2-CH_2-CO-), 3.0 (m, 8 H, βH cysteine), 3.1 (t, 6 H, βH lysine), 3.2-3.4 (m, 80 H, -CH_2-Tp), 3.48-3.54 (m, 240 H, -CH_2- Tp), 4.1-4.3 (m, 8 H, αH amino acids).

Oligomer Id: 492 Sequence: A-K-(K-(Gtt_3-C)$_2$)$_2$

δ (ppm) = 1.3-1.8 (m, 21 H, γδεH lysine, -CH_3 alanine), 2.2-2.3 (t, 48 H, -CO-CH_2-CH_2-CH_2-CO-), 1.8-1.9 (m, 24 H, -CO-CH_2-CH_2-CH_2-CO-), 3.0 (m, 8 H, βH cysteine),

3.1 (t, 6 H, βH lysine), 3.2-3.3 (m, 48 H, -CH_2- Tt), 3.4-3.5 (m, 96 H, -CH_2- Tt), 4.1-4.3 (m, 8 H, αH amino acids).

Oligomer Id: 494 Sequence: A-K-(K-(Gtt_4-C)$_2$)$_2$

δ (ppm) = 1.3-1.8 (m, 21 H, γδεH lysine, -CH_3 alanine), 2.2-2.3 (t, 64 H, -CO-CH_2-CH_2-CH_2-CO-), 1.8-1.9 (m, 32 H, -CO-CH_2-CH_2-CH_2-CH_2-CO-), 3.0 (m, 8 H, βH cysteine), 3.1 (t, 6 H, βH lysine), 3.2-3.3 (m, 64 H, -CH_2- Tt), 3.4-3.5 (m, 128 H, -CH_2- Tt), 4.1-4.3 (m, 8 H, αH amino acids).

Oligomer Id: 526 Sequence: A-K-(K-(Gtt_3-A)$_2$)$_2$

δ (ppm) = 1.3-1.8 (m, 21 H, γδεH lysine, -CH_3 alanine), 2.2-2.3 (t, 48 H, -CO-CH_2-CH_2-CH_2-CO-), 1.8-1.9 (m, 24 H, -CO-CH_2-CH_2-CH_2-CO-), 3.1 (t, 6 H, βH lysine), 3.2-3.3 (m, 48 H, -CH_2- Tt), 3.4-3.5 (m, 96 H, -CH_2- Tt), 4.1-4.3 (m, 8 H, αH amino acids).

Oligomer Id: 527 Sequence: A-K-(K-(Gtt_4-A)$_2$)$_2$

δ (ppm) = 1.3-1.8 (m, 21 H, γδεH lysine, -CH_3 alanine), 2.2-2.3 (t, 64 H, -CO-CH_2-CH_2-CH_2-CO-), 1.8-1.9 (m, 32 H, -CO-CH_2-CH_2-CH_2-CO-), 3.1 (t, 6 H, βH lysine), 3.2-3.3 (m, 64 H, -CH_2- Tt), 3.4-3.5 (m, 128 H, -CH_2- Tt), 4.1-4.3 (m, 8 H, αH amino acids).

Oligomer Id: 497 Sequence: A-K-(K-(Sph_3-C)$_2$)$_2$

δ (ppm) = 1.3-1.8 (m, 21 H, γδεH lysine, -CH_3 alanine), 2.5-2.6 (m, 48 H, -CO-CH_2-CH_2-CO-), 3.0 (m, 8 H, βH cysteine), 3.1 (t, 6 H, βH lysine), 3.2-3.4 (m, 48 H, - CH_2-Tp), 3.4-3.6 (m, 192 H, -CH_2- Tp), 4.1-4.3 (m, 8 H, αH amino acids).

Oligomer Id: 519 Sequence: A-K-(K-(Sph_4-C)$_2$)$_2$

δ (ppm) = 1.3-1.8 (m, 21 H, γδεH lysine, -CH_3 alanine), 2.5-2.6 (m, 64 H, -CO-CH_2-CH_2-CO-), 3.0 (m, 8 H, βH cysteine), 3.1 (t, 6 H, βH lysine), 3.2-3.4 (m, 64 H, - CH_2-Tp), 3.4-3.6 (m, 256 H, -CH_2- Tp), 4.1-4.3 (m, 8 H, αH amino acids).

Oligomer Id: 534 Sequence: A-K-(K-(Sph_3-A)$_2$)$_2$

δ (ppm) = 1.3-1.8 (m, 33 H, γδεH lysine, -CH_3 alanine), 2.5-2.6 (m, 48 H, -CO-CH_2-CH_2-CO-), 3.1 (t, 6 H, βH lysine), 3.2-3.4 (m, 48 H, -CH_2- Tp), 3.4-3.6 (m, 192 H, -CH_2- Tp), 4.1-4.3 (m, 8 H, αH amino acids).

Oligomer Id: 535 Sequence: A-K-(K-(Sph_4-A)$_2$)$_2$

δ (ppm) = 1.3-1.8 (m, 33 H, γδεH lysine, -CH_3 alanine), 2.5-2.6 (m, 64 H, -CO-CH_2-CH_2-CO-), 3.1 (t, 6 H, βH lysine), 3.2-3.4 (m, 64 H, -CH_2- Tp), 3.4-3.6 (m, 256 H, -CH_2- Tp), 4.1-4.3 (m, 8 H, αH amino acids).

Oligomer Id: 487 Sequence: A-K-(K-((H-Stp)$_3$-C)$_2$)$_2$

δ (ppm) = 1.3-1.8 (m, 21 H, γδεH lysine, -CH_3 alanine), 2.5-2.6 (m, 48 H, -CO-CH_2-CH_2-CO-), 3.0 (m, 8 H, βH cysteine), 3.1-3.2 (m, 32 H, βH lysine, histidine), 3.2-3.4 (m, 48 H, -CH_2- Tp), 3.48-3.54 (m, 144 H, -CH_2- Tp), 4.1-4.3 (m, 8 H, αH lysine, alanine, cysteine), 4.7 (m, 12 H, αH histidine) 7.3 (12 H, imidazole H histidine), 8.6 (12 H, imidazole H histidine).

Oligomer Id: 528 Sequence: A-K-(K-((A-Stp)$_3$-C)$_2$)$_2$

δ (ppm) = 1.3-1.8 (m, 57 H, γδεH lysine, -CH_3 alanine), 2.5-2.6 (m, 48 H, -CO-CH_2-CH_2-CO-), 3.0 (m, 8 H, βH cysteine), 3.1 (t, 6 H, βH lysine), 3.2-3.4 (m, 48 H, -CH_2-Tp), 3.48-3.54 (m, 144 H, -CH_2- Tp), 4.1-4.3 (m, 20 H, αH amino acids).

Oligomer Id: 490 Sequence: A-K-(K-((H-Stp)$_3$-A)$_2$)$_2$

δ (ppm) = 1.3-1.8 (m, 33 H, γδεH lysine, -CH_3 alanine), 2.5-2.6 (m, 48 H, -CO-CH_2-CH_2-CO-), 3.1-3.2 (m, 32 H, βH lysine, histidine), 3.2-3.4 (m, 48 H, -CH_2- Tp), 3.48-3.54 (m, 144 H, -CH_2- Tp), 4.1-4.3 (m, 8 H, αH lysine, alanine), 4.7 (m, 12 H, αH histidine) 7.3 (12 H, imidazole H histidine), 8.6 (12 H, imidazole H histidine).

Oligomer Id: 495 Sequence: A-K-(K-((A-Stp)$_3$-A)$_2$)$_2$

δ (ppm) = 1.3-1.8 (m, 69 H, γδεH lysine, -CH_3 alanine), 2.5-2.6 (m, 48 H, -CO-CH_2-CH_2-CO-), 3.1 (t, 6 H, βH lysine), 3.2-3.4 (m, 48 H, -CH_2- Tp), 3.48-3.54 (m, 144 H, -CH_2- Tp), 4.1-4.3 (m, 20 H, αH amino acids).

Oligomer Id: 521 Sequence: A-K-(K-((H-Gtt)$_3$-C)$_2$)$_2$

δ (ppm) = 1.3-1.8 (m, 21 H, γδεH lysine, -CH_3 alanine), 2.2-2.3 (t, 48 H, -CO-CH_2-CH_2-CH_2-CO-), 1.8-1.9 (m, 24 H, -CO-CH_2-CH_2-CH_2-CO-), 3.0 (m, 8 H, βH cysteine), 3.1-3.2 (m, 32 H, βH lysine, histidine), 3.2-3.3 (m, 48 H, -CH_2- Tt), 3.4-3.5 (m, 96 H, -CH_2- Tt),, 4.1-4.3 (m, 8 H, αH lysine, alanine, cysteine), 4.7 (m, 12 H, αH histidine) 7.3 (12 H, imidazole H histidine), 8.6 (12 H, imidazole H histidine).

Oligomer Id: 524 Sequence: A-K-(K-((A-Gtt)$_3$-C)$_2$)$_2$

δ (ppm) = 1.3-1.8 (m, 57 H, γδεH lysine, -CH_3 alanine), 2.2-2.3 (t, 48 H, -CO-CH_2-CH_2-CH_2-CO-), 1.8-1.9 (m, 24 H, -CO-CH_2-CH_2-CH_2-CO-), 3.0 (m, 8 H, βH cysteine), 3.1-3.2 (m, 6 H, βH lysine), 3.2-3.3 (m, 48 H, -CH_2- Tt), 3.4-3.5 (m, 96 H, -CH_2- Tt),, 4.1-4.3 (m, 20 H, αH amino acids).

Oligomer Id: 522 Sequence: A-K-(K-((H-Gtt)$_3$-A)$_2$)$_2$

δ (ppm) = 1.3-1.8 (m, 33 H, γδεH lysine, -CH_3 alanine), 2.2-2.3 (t, 48 H, -CO-CH_2-CH_2-CH_2-CO-), 1.8-1.9 (m, 24 H, -CO-CH_2-CH_2-CH_2-CO-), 3.1-3.2 (m, 32 H, βH lysine, histidine), 3.2-3.3 (m, 48 H, -CH_2- Tt), 3.4-3.5 (m, 96 H, -CH_2- Tt), 4.1-4.3 (m, 8 H, αH lysine, alanine), 4.7 (m, 12 H, αH histidine) 7.3 (12 H, imidazole H histidine), 8.6 (12 H, imidazole H histidine).

Oligomer Id: 525 Sequence: A-K-(K-((A-Gtt)$_3$-A)$_2$)$_2$

δ (ppm) = 1.3-1.8 (m, 69 H, γδεH lysine, -CH_3 alanine), 2.2-2.3 (t, 48 H, -CO-CH_2-CH_2-CH_2-CO-), 1.8-1.9 (m, 24 H, -CO-CH_2-CH_2-CH_2-CO-), 3.1-3.2 (m, 6 H, βH lysine), 3.2-3.3 (m, 48 H, -CH_2- Tt), 3.4-3.5 (m, 96 H, -CH_2- Tt), 4.1-4.3 (m, 20 H, αH amino acids).

Oligomer Id: 573 Sequence: A-K-(H-K-((H-Stp)$_3$-H-C)$_2$)$_2$

δ (ppm) = 1.3-1.8 (m, 21 H, γδεH lysine, -CH_3 alanine), 2.5-2.6 (m, 48 H, -CO-CH_2-CH_2-CO-), 3.0 (m, 8 H, βH cysteine), 3.1-3.2 (m, 36 H, βH lysine, histidine), 3.2-3.4 (m, 48 H, -CH_2- Tp), 3.48-3.54 (m, 144 H, -CH_2- Tp), 4.1-4.3 (m, 8 H, αH lysine, alanine, cysteine), 4.7 (m, 14 H, αH histidine) 7.3 (14 H, imidazole H histidine), 8.6 (14 H, imidazole H histidine).

Oligomer Id: 575 Sequence: A-K-(A-K-((A-Stp)$_3$-A-C)$_2$)$_2$

δ (ppm) = 1.3-1.8 (m, 75 H, γδεH lysine, -CH_3 alanine), 2.5-2.6 (m, 48 H, -CO-CH_2-CH_2-CO-), 3.0 (m, 8 H, βH cysteine), 3.1 (t, 6 H, βH lysine), 3.2-3.4 (m, 48 H, -CH_2-Tp), 3.48-3.54 (m, 144 H, -CH_2- Tp), 4.1-4.3 (m, 26 H, αH amino acids).

Oligomer Id: 574 Sequence: A-K-(H-K-((H-Stp)$_3$-H-A)$_2$)$_2$

δ (ppm) = 1.3-1.8 (m, 33 H, γδεH lysine, -CH_3 alanine), 2.5-2.6 (m, 48 H, -CO-CH_2-CH_2-CO-), 3.1-3.2 (m, 36 H, βH lysine, histidine), 3.2-3.4 (m, 48 H, -CH_2- Tp), 3.48-3.54 (m, 144 H, -CH_2- Tp), 4.1-4.3 (m, 8 H, αH lysine, alanine), 4.7 (m, 14 H, αH histidine) 7.3 (14 H, imidazole H histidine), 8.6 (14 H, imidazole H histidine).

Oligomer Id: 576 Sequence: A-K-(A-K-((A-Stp)$_3$-A-A)$_2$)$_2$

δ (ppm) = 1.3-1.8 (m, 87 H, γδεH lysine, -CH_3 alanine), 2.5-2.6 (m, 48 H, -CO-CH_2-CH_2-CO-), 3.1 (t, 6 H, βH lysine), 3.2-3.4 (m, 48 H, -CH_2- Tp), 3.48-3.54 (m, 144 H, -CH_2- Tp), 4.1-4.3 (m, 26 H, αH amino acids).

Oligomer Id: 577 Sequence: A-K-(H-K-((H-Gtt)$_3$-H-C)$_2$)$_2$

δ (ppm) = 1.3-1.8 (m, 21 H, γδεH lysine, -CH_3 alanine), 2.2-2.3 (t, 48 H, -CO-CH_2-CH_2-CH_2-CO-), 1.8-1.9 (m, 24 H, -CO-CH_2-CH_2-CH_2-CO-), 3.0 (m, 8 H, βH cysteine), 3.1-3.2 (m, 42 H, βH lysine, histidine), 3.2-3.3 (m, 48 H, -CH_2- Tt), 3.4-3.5 (m, 96 H, -CH_2- Tt), 4.1-4.3 (m, 8 H, αH lysine, alanine, cysteine), 4.7 (m, 18 H, αH histidine) 7.3 (18 H, imidazole H histidine), 8.6 (18 H, imidazole H histidine).

Oligomer Id: 579 Sequence: A-K-(A-K-((A-Gtt)$_3$-A-C)$_2$)$_2$

δ (ppm) = 1.3-1.8 (m, 75 H, γδεH lysine, -CH_3 alanine), 2.2-2.3 (t, 48 H, -CO-CH_2-CH_2-CH_2-CO-), 1.8-1.9 (m, 24 H, -CO-CH_2-CH_2-CH_2-CO-), 3.0 (m, 8 H, βH cysteine), 3.1-3.2 (m, 6 H, βH lysine), 3.2-3.3 (m, 48 H, -CH_2- Tt), 3.4-3.5 (m, 96 H, -CH_2- Tt), 4.1-4.3 (m, 26 H, αH amino acids).

Oligomer Id: 578 Sequence: A-K-(H-K-((H-Gtt)$_3$-H-A)$_2$)$_2$

δ (ppm) = 1.3-1.8 (m, 33 H, γδεH lysine, -CH_3 alanine), 2.2-2.3 (t, 48 H, -CO-CH_2-CH_2-CH_2-CO-), 1.8-1.9 (m, 24 H, -CO-CH_2-CH_2-CH_2-CO-), 3.1-3.2 (m, 42 H, βH lysine, histidine), 3.2-3.3 (m, 48 H, -CH_2- Tt), 3.4-3.5 (m, 96 H, -CH_2- Tt), 4.1-4.3 (m,

8 H, αH lysine, alanine), 4.7 (m, 18 H, αH histidine) 7.3 (18 H, imidazole H histidine), 8.6 (18 H, imidazole H histidine).

Oligomer Id: 580 Sequence: A-K-(A-K-((A-Gtt)$_3$-A-A)$_2$)$_2$

δ (ppm) = 1.3-1.8 (m, 87 H, γδεH lysine, -CH_3 alanine), 2.2-2.3 (t, 48 H, -CO-CH_2-CH_2-CH_2-CO-), 1.8-1.9 (m, 24 H, -CO-CH_2-CH_2-CH_2-CO-), 3.1-3.2 (m, 6 H, βH lysine), 3.2-3.3 (m, 48 H, -CH_2- Tt), 3.4-3.5 (m, 96 H, -CH_2- Tt), 4.1-4.3 (m, 26 H, αH amino acids).

Oligomer Id: 582 Sequence: A-K-(K-(K-H-(K-H_2)$_3$-K-H-K)$_2$)$_2$

δ (ppm) = 1.3-1.8 (m, 165 H, γδεH lysine, -CH_3 alanine), 2.9-3.0 (m, 54 H, βH lysine), 3.0-3.3 (m, 64 H, βH histidine), 3.9-4.3 (m, 28 H, αH lysine, alanine), 4.7 (m, 32 H, αH histidine) 7.3 (32 H, imidazole H histidine), 8.6 (32 H, imidazole H histidine).

Oligomer Id: 584 Sequence: A-K-(K-(K-H-(K-H_2)$_5$-K-H-K)$_2$)$_2$

δ (ppm) = 1.3-1.8 (m, 213 H, γδεH lysine, -CH_3 alanine), 2.9-3.0 (m, 70 H, βH lysine), 3.0-3.3 (m, 96 H, βH histidine), 3.9-4.3 (m, 36 H, αH lysine, alanine), 4.7 (m, 48 H, αH histidine) 7.3 (48 H, imidazole H histidine), 8.6 (48 H, imidazole H histidine).

7.2.2 Linear cysteine-containing Stp oligomers

Sequence: C-Stp

δ (ppm) = 2.5-2.6 (m, 4 H, -CO-CH_2-CH_2-CO-), 3.0 (m, 2 H, βH cysteine), 3.2-3.4 (m, 4 H, -CH_2- Tp), 3.48-3.54 (m, 12 H, -CH_2- Tp), 4.1-4.3 (m, 1 H, αH cysteine).

Sequence: C-Stp$_2$

δ (ppm) = 2.5-2.6 (m, 8 H, -CO-CH_2-CH_2-CO-), 3.0 (m, 2 H, βH cysteine), 3.2-3.4 (m, 8H, -CH_2- Tp), 3.48-3.54 (m, 24 H, -CH_2- Tp), 4.1-4.3 (m, 1 H, αH cysteine).

Sequence: C-Stp$_3$

δ (ppm) = 2.5-2.6 (m, 12 H, -CO-CH_2-CH_2-CO-), 3.0 (m, 2 H, βH cysteine), 3.2-3.4 (m, 12 H, -CH_2- Tp), 3.48-3.54 (m, 36 H, -CH_2- Tp), 4.1-4.3 (m, 1 H, αH cysteine).

Sequence: C-Stp$_4$

δ (ppm) = 2.5-2.6 (m, 16 H, -CO-CH_2-CH_2-CO-), 3.0 (m, 2 H, βH cysteine), 3.2-3.4 (m, 16 H, -CH_2- Tp), 3.48-3.54 (m, 48 H, -CH_2- Tp), 4.1-4.3 (m, 1 H, αH cysteine).

Sequence: C-Stp_5

δ (ppm) = 2.5-2.6 (m, 20 H, -CO-CH_2-CH_2-CO-), 3.0 (m, 2 H, βH cysteine), 3.2-3.4 (m, 20 H, -CH_2- Tp), 3.48-3.54 (m, 60 H, -CH_2- Tp), 4.1-4.3 (m, 1 H, αH cysteine).

7.2.3 PPI conjugates

Conjugate Id: 418 Sequence: PPI-(C-C-$Stp)_8$

δ (ppm) = 1.7-2.0 (m, 28 H, -CH_2-CH_2-CH_2- PPI), 2.5-2.6 (m, 32 H, -CO-CH_2-CH_2-CO-), 3.0-3.5 (m, 32 H, βH cysteine; m, 32 H, -CH_2- Tp; m, 148 H, -CH_2- Tp, -CH_2-CH_2-CH_2- PPI), 4.0-4.5 (m, 16 H, αH amino acids).

Conjugate Id: 427 Sequence: PPI-(C-C-$Stp_2)_8$

δ (ppm) = 1.7-2.0 (m, 28 H, -CH_2-CH_2-CH_2- PPI), 2.5-2.6 (m, 64 H, -CO-CH_2-CH_2-CO-), 3.0-3.5 (m, 32 H, βH cysteine; m, 64 H, -CH_2- Tp; m, 244 H, -CH_2- Tp, -CH_2-CH_2-CH_2- PPI), 4.0-4.5 (m, 16 H, αH amino acids).

Conjugate Id: 428 Sequence: PPI-(C-C-$Stp_3)_8$

δ (ppm) = 1.7-2.0 (m, 28 H, -CH_2-CH_2-CH_2- PPI), 2.5-2.6 (m, 96 H, -CO-CH_2-CH_2-CO-), 3.0-3.5 (m, 32 H, βH cysteine; m, 96 H, -CH_2- Tp; m, 340 H, -CH_2- Tp, -CH_2-CH_2-CH_2- PPI), 4.0-4.5 (m, 16 H, αH amino acids).

Conjugate Id: 526 Sequence: PPI-(C-C-$Stp_5)_8$

δ (ppm) = 1.7-2.0 (m, 28 H, -CH_2-CH_2-CH_2- PPI), 2.5-2.6 (m, 160 H, -CO-CH_2-CH_2-CO-), 3.0-3.5 (m, 32 H, βH cysteine; m, 160 H, -CH_2- Tp; m, 532 H, -CH_2- Tp, -CH_2-CH_2-CH_2- PPI), 4.0-4.5 (m, 16 H, αH amino acids).

7.3 Additional analytical Ion Exchange Chromatography traces of four-arm unmodified Stp oligomers

Analytical runs were performed after dialysis in 10 mM HCl on an Äkta Basic HPLC system, column: Resource S 1 ml (GE Healthcare). Buffer A: 10 mM HCl. Buffer B: 10 mM HCl + 3 M NaCl. Flow rate 2 ml/min. Gradient: 2% B to 100% B in 15min. UV detection at 214 nm and 280 nm.

286 Stp1

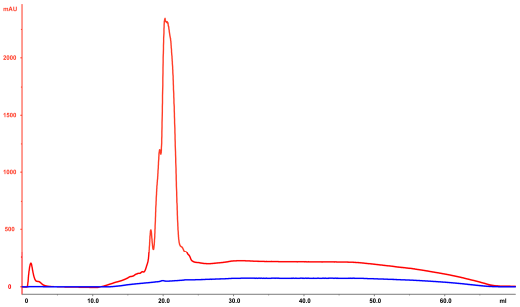

287 Stp2

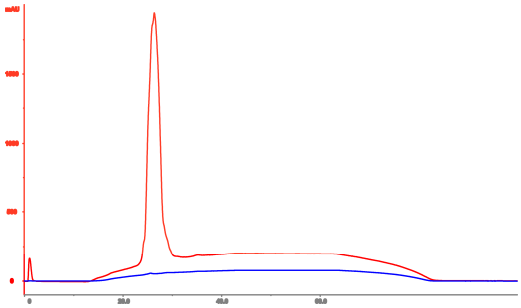

288 Stp3

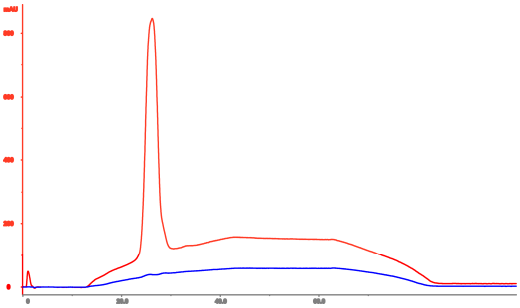

289 Stp4

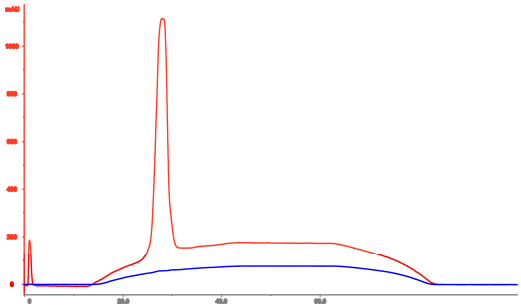

7.4 AFM images

AFM images of pDNA polyplexes formed at N/P 12 with (A) Stp-based oligomer 402 and (B) Sph-based oligomer 519. (C) Particles formed with Gtt-based oligomer 494 did not form particles detectable by AFM.

pDNA polyplexes were prepared in 20 mM HEPES, pH 7.4 at N/P 12. After 30 min incubation, samples were diluted 1:10 in 20 mM HEPES buffer pH 7.4 and 10µl of the dilution was pipetted onto a freshly cleaved mica surface. Samples were imaged in the tapping mode on a Multimode VIII AFM (Bruker AXS, Santa Barbara, USA). Experiments were performed together with Max Scheible, Department of Physics at ZNN/WSI, Biomolecular Systems and Bionanotechnology, TU Munich, Germany.

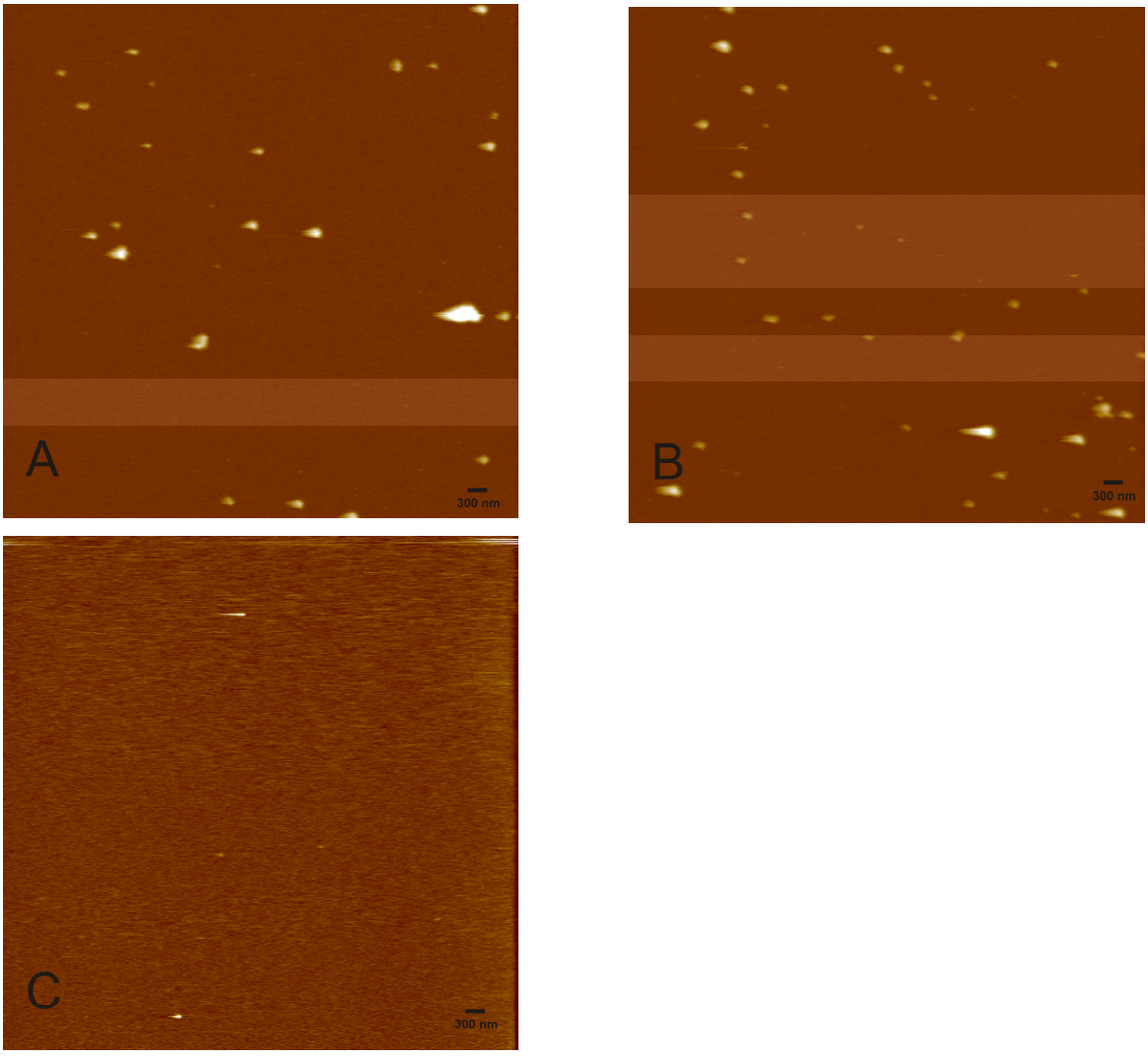

7.5 Additional particle size and zeta potential measurements

7.5.1 Five-arm oligomers after complexation with pDNA at N/P 12.

Oligomer Id	Sequence	Mean Size [nm]	Mean PdI	Mean Zeta Potential [mV]
414	A-Stp_2-K-(K-(Stp_2-C)$_2$)$_2$	539 ± 80	0.410 ± 0.01	15.3 ± 0.5
424	A-Stp_3-K-(K-(Stp_3-C)$_2$)$_2$	298 ± 47	0.282 ± 0.00	25.0 ± 0.0
425	A-Stp_4-K-(K-(Stp_4-C)$_2$)$_2$	101 ± 37	0.143 ± 0.03	25.0 ± 0.0

7.5.2 Size and zeta potential of siRNA Polyplexes.

Complexation of siRNA with four-arm oligomers at N/P 12.

Oligomer Id	Sequence	Mean Size [nm]	Mean PdI	Mean Zeta Potential [mV]
392	A-K-(K-(Stp_3-C)$_2$)$_2$	409 ± 79	0.267 ± 0.01	32.6 ± 0.4
402	A-K-(K-(Stp_4-C)$_2$)$_2$	356 ± 82	0.273 ± 0.01	34.7 ± 0.3

Oligomer Id	Sequence	Mean Size [nm]	Mean PdI	Mean Zeta Potential [mV]
519	A-K-(K-(Sph_4-C)$_2$)$_2$	506 ± 25	0.375 ± 0.06	27.8 ± 0.4
535	A-K-(K-(Sph_4-A)$_2$)$_2$	329 ± 26	0.336 ± 0.04	24.4 ± 2.2

Complexation of siRNA with five-arm oligomers at N/P 12.

Oligomer Id	Sequence	Mean Size [nm]	Mean PdI	Mean Zeta Potential [mV]
414	A-Stp_2-K-(K-(Stp_2-C)$_2$)$_2$	489 ± 44	0.338 ± 0.01	28.0 ± 0.5
424	A-Stp_3-K-(K-(Stp_3-C)$_2$)$_2$	375 ± 62	0.210 ± 0.02	30.5 ± 0.8
425	A-Stp_4-K-(K-(Stp_4-C)$_2$)$_2$	n.d.	-	n.d.

n.d. not detectable

7.6 Abbreviations

ATP	Adenosine triphosphate
BCNP	Boc-Cys(NPys)-OH
Boc	*tert*-Butyloxycarbonyl
CMPI	2-Chloro-1-methylpyridinium iodide
CMV	Cytomegalovirus
Da	Dalton
DCM	Dichloromethane
DCU	Dicyclohexylurea
DIPEA	Diisopropylethylamine
DLS	Dynamic light scattering
DMEM	Dulbecco's Modified Eagle's Medium
DMF	Dimethylformamide
DMSO	Dimethyl sulfoxide
DNTB	5,5'-dithiobis-2-nitrobenzoic acid (Ellman's reagent)
DTT	Dithiothreitol
eGFP	Enhanced green fluorescent protein
EPR	Enhanced permeability and retention
EtBr	Ethidium bromide
FBS	Foetal bovine serum
Fmoc	9-Fluorenylmethyloxycarbonyl
GSH	Glutathione
Gtt	Glutaroyl-triethylentetraamine
HBG	HEPES-buffered glucose
HEPES	N-(2-hydroxyethyl) piperazine-N'-(2-ethansulfonic acid)
HOBt	1-Hydroxybenzotriazol
IEX	Ion exchange
LL	Low load
linPEI	Linear polyethylenimine
Luc	Luciferase
MALDI	Matrix assisted laser desorption ionization mass spectrometry
MES	2-(N-morpholino)ethanesulfonic acid
MTT	Methylthiazoletetrazolium
Mw	Molecular weight

MWCO	Molecular weight cut-off
^{1}H-NMR	Proton nuclear magnetic resonance
NPys	3-Nitro-2-pyridinesulfenyl
N/P-ratio	Molar ratio of protonable nitrogens to phosphates
PBS	Phosphate-buffered saline
pDNA	Plasmid deoxyribonucleic acid
pEGFPLuc	Plasmid encoding for luciferase under control of the EGFP promoter/enhancer
PEI	Polyethylenimine
Pfp	Pentafluorophenol
Pip	Piperidine
PPI	Polypropylenimine
PyBOP®	Benzotriazol-1-yl-oxytripyrrolidinophosphonium-hexafluorophosphate
RBF	Round-bottom flask
RISC	RNA-induced silencing complex
RLU	Relative light units
RNA	Ribonucleic acid
RNAi	RNA interference
RP-HPLC	Reversed-Phase High-performance liquid chromatography
RT	Room temperature
SAR	Structure-activity relationship
SEC	Size exclusion chromatography
siRNA	Small interfering RNA
Sph	Succinyl-pentaethylenhexamine
SPS	Solid-phase synthesis
Stp	Succinoyl-tetraethylenpentamine
Succ	Succinoyl
TCEP	Tris(2-carboxyethyl) phosphine
TFA	Trifluoroacetic acid
TIS	Triisopropylsilane
TLC	Thin layer chromatography
Trt	Trityl
UV-VIS	Ultraviolett-Visible spectroscopy
w/w	Weight to weight ratio (e.g. of conjugate to nucleic acid)

7.7 Publications

7.7.1 Original papers

Schaffert, David; Troiber, Christina; Salcher, Eveline E.; Fröhlich, Thomas; Martin, Irene; Badgujar, Naresh; Dohmen, Christian; Edinger, Daniel; Kläger, Raphaela; Maiwald, Gelja; Farkasova, Katarina; Seeber, Silke; Jahn-Hofmann, Kerstin; Hadwiger, Philipp; Wagner, Ernst: *Solid-phase synthesized sequence-defined t-shape, i-shape and u-shape polymers for pDNA and siRNA delivery,* Angewandte Chemie International Edition (2011), 50, 8986-8989

Fröhlich, Thomas; Edinger, Daniel; Kläger, Raphaela; Troiber, Christina; Salcher, Edith; Badgujar, Naresh; Martin, Irene; Schaffert, David; Cengizeroglu, Arzu; Hadwiger, Philipp; Vornlocher, Hans-Peter; Wagner, Ernst: *Structure-activity relationships of siRNA carriers based on sequence-defined oligo (ethane amino) amides*, Journal of Controlled Release (2012), 160, 532-541

Salcher, Eveline E.; Kos, Petra; Fröhlich, Thomas; Badgujar, Naresh; Scheible, Max; Wagner, Ernst: *Sequence-defined Four-arm Oligo(ethanamino)amides for pDNA and siRNA Delivery: Impact of Building Blocks on Efficacy,* Journal of Controlled Release (2012), Journal of Controlled Release (2012), 164, 380-386

Lächelt, Ulrich; Kos, Petra; Mickler, Frauke M.; Salcher, Eveline E.; Rödl, Wolfgang; Badgujar, Naresh; Bräuchle, Christoph; Wagner, Ernst (2013) *Fine-tuning of proton sponges by precise diaminoethanes and histidines in pDNA polyplexes*. Submitted.

Kos, Petra; Scholz, Claudia; Salcher, Eveline E.; Herrmann, Annika; Wagner, Ernst: *Gene transfer with sequence-defined oligo(ethanamino)amides bioreducibly attached to a propylenimine dendrimer core*. Submitted.

7.7.2 Book chapters

E. Salcher and E. Wagner: *Chemically programmed polymers for targeted DNA and siRNA transfection,* Topics in Current Chemistry (2010); 296:227-249

E. Salcher and E. Wagner: *Nanoencapsulation of oligonucleotides for therapeutic use*, Nucleic Acids Nanotechnology, Manuscript submitted

7.7.3 Poster presentation

E. Salcher, D. Schaffert, Thomas Fröhlich, P. Kos, E. Wagner: *Solid-Phase Supported Synthesis of Branched Cationic Polymers for Gene Delivery,* CeNS Workshop, Venice, Italy, September 2011

7.7.4 Oral presentation

E. Salcher, D. Schaffert, Thomas Fröhlich, P. Kos, E. Wagner: *Solid-phase Synthesis of Precise Branched Polymers for Gene Delivery*, Doktorandenseminar Fakultät für Chemie und Pharmazie, LMU München, Munich, April 2011

8 REFERENCES

[1] T. Friedmann, R. Roblin, Gene therapy for human genetic disease?, Science, 178 (1972) 648-649.

[2] A. Aiuti, A.C. Bachoud-Levi, A. Blesch, M.K. Brenner, F. Cattaneo, E.A. Chiocca, G. Gao, K.A. High, A.M. Leen, N.R. Lemoine, I.A. McNeish, G. Meneguzzi, M. Peschanski, M.G. Roncarolo, D.S. Strayer, M.H. Tuszynski, D.J. Waxman, J.M. Wilson, Progress and prospects: gene therapy clinical trials (part 2), Gene Ther, 14 (2007) 1555-1563.

[3] M.L. Edelstein, M.R. Abedi, J. Wixon, Gene therapy clinical trials worldwide to 2007--an update, J Gene Med, 9 (2007) 833-842.

[4] N.C. Hasbrouck, K.A. High, AAV-mediated gene transfer for the treatment of hemophilia B: problems and prospects, Gene Ther, 15 (2008) 870-875.

[5] J.W. Bainbridge, R.R. Ali, Success in sight: The eyes have it! Ocular gene therapy trials for LCA look promising, Gene Ther, 15 (2008) 1191-1192.

[6] S.T. Crooke, Progress in antisense technology, Annu Rev Med, 55 (2004) 61-95.

[7] H. Yin, Q. Lu, M. Wood, Effective exon skipping and restoration of dystrophin expression by peptide nucleic acid antisense oligonucleotides in mdx mice, Mol Ther, 16 (2008) 38-45.

[8] E. Song, S.K. Lee, J. Wang, N. Ince, N. Ouyang, J. Min, J. Chen, P. Shankar, J. Lieberman, RNA interference targeting Fas protects mice from fulminant hepatitis, Nat Med, 9 (2003) 347-351.

[9] T.R. Brummelkamp, R. Bernards, R. Agami, A system for stable expression of short interfering RNAs in mammalian cells, Science, 296 (2002) 550-553.

[10] N. Tomita, H. Azuma, Y. Kaneda, T. Ogihara, R. Morishita, Application of decoy oligodeoxynucleotides-based approach to renal diseases, Curr Drug Targets, 5 (2004) 717-733.

[11] H. Ulrich, C.A. Trujillo, A.A. Nery, J.M. Alves, P. Majumder, R.R. Resende, A.H. Martins, DNA and RNA aptamers: from tools for basic research towards therapeutic applications, Comb Chem High Throughput Screen, 9 (2006) 619-632.

[12] A. Shir, M. Ogris, E. Wagner, A. Levitzki, EGF receptor-targeted synthetic double-stranded RNA eliminates glioblastoma, breast cancer, and adenocarcinoma tumors in mice, PLoS Med, 3 (2006) e6.

[13] D. Schaffert, M. Kiss, W. Rodl, A. Shir, A. Levitzki, M. Ogris, E. Wagner, Poly(I:C)-mediated tumor growth suppression in EGF-receptor overexpressing tumors using EGF-polyethylene glycol-linear polyethylenimine as carrier, Pharm Res, 28 (2011) 731-741.

[14] J. Mattes, M. Yang, P.S. Foster, Regulation of microRNA by antagomirs: a new class of pharmacological antagonists for the specific regulation of gene function?, Am J Respir Cell Mol Biol, 36 (2007) 8-12.

[15] J. Krutzfeldt, N. Rajewsky, R. Braich, K.G. Rajeev, T. Tuschl, M. Manoharan, M. Stoffel, Silencing of microRNAs in vivo with 'antagomirs', Nature, 438 (2005) 685-689.

[16] A. Fire, S. Xu, M.K. Montgomery, S.A. Kostas, S.E. Driver, C.C. Mello, Potent and specific genetic interference by double-stranded RNA in Caenorhabditis elegans, Nature, 391 (1998) 806-811.

[17] S.M. Elbashir, J. Harborth, W. Lendeckel, A. Yalcin, K. Weber, T. Tuschl, Duplexes of 21-nucleotide RNAs mediate RNA interference in cultured mammalian cells, Nature, 411 (2001) 494-498.

[18] M.R. Lares, J.J. Rossi, D.L. Ouellet, RNAi and small interfering RNAs in human disease therapeutic applications, Trends Biotechnol, 28 (2010) 570-579.

[19] J.C. Burnett, J.J. Rossi, K. Tiemann, Current progress of siRNA/shRNA therapeutics in clinical trials, Biotechnol J, 6 (2011) 1130-1146.

[20] B.E. Houk, G. Hochhaus, J.A. Hughes, Kinetic modeling of plasmid DNA degradation in rat plasma, AAPS PharmSci, 1 (1999) E9.

[21] B.E. Houk, R. Martin, G. Hochhaus, J.A. Hughes, Pharmacokinetics of plasmid DNA in the rat, Pharm Res, 18 (2001) 67-74.

[22] G.L. Lukacs, P. Haggie, O. Seksek, D. Lechardeur, N. Freedman, A.S. Verkman, Size-dependent DNA mobility in cytoplasm and nucleus, J Biol Chem, 275 (2000) 1625-1629.

[23] E. Dauty, A.S. Verkman, Actin cytoskeleton as the principal determinant of size-dependent DNA mobility in cytoplasm: a new barrier for non-viral gene delivery, J Biol Chem, 280 (2005) 7823-7828.

[24] W.M. Bonner, Protein migration into nuclei. I. Frog oocyte nuclei in vivo accumulate microinjected histones, allow entry to small proteins, and exclude large proteins, J Cell Biol, 64 (1975) 421-430.

[25] P.L. Paine, L.C. Moore, S.B. Horowitz, Nuclear envelope permeability, Nature, 254 (1975) 109-114.
[26] C.M. Feldherr, E. Kallenbach, N. Schultz, Movement of a karyophilic protein through the nuclear pores of oocytes, J Cell Biol, 99 (1984) 2216-2222.
[27] S. Brunner, T. Sauer, S. Carotta, M. Cotten, M. Saltik, E. Wagner, Cell cycle dependence of gene transfer by lipoplex, polyplex and recombinant adenovirus, Gene Ther, 7 (2000) 401-407.
[28] S. Brunner, E. Furtbauer, T. Sauer, M. Kursa, E. Wagner, Overcoming the nuclear barrier: cell cycle independent nonviral gene transfer with linear polyethylenimine or electroporation, Mol Ther, 5 (2002) 80-86.
[29] R. Bausinger, K. von Gersdorff, K. Braeckmans, M. Ogris, E. Wagner, C. Brauchle, A. Zumbusch, The transport of nanosized gene carriers unraveled by live-cell imaging, Angew Chem Int Ed Engl, 45 (2006) 1568-1572.
[30] K. de Bruin, N. Ruthardt, K. von Gersdorff, R. Bausinger, E. Wagner, M. Ogris, C. Brauchle, Cellular dynamics of EGF receptor-targeted synthetic viruses, Mol Ther, 15 (2007) 1297-1305.
[31] W. Walther, U. Stein, Viral vectors for gene transfer: a review of their use in the treatment of human diseases, Drugs, 60 (2000) 249-271.
[32] L. Jager, A. Ehrhardt, Emerging adenoviral vectors for stable correction of genetic disorders, Curr Gene Ther, 7 (2007) 272-283.
[33] F. Mingozzi, K.A. High, Therapeutic in vivo gene transfer for genetic disease using AAV: progress and challenges, Nat Rev Genet, 12 (2011) 341-355.
[34] J. D'Costa, S.G. Mansfield, L.M. Humeau, Lentiviral vectors in clinical trials: Current status, Curr Opin Mol Ther, 11 (2009) 554-564.
[35] L.B. Couto, K.A. High, Viral vector-mediated RNA interference, Curr Opin Pharmacol, 10 (2010) 534-542.
[36] P.J. Paddison, A.A. Caudy, E. Bernstein, G.J. Hannon, D.S. Conklin, Short hairpin RNAs (shRNAs) induce sequence-specific silencing in mammalian cells, Genes Dev, 16 (2002) 948-958.
[37] S. Nayak, R.W. Herzog, Progress and prospects: immune responses to viral vectors, Gene Ther, 17 (2010) 295-304.
[38] L. Biasco, C. Baricordi, A. Aiuti, Retroviral integrations in gene therapy trials, Mol Ther, 20 (2012) 709-716.

[39] S. Boeckle, E. Wagner, Optimizing targeted gene delivery: chemical modification of viral vectors and synthesis of artificial virus vector systems, AAPS J 8(2006) E731-E742.

[40] L. Zhu, R.I. Mahato, Lipid and polymeric carrier-mediated nucleic acid delivery, Expert Opin Drug Deliv, 7 (2010) 1209-1226.

[41] D. Schaffert, E. Wagner, Gene therapy progress and prospects: synthetic polymer-based systems, Gene Ther, 15 (2008) 1131-1138.

[42] S.D. Li, L. Huang, Non-viral is superior to viral gene delivery, J Control Release, 123 (2007) 181-183.

[43] P.L. Felgner, T.R. Gadek, M. Holm, R. Roman, H.W. Chan, M. Wenz, J.P. Northrop, G.M. Ringold, M. Danielsen, Lipofection: a highly efficient, lipid-mediated DNA-transfection procedure, Proc Natl Acad Sci U S A, 84 (1987) 7413-7417.

[44] N.J. Caplen, E.W. Alton, P.G. Middleton, J.R. Dorin, B.J. Stevenson, X. Gao, S.R. Durham, P.K. Jeffery, M.E. Hodson, C. Coutelle, et al., Liposome-mediated CFTR gene transfer to the nasal epithelium of patients with cystic fibrosis, Nat Med, 1 (1995) 39-46.

[45] W. Li, F.C. Szoka, Jr., Lipid-based nanoparticles for nucleic acid delivery, Pharm Res, 24 (2007) 438-449.

[46] A. Schroeder, C.G. Levins, C. Cortez, R. Langer, D.G. Anderson, Lipid-based nanotherapeutics for siRNA delivery, J Intern Med, 267 (2010) 9-21.

[47] C.E. Smull, E.H. Ludwig, Enhancement of the plaque-forming capacity of poliovirus ribonucleic acid with basic proteins, J Bacteriol, 84 (1962) 1035-1040.

[48] P.L. Felgner, Y. Barenholz, J.P. Behr, S.H. Cheng, P. Cullis, L. Huang, J.A. Jessee, L. Seymour, F. Szoka, A.R. Thierry, E. Wagner, G. Wu, Nomenclature for synthetic gene delivery systems, Hum Gene Ther, 8 (1997) 511-512.

[49] S.M. Moghimi, P. Symonds, J.C. Murray, A.C. Hunter, G. Debska, A. Szewczyk, A two-stage poly(ethylenimine)-mediated cytotoxicity: implications for gene transfer/therapy, Mol Ther, 11 (2005) 990-995.

[50] P. Chollet, M.C. Favrot, A. Hurbin, J.L. Coll, Side-effects of a systemic injection of linear polyethylenimine-DNA complexes, J Gene Med, 4 (2002) 84-91.

[51] P.R. Dash, M.L. Read, L.B. Barrett, M.A. Wolfert, L.W. Seymour, Factors affecting blood clearance and in vivo distribution of polyelectrolyte complexes for gene delivery 962, Gene Ther 6(1999) 643-650.

[52] R.S. Burke, S.H. Pun, Extracellular barriers to in Vivo PEI and PEGylated PEI polyplex-mediated gene delivery to the liver, Bioconjug Chem, 19 (2008) 693-704.
[53] M. Ogris, P. Steinlein, M. Kursa, K. Mechtler, R. Kircheis, E. Wagner, The size of DNA/transferrin-PEI complexes is an important factor for gene expression in cultured cells, Gene Ther, 5 (1998) 1425-1433.
[54] M. Lee, S.W. Kim, Polyethylene glycol-conjugated copolymers for plasmid DNA delivery, Pharm Res 22 (2005) 1-10.
[55] P. Erbacher, T. Bettinger, P. Belguise-Valladier, S. Zou, J.L. Coll, J.P. Behr, J.S. Remy, Transfection and physical properties of various saccharide, poly(ethylene glycol), and antibody-derivatized polyethylenimines (PEI), J Gene Med, 1 (1999) 210-222.
[56] D. Oupicky, M. Ogris, K.A. Howard, P.R. Dash, K. Ulbrich, L.W. Seymour, Importance of lateral and steric stabilization of polyelectrolyte gene delivery vectors for extended systemic circulation, Mol Ther, 5 (2002) 463-472.
[57] M. Kursa, G.F. Walker, V. Roessler, M. Ogris, W. Roedl, R. Kircheis, E. Wagner, Novel Shielded Transferrin-Polyethylene Glycol-Polyethylenimine/DNA Complexes for Systemic Tumor-Targeted Gene Transfer, Bioconjug Chem 14 (2003) 222-231.
[58] B. Brissault, A. Kichler, C. Leborgne, O. Danos, H. Cheradame, J. Gau, L. Auvray, C. Guis, Synthesis, characterization, and gene transfer application of poly(ethylene glycol-b-ethylenimine) with high molar mass polyamine block, Biomacromolecules, 7 (2006) 2863-2870.
[59] M. Ogris, G. Walker, T. Blessing, R. Kircheis, M. Wolschek, E. Wagner, Tumor-targeted gene therapy: strategies for the preparation of ligand-polyethylene glycol-polyethylenimine/DNA complexes, J Control Release, 91 (2003) 173-181.
[60] W.J. Kim, J.W. Yockman, M. Lee, J.H. Jeong, Y.H. Kim, S.W. Kim, Soluble Flt-1 gene delivery using PEI-g-PEG-RGD conjugate for anti-angiogenesis, J Control Release, 106 (2005) 224-234.
[61] S. Moffatt, C. Papasakelariou, S. Wiehle, R. Cristiano, Successful in vivo tumor targeting of prostate-specific membrane antigen with a highly efficient J591/PEI/DNA molecular conjugate, Gene Ther, 13 (2006) 761-772.
[62] V. Knorr, L. Allmendinger, G.F. Walker, F.F. Paintner, E. Wagner, An acetal-based PEGylation reagent for pH-sensitive shielding of DNA polyplexes, Bioconjug Chem, 18 (2007) 1218-1225.

[63] V. Knorr, M. Ogris, E. Wagner, An acid sensitive ketal-based polyethylene glycol-oligoethylenimine copolymer mediates improved transfection efficiency at reduced toxicity, Pharm Res, 25 (2008) 2937-2945.
[64] C. Fella, G.F. Walker, M. Ogris, E. Wagner, Amine-reactive pyridylhydrazone-based PEG reagents for pH-reversible PEI polyplex shielding, Eur J Pharm Sci, 34 (2008) 309-320.
[65] Y. Noguchi, J. Wu, R. Duncan, J. Strohalm, K. Ulbrich, T. Akaike, H. Maeda, Early phase tumor accumulation of macromolecules: a great difference in clearance rate between tumor and normal tissues, Jpn.J Cancer Res, 89 (1998) 307-314.
[66] H. Maeda, The enhanced permeability and retention (EPR) effect in tumor vasculature: the key role of tumor-selective macromolecular drug targeting, Adv Enzyme Regul, 41 (2001) 189-207.
[67] G.Y. Wu, C.H. Wu, Receptor-mediated in vitro gene transformation by a soluble DNA carrier system, J Biol Chem, 262 (1987) 4429-4432.
[68] N. Tietze, J. Pelisek, A. Philipp, W. Roedl, T. Merdan, P. Tarcha, M. Ogris, E. Wagner, Induction of apoptosis in murine neuroblastoma by systemic delivery of transferrin-shielded siRNA polyplexes for downregulation of Ran, Oligonucleotides, 18 (2008) 161-174.
[69] Y. Ikeda, K. Taira, Ligand-targeted delivery of therapeutic siRNA, Pharm Res, 23 (2006) 1631-1640.
[70] I. Martin, C. Dohmen, C. Mas-Moruno, C. Troiber, P. Kos, D. Schaffert, U. Lachelt, M. Teixido, M. Gunther, H. Kessler, E. Giralt, E. Wagner, Solid-phase-assisted synthesis of targeting peptide-PEG-oligo(ethane amino)amides for receptor-mediated gene delivery, Org Biomol Chem, 10 (2012) 3258-3268.
[71] S.H. Kim, H. Mok, J.H. Jeong, S.W. Kim, T.G. Park, Comparative evaluation of target-specific GFP gene silencing efficiencies for antisense ODN, synthetic siRNA, and siRNA plasmid complexed with PEI-PEG-FOL conjugate, Bioconjug Chem, 17 (2006) 241-244.
[72] B. Liang, M.L. He, Z.P. Xiao, Y. Li, C.Y. Chan, H.F. Kung, X.T. Shuai, Y. Peng, Synthesis and characterization of folate-PEG-grafted-hyperbranched-PEI for tumor-targeted gene delivery, Biochem Biophys Res Commun, 367 (2008) 874-880.
[73] I. Mellman, Endocytosis and molecular sorting, Annu.Rev.Cell Dev.Biol, 12 (1996) 575-625.

[74] D. Fischer, T. Bieber, Y. Li, H.P. Elsasser, T. Kissel, A novel non-viral vector for DNA delivery based on low molecular weight, branched polyethylenimine: effect of molecular weight on transfection efficiency and cytotoxicity, Pharm Res, 16 (1999) 1273-1279.

[75] L. Wightman, R. Kircheis, V. Rossler, S. Carotta, R. Ruzicka, M. Kursa, E. Wagner, Different behavior of branched and linear polyethylenimine for gene delivery in vitro and in vivo, J Gene Med, 3 (2001) 362-372.

[76] O. Boussif, F. Lezoualc'h, M.A. Zanta, M.D. Mergny, D. Scherman, B. Demeneix, J.P. Behr, A versatile vector for gene and oligonucleotide transfer into cells in culture and in vivo: polyethylenimine, Proc Natl Acad Sci U.S.A, 92 (1995) 7297-7301.

[77] J.P. Behr, The proton sponge: A trick to enter cells viruses did not exploit, Chimia, 51 (1997) 34-36.

[78] E. Wagner, Polymers for siRNA delivery: inspired by viruses to be targeted, dynamic, and precise, Acc Chem Res, 45 (2012) 1005-1013.

[79] A. Akinc, M. Thomas, A.M. Klibanov, R. Langer, Exploring polyethylenimine-mediated DNA transfection and the proton sponge hypothesis, J Gene Med, 7 (2005) 657-663.

[80] M.C. Garnett, Gene-delivery systems using cationic polymers, Crit Rev Ther Drug Carrier Syst, 16 (1999) 147-207.

[81] H. Uchida, K. Miyata, M. Oba, T. Ishii, T. Suma, K. Itaka, N. Nishiyama, K. Kataoka, Odd-even effect of repeating aminoethylene units in the side chain of N-substituted polyaspartamides on gene transfection profiles, J Am Chem Soc, 133 (2011) 15524-15532.

[82] T. Suma, K. Miyata, T. Ishii, S. Uchida, H. Uchida, K. Itaka, N. Nishiyama, K. Kataoka, Enhanced stability and gene silencing ability of siRNA-loaded polyion complexes formulated from polyaspartamide derivatives with a repetitive array of amino groups in the side chain, Biomaterials, 33 (2012) 2770-2779.

[83] K. Miyata, N. Nishiyama, K. Kataoka, Rational design of smart supramolecular assemblies for gene delivery: chemical challenges in the creation of artificial viruses, Chem Soc Rev, 41 (2012) 2562-2574.

[84] P. Midoux, M. Monsigny, Efficient gene transfer by histidylated polylysine/pDNA complexes, Bioconjug Chem, 10 (1999) 406-411.

[85] T. Okuda, A. Sugiyama, T. Niidome, H. Aoyagi, Characters of dendritic poly(L-lysine) analogues with the terminal lysines replaced with arginines and histidines as gene carriers in vitro, Biomaterials, 25 (2004) 537-544.

[86] A. Swami, A. Aggarwal, A. Pathak, S. Patnaik, P. Kumar, Y. Singh, K.C. Gupta, Imidazolyl-PEI modified nanoparticles for enhanced gene delivery, Int J Pharm, 335 (2007) 180-192.

[87] O. Germershaus, G. Pickaert, J. Konrad, U. Kruger, T. Kissel, R. Haag, Imidazole and dimethyl aminopropyl-functionalized hyperbranched polymers for nucleic acid transfection, Macromol Biosci, 10 (2010) 1055-1062.

[88] E. Bertrand, C. Goncalves, L. Billiet, J.P. Gomez, C. Pichon, H. Cheradame, P. Midoux, P. Guegan, Histidinylated linear PEI: a new efficient non-toxic polymer for gene transfer, Chem Commun (Camb), 47 (2011) 12547-12549.

[89] G.S. Yu, Y.M. Bae, H. Choi, B. Kong, I.S. Choi, J.S. Choi, Synthesis of PAMAM dendrimer derivatives with enhanced buffering capacity and remarkable gene transfection efficiency, Bioconjug Chem, 22 (2011) 1046-1055.

[90] S. Asayama, T. Kumagai, H. Kawakami, Synthesis and Characterization of Methylated Poly(l-histidine) To Control the Stability of Its siRNA Polyion Complexes for RNAi, Bioconjug Chem, (2012).

[91] D.B. Rozema, D.L. Lewis, D.H. Wakefield, S.C. Wong, J.J. Klein, P.L. Roesch, S.L. Bertin, T.W. Reppen, Q. Chu, A.V. Blokhin, J.E. Hagstrom, J.A. Wolff, Dynamic PolyConjugates for targeted in vivo delivery of siRNA to hepatocytes, Proc.Natl.Acad.Sci U.S.A, 104 (2007) 12982-12987.

[92] E. Wagner, C. Plank, K. Zatloukal, M. Cotten, M.L. Birnstiel, Influenza virus hemagglutinin HA-2 N-terminal fusogenic peptides augment gene transfer by transferrin-polylysine-DNA complexes: toward a synthetic virus-like gene-transfer vehicle, Proc Natl Acad Sci U S A, 89 (1992) 7934-7938.

[93] K. Mechtler, E. Wagner, Gene transfer mediated by influenza virus peptides: the role of peptide sequence, New J Chem, 21 (1997) 105-111.

[94] S. Boeckle, E. Wagner, M. Ogris, C- versus N-terminally linked melittin-polyethylenimine conjugates: the site of linkage strongly influences activity of DNA polyplexes, J Gene Med, 7 (2005) 1335-1347.

[95] M. Ogris, R.C. Carlisle, T. Bettinger, L.W. Seymour, Melittin enables efficient vesicular escape and enhanced nuclear access of nonviral gene delivery vectors, J Biol Chem, 276 (2001) 47550-47555.

[96] J. Kloeckner, S. Boeckle, D. Persson, W. Roedl, M. Ogris, K. Berg, E. Wagner, DNA polyplexes based on degradable oligoethylenimine-derivatives: Combination with EGF receptor targeting and endosomal release functions, J.Control Release, 116 (2006) 115-122.

[97] T. Bettinger, R.C. Carlisle, M.L. Read, M. Ogris, L.W. Seymour, Peptide-mediated RNA delivery: a novel approach for enhanced transfection of primary and post-mitotic cells, Nucleic Acids Res., 29 (2001) 3882-3891.

[98] C.E. Dempsey, The actions of melittin on membranes, Biochim Biophys Acta, 1031 (1990) 143-161.

[99] D.B. Rozema, K. Ekena, D.L. Lewis, A.G. Loomis, J.A. Wolff, Endosomolysis by Masking of a Membrane-Active Agent (EMMA) for Cytoplasmic Release of Macromolecules, Bioconjug Chem 14 (2003) 51-57.

[100] S. Boeckle, J. Fahrmeir, W. Roedl, M. Ogris, E. Wagner, Melittin analogs with high lytic activity at endosomal pH enhance transfection with purified targeted PEI polyplexes, J.Control Release, 112 (2006) 240-248.

[101] M. Meyer, A. Philipp, R. Oskuee, C. Schmidt, E. Wagner, Breathing life into polycations: functionalization with pH-responsive endosomolytic peptides and polyethylene glycol enables siRNA delivery, J Am Chem Soc, 130 (2008) 3272-3273.

[102] M. Meyer, C. Dohmen, A. Philipp, D. Kiener, G. Maiwald, C. Scheu, M. Ogris, E. Wagner, Synthesis and biological evaluation of a bioresponsive and endosomolytic siRNA-polymer conjugate, Mol Pharm, 6 (2009) 752-762.

[103] G. Grandinetti, A.E. Smith, T.M. Reineke, Membrane and nuclear permeabilization by polymeric pDNA vehicles: efficient method for gene delivery or mechanism of cytotoxicity?, Mol Pharm, 9 (2012) 523-538.

[104] Y.H. Kim, J.H. Park, M. Lee, T.G. Park, S.W. Kim, Polyethylenimine with acid-labile linkages as a biodegradable gene carrier, J Control Release, 103 (2005) 209-219.

[105] M.S. Shim, Y.J. Kwon, Acid-Responsive Linear Polyethylenimine for Efficient, Specific, and Biocompatible siRNA Delivery., Bioconjug Chem, 20 (2009) 488-499.

[106] D.G. Anderson, D.M. Lynn, R. Langer, Semi-Automated Synthesis and Screening of a Large Library of Degradable Cationic Polymers for Gene Delivery, Angew Chem Int Ed Engl, 42 (2003) 3153-3158.

[107] J. Kloeckner, S. Bruzzano, M. Ogris, E. Wagner, Gene carriers based on hexanediol diacrylate linked oligoethylenimine: effect of chemical structure of polymer on biological properties, Bioconjug Chem, 17 (2006) 1339-1345.
[108] M. Thomas, J.J. Lu, C. Zhang, J. Chen, A.M. Klibanov, Identification of novel superior polycationic vectors for gene delivery by high-throughput synthesis and screening of a combinatorial library, Pharm Res, 24 (2007) 1564-1571.
[109] G. Saito, J.A. Swanson, K.D. Lee, Drug delivery strategy utilizing conjugation via reversible disulfide linkages: role and site of cellular reducing activities, Adv Drug Deliv Rev 55 (2003) 199-215.
[110] M.L. Read, K.H. Bremner, D. Oupicky, N.K. Green, P.F. Searle, L.W. Seymour, Vectors based on reducible polycations facilitate intracellular release of nucleic acids, J Gene Med, 5 (2003) 232-245.
[111] L.V. Christensen, C.W. Chang, W.J. Kim, S.W. Kim, Z. Zhong, C. Lin, J.F. Engbersen, J. Feijen, Reducible poly(amido ethylenimine)s designed for triggered intracellular gene delivery, Bioconjug Chem, 17 (2006) 1233-1240.
[112] C. Lin, Z. Zhong, M.C. Lok, X. Jiang, W.E. Hennink, J. Feijen, J.F. Engbersen, Linear poly(amido amine)s with secondary and tertiary amino groups and variable amounts of disulfide linkages: synthesis and in vitro gene transfer properties., J Control Release, 116 (2006) 130-137.
[113] Q. Peng, C. Hu, J. Cheng, Z. Zhong, R. Zhuo, Influence of disulfide density and molecular weight on disulfide cross-linked polyethylenimine as gene vectors., Bioconjug Chem, 20 (2009) 340-346.
[114] M.A. Gosselin, W. Guo, R.J. Lee, Efficient gene transfer using reversibly cross-linked low molecular weight polyethylenimine, Bioconjug Chem, 12 (2001) 989-994.
[115] J.H. Jeong, L.V. Christensen, J.W. Yockman, Z. Zhong, J.F. Engbersen, W.J. Kim, J. Feijen, S.W. Kim, Reducible poly(amido ethylenimine) directed to enhance RNA interference., Biomaterials, 28 (2007) 1912-1917.
[116] M. Breunig, C. Hozsa, U. Lungwitz, K. Watanabe, I. Umeda, H. Kato, A. Goepferich, Mechanistic investigation of poly(ethylene imine)-based siRNA delivery: Disulfide bonds boost intracellular release of the cargo., J Control Release, 130 (2008) 57-63.
[117] W.J. Kim, S.W. Kim, Efficient siRNA delivery with non-viral polymeric vehicles., Pharm Res, 26 (2009) 657-666.

[118] J.J. Green, J. Shi, E. Chiu, E.S. Leshchiner, R. Langer, D.G. Anderson, Biodegradable polymeric vectors for gene delivery to human endothelial cells, Bioconjug Chem, 17 (2006) 1162-1169.

[119] V. Russ, H. Elfberg, C. Thoma, J. Kloeckner, M. Ogris, E. Wagner, Novel degradable oligoethylenimine acrylate ester-based pseudodendrimers for in vitro and in vivo gene transfer, Gene Ther, 15 (2008) 18-29.

[120] D.A. Tomalia, H. Baker, J. Dewald, M. Hall, G. Kallos, S. Martin, J. Roeck, J. Ryder, P. Smith, A new class of polymers: starburst-dendritic macromolecules, Polym J, 17 (1985) 117-132.

[121] D.A. Tomalia, H. Baker, J. Dewald, M. Hall, G. Kallos, S. Martin, J. Roeck, J. Ryder, P. Smith, Dendritic macromolecules: synthesis of starburst dendrimers, Macromolecules, 19 (1986) 2466-2468.

[122] C. Worner, R. Mulhaupt, Polynitrile- and polyamine-functional poly(trimethylene imine) dendrimers 721, Angew.Chem.Int.Ed.Engl., 32 (1993) 1306-1311.

[123] J. Haensler, F.C. Szoka, Jr., Polyamidoamine cascade polymers mediate efficient transfection of cells in culture, Bioconjug Chem, 4 (1993) 372-379.

[124] A. Bielinska, J.F. Kukowska-Latallo, J. Johnson, D.A. Tomalia, J.R. Baker, Jr., Regulation of in vitro gene expression using antisense oligonucleotides or antisense expression plasmids transfected using starburst PAMAM dendrimers, Nucleic Acids Res, 24 (1996) 2176-2182.

[125] H. Yoo, P. Sazani, R.L. Juliano, PAMAM dendrimers as delivery agents for antisense oligonucleotides, Pharm Res, 16 (1999) 1799-1804.

[126] B.H. Zinselmeyer, S.P. Mackay, A.G. Schatzlein, I.F. Uchegbu, The lower-generation polypropylenimine dendrimers are effective gene-transfer agents, Pharm Res, 19 (2002) 960-967.

[127] A.G. Schatzlein, B.H. Zinselmeyer, A. Elouzi, C. Dufes, Y.T. Chim, C.J. Roberts, M.C. Davies, A. Munro, A.I. Gray, I.F. Uchegbu, Preferential liver gene expression with polypropylenimine dendrimers, J Control Release, 101 (2005) 247-258.

[128] A. Harada, M. Kawamura, T. Matsuo, T. Takahashi, K. Kono, Synthesis and characterization of a head-tail type polycation block copolymer as a nonviral gene vector, Bioconjug.Chem., 17 (2006) 3-5.

[129] J.S. Choi, K. Nam, J.Y. Park, J.B. Kim, J.K. Lee, J.S. Park, Enhanced transfection efficiency of PAMAM dendrimer by surface modification with l-arginine, J Control Release, 99 (2004) 445-456.

[130] H. Arima, F. Kihara, F. Hirayama, K. Uekama, Enhancement of gene expression by polyamidoamine dendrimer conjugates with alpha-, beta-, and gamma-cyclodextrins, Bioconjug.Chem., 12 (2001) 476-484.

[131] K.C. Wood, S.M. Azarin, W. Arap, R. Pasqualini, R. Langer, P.T. Hammond, Tumor-targeted gene delivery using molecularly engineered hybrid polymers functionalized with a tumor-homing peptide, Bioconjug Chem, 19 (2008) 403-405.

[132] J.W. Lee, Y.H. Ko, S.H. Park, K. Yamaguchi, K. Kim, Novel Pseudorotaxane-Terminated Dendrimers: Supramolecular Modification of Dendrimer Periphery, Angew Chem Int Ed Engl, 40 (2001) 746-749.

[133] Y.B. Lim, T. Kim, J.W. Lee, S.M. Kim, H.J. Kim, K. Kim, J.S. Park, Self-assembled ternary complex of cationic dendrimer, cucurbituril, and DNA: noncovalent strategy in developing a gene delivery carrier., Bioconjug Chem, 13 (2002) 1181-1185.

[134] T.I. Kim, J.U. Baek, C. Zhe Bai, J.S. Park, Arginine-conjugated polypropylenimine dendrimer as a non-toxic and efficient gene delivery carrier., Biomaterials, 28 (2007) 2061-2067.

[135] V. Russ, M. Gunther, A. Halama, M. Ogris, E. Wagner, Oligoethylenimine-grafted polypropylenimine dendrimers as degradable and biocompatible synthetic vectors for gene delivery, J Control Release, 132 (2008) 131-140.

[136] O. Taratula, O.B. Garbuzenko, P. Kirkpatrick, I. Pandya, R. Savla, V.P. Pozharov, H. He, T. Minko, Surface-engineered targeted PPI dendrimer for efficient intracellular and intratumoral siRNA delivery, J Control Release, 140 (2009) 284-293.

[137] A. Akinc, A. Zumbuehl, M. Goldberg, E.S. Leshchiner, V. Busini, N. Hossain, S.A. Bacallado, D.N. Nguyen, J. Fuller, R. Alvarez, A. Borodovsky, T. Borland, R. Constien, A. de Fougerolles, J.R. Dorkin, K. Narayanannair Jayaprakash, M. Jayaraman, M. John, V. Koteliansky, M. Manoharan, L. Nechev, J. Qin, T. Racie, D. Raitcheva, K.G. Rajeev, D.W. Sah, J. Soutschek, I. Toudjarska, H.P. Vornlocher, T.S. Zimmermann, R. Langer, D.G. Anderson, A combinatorial library of lipid-like materials for delivery of RNAi therapeutics, Nat Biotechnol, 26 (2008) 561-569.

[138] K.P. Mahon, K.T. Love, K.A. Whitehead, J. Qin, A. Akinc, E. Leshchiner, I. Leshchiner, R. Langer, D.G. Anderson, Combinatorial approach to determine

functional group effects on lipidoid-mediated siRNA delivery, Bioconjug Chem, 21 (2010) 1448-1454.
[139] T. Blessing, J.S. Remy, J.P. Behr, Monomolecular collapse of plasmid DNA into stable virus-like particles, Proc Natl Acad Sci U S A, 95 (1998) 1427-1431.
[140] E. Dauty, J.S. Remy, T. Blessing, J.P. Behr, Dimerizable cationic detergents with a low cmc condense plasmid DNA into nanometric particles and transfect cells in culture, J Am Chem Soc, 123 (2001) 9227-9234.
[141] C. Chittimalla, L. Zammut-Italiano, G. Zuber, J.P. Behr, Monomolecular DNA nanoparticles for intravenous delivery of genes, J Am Chem Soc, 127 (2005) 11436-11441.
[142] R.B. Merrifield Solid Phase Peptide Synthesis. I. The Synthesis of a Tetrapeptide, J Amer Chem Soc, 85 (1963) 2149–2154.
[143] R.B. Merrifield, Solid-Phase Peptide Synthesis. 3. An Improved Synthesis of Bradykinin, Biochemistry, 3 (1964) 1385-1390.
[144] J.P. Tam, Synthetic peptide vaccine design: synthesis and properties of a high-density multiple antigenic peptide system, Proc Natl Acad Sci U S A, 85 (1988) 5409-5413.
[145] Q.R. Chen, L. Zhang, P.W. Luther, A.J. Mixson, Optimal transfection with the HK polymer depends on its degree of branching and the pH of endocytic vesicles, Nucleic Acids Res, 30 (2002) 1338-1345.
[146] Q. Leng, A.J. Mixson, Modified branched peptides with a histidine-rich tail enhance in vitro gene transfection, Nucleic Acids Res, 33 (2005) e40.
[147] Q. Leng, P. Scaria, O.B. Ioffe, M. Woodle, A.J. Mixson, A branched histidine/lysine peptide, H2K4b, in complex with plasmids encoding antitumor proteins inhibits tumor xenografts, J Gene Med, 8 (2006) 1407-1415.
[148] X.L. Wang, S. Ramusovic, T. Nguyen, Z.R. Lu, Novel polymerizable surfactants with pH-sensitive amphiphilicity and cell membrane disruption for efficient siRNA delivery, Bioconjug Chem, 18 (2007) 2169-2177.
[149] N.J. Wells, A. Basso, M. Bradley, Solid-phase dendrimer synthesis, Peptide Science, 47 (1998) 381-396.
[150] S. Manku, C. Laplante, D. Kopac, T. Chan, D.G. Hall, A mild and general solid-phase method for the synthesis of chiral polyamines. Solution studies on the cleavage of borane-amine intermediates from the reduction of secondary amides, J Org Chem, 66 (2001) 874-885.

[151] M.R. Jorgensen, J.W. Jaroszewski, M. Witt, H. Franzyk, On-Resin Carboxy Group Activation of w-Amino Acids in Solid-Phase Synthesis of Philanthotoxin Analogues, Synthesis, 16 (2005) 2687-2694.
[152] L. Hartmann, E. Krause, M. Antonietti, H.G. Borner, Solid-phase supported polymer synthesis of sequence-defined, multifunctional poly(amidoamines), Biomacromolecules, 7 (2006) 1239-1244.
[153] L. Hartmann, S. Hafele, R. Peschka-Suss, M. Antonietti, H.G. Borner, Tailor-Made Poly(amidoamine)s for Controlled Complexation and Condensation of DNA, Chemistry, 14 (2008) 2025-2033.
[154] D. Schaffert, N. Badgujar, E. Wagner, Novel Fmoc-polyamino acids for solid-phase synthesis of defined polyamidoamines, Org Lett, 13 (2011) 1586-1589.
[155] D. Schaffert, C. Troiber, E.E. Salcher, T. Frohlich, I. Martin, N. Badgujar, C. Dohmen, D. Edinger, R. Klager, G. Maiwald, K. Farkasova, S. Seeber, K. Jahn-Hofmann, P. Hadwiger, E. Wagner, Solid-phase synthesis of sequence-defined T-, i-, and U-shape polymers for pDNA and siRNA delivery, Angew Chem Int Ed Engl, 50 (2011) 8986-8989.
[156] E.E. Salcher, P. Kos, T. Frohlich, N. Badgujar, M. Scheible, E. Wagner, Sequence-defined four-arm oligo(ethanamino)amides for pDNA and siRNA delivery: Impact of building blocks on efficacy, J Control Release, 164 (2012) 380-386.
[157] G. Mezo, N. Mihala, D. Andreu, F. Hudecz, Conjugation of epitope peptides with SH group to branched chain polymeric polypeptides via Cys(Npys), Bioconjug Chem, 11 (2000) 484-491.
[158] G.L. Ellman, Tissue sulfhydryl groups, Arch Biochem Biophys, 82 (1959) 70-77.
[159] A. Zintchenko, A. Philipp, A. Dehshahri, E. Wagner, Simple modifications of branched PEI lead to highly efficient siRNA carriers with low toxicity, Bioconjug Chem, 19 (2008) 1448-1455.
[160] T. Frohlich, D. Edinger, R. Klager, C. Troiber, E. Salcher, N. Badgujar, I. Martin, D. Schaffert, A. Cengizeroglu, P. Hadwiger, H.P. Vornlocher, E. Wagner, Structure-activity relationships of siRNA carriers based on sequence-defined oligo (ethane amino) amides, J Control Release, 160 (2012) 532-541.
[161] P. Midoux, C. Pichon, J.J. Yaouanc, P.A. Jaffres, Chemical vectors for gene delivery: a current review on polymers, peptides and lipids containing histidine or imidazole as nucleic acids carriers, Br J Pharmacol, 157 (2009) 166-178.

[162] Y. Wen, Z. Guo, Z. Du, R. Fang, H. Wu, X. Zeng, C. Wang, M. Feng, S. Pan, Serum tolerance and endosomal escape capacity of histidine-modified pDNA-loaded complexes based on polyamidoamine dendrimer derivatives, Biomaterials, 33 (2012) 8111-8121.

[163] J.J. Thomas, M.R. Rekha, C.P. Sharma, Unraveling the intracellular efficacy of dextran-histidine polycation as an efficient nonviral gene delivery system, Mol Pharm, 9 (2012) 121-134.

[164] J. Gu, X. Wang, X. Jiang, Y. Chen, L. Chen, X. Fang, X. Sha, Self-assembled carboxymethyl poly (L-histidine) coated poly (beta-amino ester)/DNA complexes for gene transfection, Biomaterials, 33 (2012) 644-658.

[165] M. Hashemi, B.H. Parhiz, A. Hatefi, M. Ramezani, Modified polyethyleneimine with histidine-lysine short peptides as gene carrier, Cancer Gene Ther, 18 (2011) 12-19.

[166] F. Perche, O. Lambert, M. Berchel, P.A. Jaffres, C. Pichon, P. Midoux, Gene transfer by histidylated lipopolyplexes: A dehydration method allowing preservation of their physicochemical parameters and transfection efficiency, Int J Pharm, 423 (2012) 144-150.

[167] F. Perche, D. Gosset, M. Mevel, M.L. Miramon, J.J. Yaouanc, C. Pichon, T. Benvegnu, P.A. Jaffres, P. Midoux, Selective gene delivery in dendritic cells with mannosylated and histidylated lipopolyplexes, J Drug Target, 19 (2011) 315-325.

[168] C.M. Ward, M.L. Read, L.W. Seymour, Systemic circulation of poly(L-lysine)/DNA vectors is influenced by polycation molecular weight and type of DNA: differential circulation in mice and rats and the implications for human gene therapy, Blood, 97 (2001) 2221-2229.

[169] C.H. Ahn, S.Y. Chae, Y.H. Bae, S.W. Kim, Biodegradable poly(ethylenimine) for plasmid DNA delivery, J Control Release, 80 (2002) 273-282.

[170] H. Zhang, S.V. Vinogradov, Short biodegradable polyamines for gene delivery and transfection of brain capillary endothelial cells, J Control Release, 143 (2010) 359-366.

[171] A.A. Eltoukhy, D.J. Siegwart, C.A. Alabi, J.S. Rajan, R. Langer, D.G. Anderson, Effect of molecular weight of amine end-modified poly(beta-amino ester)s on gene delivery efficiency and toxicity, Biomaterials, 33 (2012) 3594-3603.

[172] E. Wagner, J. Kloeckner, Gene delivery using polymer therapeutics, Adv.Polym.Sci, 192 (2006) 135-173.

[173] M.L. Forrest, J.T. Koerber, D.W. Pack, A degradable polyethylenimine derivative with low toxicity for highly efficient gene delivery, Bioconjug.Chem., 14 (2003) 934-940.

[174] M. Breunig, U. Lungwitz, R. Liebl, A. Goepferich, Breaking up the correlation between efficacy and toxicity for nonviral gene delivery, Proc.Natl.Acad.Sci U.S.A, 104 (2007) 14454-14459.

[175] L. Hartmann, H.G. Börner, Precision Polymers: Monodisperse, Monomer-Sequence-Defined Segments to Target Future Demands of Polymers in Medicine, Advanced Materials, 21 (2009) 3425-3431.

[176] L. Hartmann, Polymers for Control Freaks: Sequence-Defined Poly(amidoamine)s and Their Biomedical Applications, Macromolecular Chemistry and Physics, 212 (2011) 8-13.

[177] C. Troiber, E. Wagner, Nucleic acid carriers based on precise polymer conjugates, Bioconjug Chem, 22 (2011) 1737-1752.

[178] M.L. Read, K.H. Bremner, D. Oupicky, N.K. Green, P.F. Searle, L.W. Seymour, Vectors based on reducible polycations facilitate intracellular release of nucleic acids, J.Gene Med., 5 (2003) 232-245.

[179] C. Lin, C.J. Blaauboer, M.M. Timoneda, M.C. Lok, M. van Steenbergen, W.E. Hennink, Z. Zhong, J. Feijen, J.F. Engbersen, Bioreducible poly(amido amine)s with oligoamine side chains: synthesis, characterization, and structural effects on gene delivery, J Control Release, 126 (2008) 166-174.

[180] V. Russ, T. Frohlich, Y. Li, A. Halama, M. Ogris, E. Wagner, Improved in vivo gene transfer into tumor tissue by stabilization of pseudodendritic oligoethylenimine-based polyplexes, J Gene Med, 12 (2010) 180-193.

[181] M.E. Bonnet, P. Erbacher, A.L. Bolcato-Bellemin, Systemic delivery of DNA or siRNA mediated by linear polyethylenimine (L-PEI) does not induce an inflammatory response, Pharm Res, 25 (2008) 2972-2982.

[182] C.C. Lee, Y. Liu, T.M. Reineke, General Structure-Activity Relationship for Poly(glycoamidoamine)s: The Effect of Amine Density on Cytotoxicity and DNA Delivery Efficiency, Bioconjug Chem, 19 (2008) 428-440.

9 ACKNOWLEDGEMENTS

The completion of this thesis would not have been possible without the support of various people I would like to acknowledge in the following lines.
First of all, I would like to thank my supervisor Prof. Ernst Wagner for giving me the opportunity to be a part of his group. His scientific support, the creative freedom he offered and his great patience motivated my work all through the years.
A huge thank you goes to Dr. David Schaffert for introducing me to the daily lab work and the willingness to share his profound knowledge not only of SPS.
A great thank you goes to my colleagues of the “polymer group”: Christina, Christian D., Naresh, Uli, Claudia, Petra and Thomas for the good teamwork, helpful discussions and for being great colleagues I could always rely on. Additionally, thank you to Petra and Thomas for performing uncountable transfection experiments.
Thank-you to my (former) lab buddies Terese, Claudia (mmmmhh), Christian D., Kevin and Wolfgang for sharing joy and frustration all through the years. Thank-you to my “downstairs buddies” Christian M., Uli and Arzu for funny and fruitful conversations and also to the other members of the Wagner lab I did not mention by name for contributing to a pleasant working atmosphere.
I would also like to thank to Dr. Martina Rüffer for patiently introducing me (again) to the secrets of cellular plant drawing and Bavarian fauna. Her deep knowledge on plants and enthusiasm of sharing it made me look forward to the summer terms. I thank her also for sharing her passion for contemporary literature by providing me with interesting new books.
I am also very grateful to Wolfgang Rödl, who heard the most silent cries of desperation whenever some device was not working and was immediately there to help.
I would also like to thank the people from our former cooperation partner Axolabs GmbH (formerly: Roche Kulmbach GmbH) for the great collaboration and support.
Thank you also Dr. Lars Allmendinger and his team for measuring uncountable NMRs. Also, thank-you to Max Scheible from the Simmel lab for performing the AFM measurements.
My gratitude goes also, more than words can say, to my parents and my husband Christian. For always catching me when I was about to fall and making dark days

sunny. For always showing me the way back when I was about to get lost. For laughing with me. For drying my tears. For being in my life. Thank you.